Molecular Basis for G-protein-Coupled Receptor (GPCR) Activation and Biased Signalling at the Platelet Thrombin Receptor Proteinase Activated Receptor-4 (PAR4).

Pierre E. Thibeault[1], Jordan C. LeSarge[2], D'Arcy Arends[1], Michaela Fernandes[2], Peter Chidiac[1], Peter B. Stathopulos[1], Leonard G. Luyt[2,3,4], and Rithwik Ramachandran[1*]

[1)] Department of Physiology and Pharmacology, University of Western Ontario, London, ON, N6A5C1, Canada.

[2)] Department of Chemistry, The University of Western Ontario, London, ON, N6A5C1, Canada.

[3)] Departments of Oncology, The University of Western Ontario, London, ON, N6A5C1, Canada.

[4)] London Regional Cancer Program, Lawson Health Research Institute, London, ON, N6C2R5, Canada.

* For correspondence:

Rithwik Ramachandran,
Department of Physiology and Pharmacology,
Schulich School of Medicine and Dentistry,
University of Western Ontario, London,
Ontario, Canada.
Phone: 519-661-2142
email: rramach@uwo.ca

Abstract:
Proteinase Activated Receptor-4 (PAR4) is a member of the proteolytically-activated PAR family of G-Protein-coupled Receptors (GPCRs). PARs are activated following proteolytic cleavage of the receptor N-terminus by enzymes such as thrombin, trypsin, and cathepsin-G to reveal the receptor-activating motif termed the tethered ligand. The tethered ligand binds intramolecularly to the receptor and triggers receptor signalling and cellular responses. In spite of this unusual mechanism of activation, PARs are fundamentally peptide receptors and can also be activated by exogenous application of short synthetic peptides derived from the tethered ligand sequence. In order to gain a better understanding of the molecular basis for PAR4-dependent signalling, we examined signalling responses to a library of peptides derived from the canonical PAR4 activating peptide (PAR4-AP), AYPGKF-NH_2. We examined residues involved in activation of the $G\alpha_{q/11}$-coupled calcium signalling pathway, β-arrestin recruitment, and mitogen-activated protein kinase pathway activation. The peptide *N*-methyl-alanine-YPGKF-NH_2 was identified as a compound that is a poor activator of PAR4-dependent calcium signalling but was fully competent in recruiting β-arrestin-1 and -2. In order to gain a better understanding of the ligand-binding pocket, we used *in silico* docking to identify key residues involved in PAR4 interaction with AYPGKF-NH_2. The predicted interactions were verified by site-directed mutagenesis and analysis of calcium signalling and β-arrestin-1/-2 recruitment following proteolytic activation (with thrombin) or activation with the synthetic agonist peptide (AYPGKF-NH_2). We determined that a key extracellular loop-2 aspartic acid residue (Asp^{230}) is critical for signalling following both proteolytic and peptide activation of PAR4. Finally, we investigated platelet aggregation in response to A**y**PGKF-NH_2 (a peptide with D-tyrosine in position two) which is unable to activate calcium signalling, and AYPG**R**F-NH_2 a peptide that is equipotent to the parental peptide AYPGKF-NH_2 for calcium signalling but is more potent at recruiting β-arrestins. We found that A**y**PGKF-NH_2 fails to activate platelets while AYPG**R**F-NH_2 causes a platelet aggregation response that is greater than that seen with the parental peptide and is comparable to that seen with thrombin stimulation. Overall, these studies uncover molecular determinants for agonist binding and signalling through a non-canonically activated GPCR and provide a template for development of small molecule modulators of PAR4.

Introduction:

G-Protein-coupled receptors (GPCRs) are the largest family of cell surface receptors and regulate a host of important physiological responses (Fredriksson and Schioth, 2005; Pierce et al., 2002). GPCRs respond to a variety of extracellular signals and regulate cellular behaviour through engaging intracellular effector molecules to activate various cell-signalling pathways (Erlandson et al., 2018; Hilger et al., 2018). In drug discovery, GPCRs are a valuable and highly tractable class of drug targets with over 30% of all currently approved drugs acting on GPCRs (Sriram and Insel, 2018). GPCR activation occurs typically through binding of a soluble ligand and conformational changes that enable engagement of G-protein-dependent or β-arrestin-mediated signal transduction. The Proteinase Activated Receptors (PARs) are a four-member family of GPCRs with a distinct mechanism of activation that involves limited proteolysis and unmasking of a receptor activating motif called the tethered ligand. PARs were first discovered in an effort to identify the cellular receptors responsible for actions of thrombin that were independent from its role in the coagulation cascade (Vu et al., 1991). Various proteinases have now been described as activators of the different members of the PAR family, but canonically PAR1 and PAR4 are described as thrombin-activated receptors, while PAR2 is activated by trypsin and other trypsin-like serine proteinases. PAR4 can also be activated by trypsin. Whether PAR3 signals independently is unclear, though thrombin can cleave the PAR3 N-terminus to reveal a tethered ligand (Adams et al., 2011; Ishihara et al., 1997). Following the discovery of PARs it was quickly realized that two receptors, PAR1 and PAR4, serve as the thrombin receptors on human platelets (Coughlin, 2005, 1999). PAR1 and PAR4 both trigger platelet activation and aggregation. Given that anti-platelet agents are an important class of drugs for the treatment of various cardiovascular diseases, there has been a concerted effort aimed at understanding the role of these receptors in platelet activation and in identifying molecules that can act as PAR1 and PAR4 antagonists. A PAR1 antagonist was recently identified and approved for clinical use, however significant bleeding side effects were noted in patients administered this drug (Morrow et al., 2012, 2009; Scirica et al., 2012). While bleeding is a frequently encountered side effect of therapeutically targeting pathways involved in blood coagulation, it was hoped that targeting PAR1 would not present such liability. Much attention has now shifted to understanding and targeting the other thrombin receptor PAR4. Though both PAR1 and PAR4 are activated by thrombin, there are some key differences reported in the activation of these two receptors on platelets that argue for PAR4 being a better anti-platelet drug target than PAR1. PAR1 possesses a hirudin-like binding site that enables it to bind thrombin with relatively high affinity (Jacques et al., 2000; Liu et al., 1991). In lacking this thrombin-binding site, PAR4 can only be activated at much higher concentrations of thrombin, such as may be encountered on a growing platelet thrombus. There are also reported differences in the kinetics of PAR1 and PAR4-dependent calcium signalling, with PAR4 causing a delayed but more sustained signal compared to PAR1 (Shapiro et al., 2000). This is thought to be due to dual proline residues in the PAR4 exodomain that provide low-affinity interactions with the thrombin active site and an anionic cluster that slows dissociation from thrombin (Jacques and Kuliopulos, 2003). Overall, PAR1 is thought to initiate platelet activation in response to low concentrations of thrombin while PAR4 is engaged at higher concentrations to further consolidate and stabilize the clot.

102 Given the liabilities seen with targeting PAR1 as a platelet thrombin receptor there has been
103 renewed interest in developing small molecule PAR4 antagonists (Rwibasira Rudinga et al.,
104 2018; Wu et al., 2000; Young et al., 2010). Recently small molecule antagonists of PAR4 have
105 been described with efficacy in inhibiting injury induced thrombosis in both non-human
106 primates and humans (Miller et al., 2019; Wilson et al., 2017; Wong et al., 2017). Despite these
107 promising advances there remains the question of whether a complete inhibition of PAR4 might
108 also lead to bleeding liability. Our efforts have therefore focused on examining biased
109 signalling through PAR4 in order to identify pathways that are responsible for platelet
110 aggregation and that could be selectively manipulated for therapeutic efficacy. PAR4 can
111 activate multiple signalling pathways through coupling to $G\alpha_{q/11}$, $G\alpha_{12/13}$ and β-arrestin
112 (Holinstat et al., 2006; Li et al., 2011; Ramachandran et al., 2017). In previous work, we and
113 others showed that pepducins targeting different intracellular motifs in PAR4 could be
114 employed to differentially inhibit platelet activation by blocking G-protein-coupled or β-
115 arrestin-dependent signalling (Covic et al., 2002; Ramachandran et al., 2017). The ability to
116 selectively activate or inhibit GPCR signalling in a biased manner is of great interest and has
117 been proposed as a strategy for obtaining therapeutically superior drugs for a number of
118 conditions (Bar-Shavit et al., 2016; Hollenberg et al., 2014; Seyedabadi et al., 2019). In the
119 case of the finely balanced signalling systems involved in coagulation and platelet activation,
120 such subtle perturbations may be key to obtaining drugs which do not result in bleeding
121 liability.
122
123 Here we seek to gain an understanding of the molecular interactions responsible for agonist
124 docking to PAR4 and to identify interactions that can be manipulated to obtain biased ligands
125 for PAR4. By screening a peptide library derived from the most widely used PAR4 agonist
126 peptide, AYPGKF-NH_2, we have identified key residues that confer selective activation of
127 $G\alpha_{q/11}$ coupled calcium signalling and/or β-arrestin recruitment. Through *in silico* docking and
128 confirmatory mutagenesis experiments we further identify an extracellular loop 2 residue that
129 is critical for receptor activation and signalling. We also examine platelet activation by peptides
130 that show differential activation of PAR4 signalling. Overall, these studies advance our
131 understanding of PAR4 activation and signalling and will help guide future drug discovery
132 efforts targeting this receptor.

133 **Results:**

134 **Experimental design and data analysis.** In order to understand the rules governing agonist
135 peptide activation of PAR4 we synthesized 37 hexapeptides through modification to the
136 synthetic PAR4 agonist peptide AYPGKF-NH_2. A number of different modifications were
137 examined at each of the six positions, including alanine substitutions, D-isomer substitutions,
138 *N*-methyl substitutions, as well as other modifications aimed at further probing each of the six
139 positions. Henceforth, the parental PAR4 agonist peptide for this study, AYPGKF-NH_2 (Ala^1-
140 Tyr^2-Pro^3-Gly^4-Lys^5-Phe^6-NH_2; superscript denotes position from N-terminus), will be referred
141 to as PAR4-AP. $G\alpha_{q/11}$-coupled calcium signalling, β-arrestin-1/-2 recruitment, and p44/42
142 mitogen-activated protein kinase (MAPK) signalling by each of these peptides was monitored
143 and compared to responses triggered by PAR4-AP (Table 1). Whereas PAR4-AP triggered
144 $G\alpha_{q/11}$ signalling reached a clear plateau over the range of concentrations tested (0.3 – 300
145 μM), β-arrestin recruitment did not and therefore the effective concentration required to
146 achieve half-maximal response (EC_{50}) values could not be accurately assessed. In contrast, with
147 the substituted peptides, $G\alpha_{q/11}$ signalling concentration-effect curves in some cases did not
148 clearly plateau, whereas β-arrestin recruitment did. Where possible, EC_{50} values are compared
149 between PAR4-AP and substituted peptides. However, since clear maxima were not always
150 obtained, comparisons of signal magnitude throughout the present study are presented as the
151 response elicited by a given compound at 100 μM shown as a percentage of responses elicited
152 by PAR4-AP at the same concentration. Since the concentration-effect curve for PAR4-AP
153 exhibits a saturating calcium signal, peptides that failed to saturate calcium signalling responses
154 are depicted as having EC_{50} values that were 'not determined' (*n.d.*). Maximal calcium signal
155 responses are shown as a percentage of the response obtained with the calcium ionophore
156 A23187 (Table 1, Max; % of A23187 calcium ionophore) and are referred to throughout the
157 results as a change in maximal calcium signalling as a measure of the efficacy of the peptides.
158 Throughout the results, β-arrestin recruitment values are presented as a percentage (%) of the
159 PAR4-AP-induced recruitment at 100 μM concentration. For ease of comparison,
160 concentration-effect curves for PAR4-AP-mediated $G\alpha_{q/11}$ calcium signalling and β-arrestin
161 recruitment are displayed as reference values in each of the Figures 1 through 7.
162
163 **Effect of alanine substitution on PAR4-AP-mediated signalling responses.** Our first set of
164 changes involved alanine substitutions at positions 2-6 of the PAR4-AP (calcium EC_{50} = 12.1
165 ± 3.1 μM; β-arrestin-1 recruitment at 100 μM for comparison is considered 100 ± 3.9%, and
166 100 ± 3.5% for β-arrestin-2) (Fig. 1, Table 1). Potency was decreased with respect to calcium
167 signalling when $tyrosine^2$ was substituted with alanine, and failed to reach a plateau over the
168 concentration range tested (A**A**PGKF-NH_2; EC_{50} = *n.d.*). Correspondingly, β-arrestin
169 recruitment was reduced compared to PAR4-AP at the same concentration (β-arr-1 47.3 ±
170 3.6%; β-arr-2 46.4 ± 3.2%). Substitution of $proline^3$ with alanine resulted in a significant
171 decrease in potency for calcium signalling (AY**A**GKF-NH_2 EC_{50} = 63.7 ± 20.8 μM) and yielded
172 reduced β-arrestin recruitment (β-arr-1 48.5 ± 7.9%; β-arr-2 43.4 ± 7.1%). Either $glycine^4$ or
173 $phenylalanine^6$ substitution to alanine resulted in reduced maximal calcium signalling
174 compared to PAR4-AP at the same concentration, with no significant effect on potency (EC_{50}

175 = 21.2 ± 6.6 μM; EC_{50} = 17.3 ± 5.0 μM, respectively). Additionally, alanine substitutions in
176 these positions resulted in significantly reduced β-arrestin recruitment, to levels approximately
177 half of those observed with PAR4-AP (AYP**A**KF-NH_2 β-arr-1 56.4 ± 5.6%, β-arr-2 54.6 ±
178 5.1%; AYPGK**A**-NH_2 β-arr-1 47.9 ± 3.8%, β-arr-2 52.6 ± 3.5%). Interestingly, we observed
179 that lysine[5] to alanine substitution had no appreciable impact on potency with respect to
180 calcium signalling (AYPG**A**F-NH_2 EC_{50} = 9.8 ± 2.9 μM); however, this substitution did reduce
181 recruitment of β-arrestin-1 (59.3 ± 7.2%) and -2 (70.8 ± 6.5%). Collectively, alanine
182 substitutions of positions 2-6 resulted in decreased β-arrestin recruitment compared to the
183 parental peptide (Fig. 1 B. and C.; Table 1). Interestingly, we observe differential effects on
184 calcium signalling with significant detriment to potency attributed to tyrosine substitution (Fig.
185 1 A.). Additionally, substitution of glycine and phenylalanine moderately decreased maximal
186 calcium signalling responses, perhaps indicating that these residues are important for full
187 agonism of this pathway comparative to that achieved with the parental peptide. Notably, all
188 single alanine substitutions of positions 2-6 of the PAR4-AP retained some agonist activity
189 indicating that signalling is not wholly reliant on any single residue alone.
190
191 **Effect of D-isomer amino acid substitutions on PAR4-AP-mediated signalling responses.**
192 To assess the impact of stereochemical inversion at each residue we generated five peptides
193 with single amino acid substitutions to their respective D-isomers (Fig. 2, Table 1). Glycine
194 possesses only one isomeric form and thus is not substituted. Both L-alanine to D-alanine
195 (**a**YPGKF-NH_2) and L-lysine to D-lysine (AYPG**k**F-NH_2) substitutions resulted in significant
196 losses of potency in calcium signalling assays compared to PAR4-AP. Consistent with calcium
197 data, we observed a significant decrease in β-arrestin recruitment compared to the parental
198 PAR4-AP (**a**YPGKF-NH_2 β-arr-1 48.7 ± 2.6%, β-arr-2 47.5 ± 2.4%; AYPG**k**F-NH_2 β-arr-1
199 47.4 ± 1.0%, β-arr-2 36.5 ± 0.9%). Interestingly, both D-tyrosine (A**y**PGKF-NH_2) and D-
200 proline (AY**p**GKF-NH_2) substitutions completely abolished calcium signalling. Comparably,
201 β-arrestin recruitment was significantly reduced with stimulation by either peptide (A**y**PGKF-
202 NH_2 β-arr-1 50.7 ± 4.6%, β-arr-2 46.4 ± 4.2%; AY**p**GKF-NH_2 β-arr-1 45.2 ± 10.5%, β-arr-2
203 38.1 ± 9.5%). In keeping with what we observed with phenylalanine to alanine substitution
204 (Fig. 1), D-phenylalanine substitution in position 6 (AYPGK**f**-NH_2) resulted in less efficacious
205 agonism of both calcium (EC_{50} = 22.2 ± 4.7 μM) and β-arrestin recruitment (β-arr-1 80.3 ±
206 6.6%, β-arr-2 74.1 ± 6.0%). Overall, D-isomers substitutions of amino acids alanine[1], tyrosine[2],
207 proline[3], and lysine[5] all result in significant reduction of (D-alanine, D-lysine) or abolition of
208 (D-tyrosine, D-proline) calcium signalling while causing significant reductions in β-arrestin
209 recruitment. Substitution of L-phenylalanine[6] for D-phenylalanine was the only D-isomer
210 substitution that is somewhat tolerated, resulting in modest reductions in potency with respect
211 to both calcium signalling and β-arrestin recruitment. These data reveal that the sidechain
212 stereochemistry of residues within the AYPGKF-NH_2 peptide perform a role in agonism.
213
214 **Effect of *N*-methylation on PAR4-AP-mediated signalling responses.** We generated a series
215 of peptides to investigate the pharmacological impact of *N*-methylation along the peptide
216 backbone (Fig. 3, Table 1). In contrast to the parental PAR4-AP, all but one of the N-
217 methylated peptides evaluated yielded clear plateaus and discernible EC_{50} values in β-arrestin
218 recruitment assays, and where applicable these are indicated below along with their relative

219 responses compared to PAR4-AP at 100 μM. Substitution of alanine[1] with *N*-methyl-alanine
220 [(***N*-Me-A)**-YPGKF-NH_2] almost completely abolished calcium signalling (EC_{50} = *n.d.*).
221 Interestingly, this peptide was able to initiate β-arrestin-1/-2 recruitment comparable to levels
222 obtained with PAR4-AP (β-arr-1 119.2 ± 11.9%, EC_{50} = 6.8 ± 2.6 μM; β-arr-2 80.6 ± 10.8%;
223 EC_{50} = 2.0 ± 0.7 μM). These results suggest that increasing steric bulk and hydrophobicity of
224 the backbone at amide positions through the addition of an N-terminal methyl group drives
225 PAR4 signalling towards β-arrestin pathways and causes only modest activation of calcium
226 signalling. Substitution of tyrosine[2] for *N*-methyl-tyrosine [A-**(*N*-Me-Y)**-PGKF-NH_2]
227 abolished calcium signalling up to 300 μM (EC_{50} = *n.d.*). Consistent with calcium signalling,
228 we observed decreased signal magnitude in β-arrestin recruitment assays compared to PAR4-
229 AP (β-arr-1 71.4 ± 10.8%, EC_{50} = 14.2 ± 8.6 μM; β-arr-2 61.5 ± 9.8%, EC_{50} = 11.8 ± 5.7 μM).
230 Substitution of the PAR4-AP glycine[4] with sarcosine (Sar., a.k.a *N*-methyl-glycine; AYP-**Sar**-
231 KF-NH_2) resulted in significantly reduced calcium potency (EC_{50} = *n.d.*) and significantly
232 reduced β-arrestin-1/-2 recruitment (35.9 ± 4.3%, 36.1 ± 3.9% respectively). *N*-methylation of
233 the alpha (α) amine of lysine[5] [AYPG-**(N_α-Me-K)**-F-NH_2] resulted in significantly reduced
234 calcium signalling (EC_{50} = *n.d.*) with no significant effect on maximal β-arrestin recruitment
235 (β-arr-1 126.7 ± 18.6%, EC_{50} = 12.2 ± 4.3 μM; β-arr-2 77.1 ± 16.9%, EC_{50} = 2.5 ± 1.0 μM).
236 Substitution of phenylalanine[6] with *N*-methyl-phenylalanine [AYPGK-**(*N*-Me-F)**-NH_2] was
237 equipotent for calcium signalling compared to PAR4-AP (EC_{50} = 7.6 ± 1.9 μM). Interestingly,
238 this peptide showed increased recruitment of both β-arrestins (β-arr-1 136.9 ± 18.0%, EC_{50} =
239 10.4 ± 3.3 μM; β-arr-2 96.6 ± 16.4%, EC_{50} = 15.3 ± 4.6 μM). Together, these data reveal that
240 *N*-methylation of positions 1, 2, 4, and 5 are deleterious to calcium signalling.
241
242 We were excited to observe evidence of β-arrestin-biased peptides within this group, all of
243 which showed decreased calcium signalling and/or increased β-arrestin recruitment. Moreover,
244 the leftward shifts in their associated β-arrestin concentration-effect profiles imply that
245 substitution of *N*-methylated alanine[1], tyrosine[2], lysine[5], or phenylalanine[6] residues increases
246 peptide potency with respect to G-protein-independent signalling. Only *N*-methylation of
247 glycine[4] (sarcosine) resulted in a reduced overall ability to activate PAR4, with relative calcium
248 and β-arrestin signals being reduced by approximately 90% and 60%, respectively.
249
250 **Effect of N-terminal and position 1 modifications on PAR4-AP-mediated signalling**
251 **responses.** To further investigate the impact of *N*-terminal alterations to the PAR4-AP we
252 examined the impact of N-terminal acetylation and substitutions of position 1 (Fig. 4, Table 1).
253 Previously it was demonstrated that protonation of the N-terminus of the PAR1 tethered ligand
254 (SFLLRN) is critical for agonist function (Scarborough et al., 1992). Additionally, substitution
255 of glycine for mercaptoproprionic acid (Mpr), which lacks an amino-terminal protonated amine
256 in the native tethered-ligand-mimicking peptide GYPGQV, resulted in complete loss of agonist
257 activity (Faruqi et al., 2000). Given the evidence for N-terminal protonation in PAR agonism,
258 we sought to determine the impact of N-terminal acetylation on PAR4-AP activity. N-terminal
259 acetylation of the PAR4-AP (**Ac**-AYPGKF-NH2) negatively impacted both calcium signalling
260 (EC_{50} = *n.d.*) as well as the magnitude of β-arrestin recruitment to PAR4 as expected (β-arr-1
261 47.3 ± 3.1%, EC_{50} = 15.0 ± 4.3 μM; β-arr-2 45.5 ± 2.8%, EC_{50} = 26.7 ± 5.6 μM). In contrast

262 to the previously reported loss of activity with Mpr-YPGQV peptide, we observe partial
263 agonism with the loss of protonation in the PAR4-AP.
264
265 In both the native human PAR4 tethered-ligand sequence and the PAR4-AP, position 1 is
266 occupied by small (tethered ligand – glycine, PAR4-AP – alanine) and non-polar (PAR4-AP –
267 alanine) residues. To investigate the role of position 1 in the PAR4-AP, we generated seven
268 peptides with position 1 substitutions. Introduction of steric bulk and increased hydrophobicity
269 through substitution of alanine[1] for valine resulted in partial agonism of both calcium signalling
270 and β-arrestin recruitment (**V**YPGKF-NH_2 EC_{50} = 22.9 ± 8.3 μM; β-arr-1 73.6 ± 13.0%, EC_{50}
271 = 33.8 ± 13.7 μM; β-arr-2 55.2 ± 11.8%, EC_{50} = 13.7 ± 8.2 μM). Additionally, increasing
272 hydrophobic bulk at position 1 through substitution with norleucine completely abolished
273 calcium signalling (**Nle**-YPGKF-NH_2, EC_{50} = *n.d.*) and resulted in partial agonism of β-arrestin
274 recruitment (β-arr-1 40.2 ± 9.7%; β-arr-2 36.5 ± 8.8%). Together, data from these substitutions
275 indicate that the precise steric bulk of the side chain in position 1 is important for PAR4
276 agonism.
277
278 Next, we evaluated the impact of steric bulk relocation in position 1. Relocation of the methyl
279 group in alanine to the N-terminus and loss of side chain through substitution with sarcosine
280 (**Sar**-YPGKF-NH_2) resulted in poor agonism at both calcium signalling (EC_{50} = *n.d.*) and β-
281 arrestin recruitment (β-arr-1 35.6 ± 2.0%, β-arr-2 39.8 ± 1.8%). Further, the addition of an α-
282 methyl group through substitution of alanine[1] with 2-aminoisobutyric acid (**Aib**-YPGKF-NH_2)
283 resulted in a significantly less potent partial agonist for calcium signalling (EC_{50} = 50.2 ± 15.3
284 μM) and also resulted in a significant reduction in β-arrestin recruitment (β-arr-1 38.6 ± 3.9%;
285 β-arr-2 37.3 ± 3.6%). Similarly, replacement with *N*-methyl-serine [**(N-Me-S)**-YPGKF-NH_2]
286 also caused a significant attenuation of calcium signalling (EC_{50} = *n.d.*), while also revealing a
287 decrease in β-arrestin recruitment compared to PAR4-AP (β-arr-1 78.1 ± 6.9%, β-arr-2 51.7 ±
288 6.3%). Thus, it is apparent that the precise position of the side chain in position 1 is important
289 for agonism.
290
291 To further probe the importance of charge localization at the N-terminal region of the peptide,
292 we examined the effect of changing the localization of the positive charge in position 1.
293 Substitution of alanine with either beta-alanine or isonipecotic acid significantly reduced the
294 potency and activity of the PAR4-AP, similar to the results with PAR4-AP N-terminal
295 acetylation (**betaAla**-YPGKF-NH2 calcium EC_{50} = *n.d.*, β-arr-1 25.7 ± 4.8%, β-arr-2 31.8 ±
296 4.4%; **Inp**-YPGKF-NH_2 calcium EC_{50} = *n.d.*, β-arr-1 32.0 ± 3.3%, β-arr-2 26.9 ± 3.0%).
297 Together these data suggest a role for N-terminal charge localization in agonist activity.
298
299 **Effect of additional substitutions in positions 2-4 on PAR4-AP-mediated signalling.**
300 Previously structure activity studies with PAR4 activating peptides revealed an apparent
301 requirement for an aromatic residue in position 2 (tyrosine) and found that alterations to
302 position 3 (proline) and position 4 (glycine) were not well tolerated (Faruqi et al., 2000). In the
303 present study, we observed that substitution of either tyrosine, proline, or glycine with alanine
304 reduced calcium signalling potency and β-arrestin recruitment, however none of these

305 substitutions completely abolished activity of the peptide (Fig. 1). Interestingly, substitution of
306 either L-tyrosine or L-proline with the respective D-isomer significantly reduced the activity
307 of the PAR4-AP (Fig. 2, Table 1). Together, these data suggest that while no individual residue
308 is strictly required for agonist activity, the side chains of these residues and their positioning
309 are important for agonist function. To further probe the contribution of these residues to the
310 PAR4-AP, we generated peptides with alterations in the aromatic side chain of position 2, the
311 backbone conformation of position 3, or position 4 (Fig. 5, Table 1).
312
313 Peptides with substitution of tyrosine[2] with either 4-fluoro-L-phenylalanine [A-**F(4-fluoro)**-
314 PGKF-NH2] or *O*-methyl-tyrosine [A-**Tyr(Me)**-PGKF-NH_2] retained calcium signalling and
315 β-arrestin recruitment with no significant changes in potency compared to the PAR4-AP. These
316 data suggest that the side chain of tyrosine may be a site in which further modifications can be
317 made to the peptide without affecting agonist potential; however, by comparing A**A**PGKF-
318 NH_2 the presence of an aromatic ring in position 2 is of importance. Given the results obtained
319 with alanine or D-proline substitution of proline[3] (Fig. 1 & 2, respectively), we furthered
320 probed conformational contributions of this residue to the parental PAR4-AP. Proline was
321 substituted with pipecolic acid (2-piperidinecarboxylic acid; Pip) which is structurally similar
322 to proline but has an increased steric bulk and backbone elongation provided by a six-
323 membered ring compared to the five-membered ring of proline. We observed partial agonism
324 of calcium signalling in response to AY-**Pip**-GKF-NH_2 stimulation with no significant
325 difference in agonist potency (EC_{50} = 30.7 ± 4.9 μM) with a correlating partial agonism of β-
326 arrestin recruitment (β-arr-1 38.8 ± 3.0%; β-arr-2 44.0 ± 2.7%). Thus, it appears that increasing
327 steric bulk/backbone length may affect efficacy but still results in agonism. To further
328 investigate the role of backbone conformation provided at position 3, proline was substituted
329 with nipecotic acid (3-piperidinecarboxylic acid; Nip) which is similar to pipecotic acid,
330 however, results in change of the peptide backbone direction (AY-**Nip**-GKF-NH_2). With this
331 modification, both calcium signalling (EC_{50} = *n.d.*) and β-arrestin recruitment (β-arr-1 32.9 ±
332 4.9%; β-arr-2 30.9 ± 4.5%) were significantly decreased in response to PAR4 stimulation.
333 Elongation of the backbone in position four (glycine) by substitution with beta-alanine (AYP-
334 **betaAla**-KF-NH_2) was also significantly detrimental to both calcium signalling (EC_{50} = *n.d.*)
335 and β-arrestin recruitment (β-arr-1 42.5 ± 1.8%, β-arr-2 24.9 ± 1.6%). Together these data
336 suggest an important role for backbone conformation contributed by proline[3] and glycine[4]
337 compactness in the PAR4-AP. As well, these data suggest peptide backbone length at proline[3]
338 and glycine[4] has an important role; consistent with what we have observed with backbone
339 elongation modifications at position 1 (**Inp**-YPGKF-NH_2 and **betaAla**-YPGKF-NH_2; Fig. 4,
340 Table 1).
341
342 **Effect of additional substitutions in position 5 on PAR4-AP-mediated signalling**
343 **responses.** Previously, investigations into glutamine substitutions in the native tethered ligand
344 mimicking peptide, GYPGQV, revealed that agonism is maintained when this position is
345 substituted with a charged residue such as arginine or ornithine (Faruqi et al., 2000). In the
346 present study, we have identified that substitution of position 5 (lysine) of the PAR4-AP
347 (AYPGKF-NH_2) with alanine does not significantly affect the agonist capacity of the peptide

348 (Fig. 1). Further, we identified that substitution of L-lysine with D-lysine significantly
349 decreases agonist stimulation of calcium signalling and β-arrestin recruitment (Fig. 2). To
350 further probe the effect of positively charged residues in position 5, we generated several
351 PAR4-AP analogues with lysine[5] substitutions by either arginine or ornithine (Fig. 6, Table 1).
352 Substitution of lysine[5] with arginine resulted in a partial agonist with respect to calcium
353 signalling but increased β-arrestin recruitment compared to the parental peptide (AYPG**R**F-
354 NH_2 calcium EC_{50} = 4.0 ± 1.1 μM, β-arr-1 154.2 ± 10.3%, β-arr-2 140.1 ± 9.4%). This
355 substitution delocalizes the positive charge of the side chain compared to lysine and increases
356 steric bulk. Interestingly, substitution with ornithine, which is similarly charged but has a
357 shortened distance between the charge and the peptide backbone compared to lysine, also
358 resulted in partial agonism of PAR4-mediated calcium signalling accompanied by a modest
359 increase in the recruitment of β-arrestins (AYPG**O**F-NH_2 calcium EC_{50} = 4.2 ± 1.1 μM, β-arr-
360 1 121.7 ± 8.5%, β-arr-2 112.1 ± 7.7%). To further probe if steric bulk in the side chain of
361 position 5 affects PAR4-AP potency, we increased steric bulk through methylation of the
362 epsilon (ε) amine of lysine [AYPG-**(N_ε-Me-K)**-F-NH_2]. This substitution yielded a full agonist
363 for calcium signalling (EC_{50} = 6.7 ± 1.9 μM) and a modestly more efficacious agonist for the
364 recruitment of β-arrestins (β-arr-1 122.5 ± 12.4%; β-arr-2 116.7 ± 11.2%). All of these
365 substitutions maintain a positive charge and are able to act as agonists for PAR4. To determine
366 if charge in position 5 is required, we substituted lysine with citrulline, which maintains similar
367 structure to arginine and lysine while removing a positive charge (AYPG-**Cit**-F-NH_2).
368 Interestingly, we observed partial agonism with respect to calcium signalling (EC_{50} = 5.4 ± 0.8
369 μM) with equipotent β-arrestin recruitment compared to the PAR4-AP, consistent with the
370 alanine scan data for this position. Thus, positively charged residues in position 5 seem to
371 contribute to agonism. Interestingly, we observed similar increases in β-arrestin recruitment
372 and equipotent calcium signalling when stericity was either increased (AYPG**R**F-NH_2) or
373 decreased (AYPG**O**F-NH_2), suggesting that the positive charge in this position is more
374 important than the size of the side chain. Finally, although both the charge and size of the size
375 chain have an effect, all modifications to position 5, with the exception of D-lysine (Fig. 2,
376 Table 1) and N_α-methyl-lysine (Fig. 3, Table 1) modifications, were generally well-tolerated
377 and there appears to be modest freedom in the side-chain of this position. This makes the side
378 chain a good candidate for further investigations of structure-activity relationships as well as a
379 good region to label with an imagine modality.
380
381 **Effect of additional substitutions in position 6 on PAR4-AP-mediated signalling**
382 **responses.** Through our initial investigations into position 6 substitutions, we observed that
383 replacement of phenylalanine[6] with either alanine, D-phenylalanine, or *N*-methyl-
384 phenylalanine had varied effects on PAR4-AP potency and efficacy. Interestingly, while
385 signalling was modulated, we did not observe a loss of activity with any of these substitutions.
386 Previous investigations into position 6 substitutions in the native tethered ligand (GYPGQV)
387 revealed the requirement for an aromatic residue, as substitution with non-aromatic residues
388 such as lysine or ornithine significantly decreased or abolished the activity of the peptide
389 (Faruqi et al., 2000). In addition to being an aromatic residue, phenylalanine is a hydrophobic

390 residue so we investigated the impact of altering the hydrophobicity/hydrophilicity and stericity
391 while maintaining an aromatic residue (Fig. 7, Table 1).
392
393 First, we investigated the effect of polar changes that decrease hydrophobicity. Substitution of
394 phenylalanine[6] with tyrosine results in the addition of a hydroxyl group to position 6
395 (AYPGK**Y**-NH_2). We observed partial agonism of calcium signalling with no significant
396 change in potency compared to the PAR4-AP (AYPGK**Y**-NH_2, EC_{50} = 5.2 ± 1.0 μM).
397 Interestingly, the peptide was able to recruit β-arrestins at least as well as the PAR4-AP (β-arr-
398 1 120.5 ± 12.5%; β-arr-2 109.9 ± 11.4%). Further increasing polarity through substitution with
399 4-fluoro-L-phenylalanine, caused significant impairment of agonist activity, both decreasing
400 calcium signalling and significantly decreasing β-arrestin recruitment [AYPGK-**F(4-fluoro)**-
401 NH_2, calcium EC_{50} = *n.d.,* β-arr-1 25.2 ± 6.5%; β-arr-2 41.3 ± 5.9%]. The results of these two
402 substitutions suggest that altering the polarity, while maintaining aromaticity, in position 6
403 reduces efficacy (Hoffmann et al., 2019). Since decreasing hydrophobicity did not increase
404 PAR4-AP activity, we next investigated alterations that increase stericity and hydrophobicity.
405 Substitution with 4-methyl-L-phenylalanine reduced the efficacy of the PAR4-AP to a partial
406 agonist for both calcium signalling and β-arrestin recruitment [AYPGK-**F(4-Me)**-NH_2 calcium
407 EC_{50} = 9.4 ±3.0 μM, β-arr-1 56.4 ± 1.2%; β-arr-2 63.2 ± 1.1%]. Given these results, we wanted
408 to assess the pharmacological impact of substituting phenylalanine with (1-naphthyl)-L-alanine
409 (1Nal) and (2-naphthyl)-L-alanine (2Nal) which not only increase hydrophobicity but also have
410 a modest increase in steric bulk and π-stacking potential. Substitution of phenylalanine[6] with
411 (1-naphthyl)-L-alanine (1Nal; AYPGK-**1Nal**-NH_2) generated a partial agonist for both calcium
412 signalling (EC_{50} = 9.6 ±1.9 μM) and β-arrestin recruitment (β-arr-1 77.5 ± 2.3%; β-arr-2 64.1
413 ± 2.0%) compared to PAR4-AP. Notably, substitution to (2-naphthyl)-L-alanine (2Nal;
414 AYPGK-**2Nal**-NH_2), which differs in orientation compared to (1-naphthyl)-L-alanine such that
415 the alkyl chain is connected to position 2 of naphthyl group (instead of position one as in 1Nal),
416 restored potency of the peptide to the levels observed with PAR4-AP. AYPGK-**2Nal**-NH_2 was
417 an equipotent agonist for calcium signalling (EC_{50} = 11.1 ± 2.3 μM) and β-arrestin recruitment
418 (β-arr-1 77.0 ± 7.0%; β-arr-2 91.6 ± 6.4%). Together, these results indicate that there is a
419 balance needed between hydrophobicity, stericity, and side chain positioning in the C-terminal
420 residue.
421
422 **Probing antagonism of PAR4-AP-stimulated calcium signalling by calcium signalling null**
423 **peptides.** The failure of some substituted peptides to stimulate calcium signalling could reflect
424 either a failure to bind or a loss of efficacy. To determine if such peptides can act as antagonists
425 of PAR4-AP stimulated calcium signalling, we pre-incubated HEK293 cells stably expressing
426 PAR4-YFP prior to stimulation with PAR4-AP. Pre-treatment and competition with 100 μM
427 of calcium null peptides were largely unable to affect the calcium response elicited by 30 μM
428 PAR4-AP (AYPGKF-NH_2) compared to vehicle treated controls. Interestingly, two calcium
429 null peptides with substitution in position 3 or 4 were able to decrease calcium signals elicited
430 by PAR4-AP. Calcium signalling reached a mean of 20.8 ± 1.3% of A23187 (3 μM) in response
431 to 30 μM AYPGKF-NH_2. Signalling in response to AYPGKF-NH_2 thus was significantly

432 reduced following pre-treatment with AY-**Nip**-GKF-NH_2 (10.6 ± 0.9% of A23187; $p<0.05$) or
433 AYP-**Sar**-KF-NH_2 (13.0 ± 1.5% of A23187; $p<0.05$) (Fig. 8).
434
435 **PAR4-dependent calcium signalling is $G\alpha_{q/11}$-dependent.** In order to verify that PAR4
436 dependent calcium signalling was $G\alpha_{q/11}$-dependent, HEK293 cells stably expressing PAR4-
437 YFP were stimulated with 100 µM AYPGKF-NH_2 following pre-incubation with selective
438 $G\alpha_{q/11}$-inhibitor YM254890. YM254890 inhibited AYPGKF-NH_2-stimulated calcium
439 signalling in a concentration-dependent manner, with complete inhibition observed at 100 nM
440 YM254890. The control vehicle (0.001% DMSO) had no effect on calcium signalling (Fig. 9).
441
442 **Calcium signalling-null peptides do not activate MAPK signalling.** Activation of G-protein
443 and β-arrestin pathways downstream of GPCRs often converge on the activation of the p44/42
444 MAP kinase-signalling pathway (Jean-Charles et al., 2017). We therefore monitored
445 phosphorylation of p44/42 MAPK in response to the 37 AYPGKF-NH_2 derivative peptides.
446 HEK293 cells, stably expressing PAR4-YFP, were incubated with control vehicle (0.001%
447 DMSO), 100 µM of AYPGKF-NH_2, or derivative peptides (100 µM) for 10 minutes. Data were
448 normalized as a ratio of phosphorylated-p44/42 (p-p44/42) to total-p44/42 (p44/42).
449 Interestingly, we find that most peptides that were unable to stimulate calcium signalling were
450 also unable to activate p44/42 MAPK signalling (*i.e.* A**y**PGKF-NH_2, AY**p**GKF-NH_2, **(*N*-Me-**
451 **S)**-YPGKF-NH_2, **Inp**-YPGKF-NH_2, **Sar**-YPGKF-NH_2, AY-**Nip**-GKF-NH_2, AYP-**Sar**-KF-
452 NH_2). Similarly, peptides that perform as partial agonists of $G\alpha_{q/11}$-mediated calcium signalling
453 were also partial agonists for p44/42 phosphorylation. Several peptides were able to cause a
454 significantly greater increase in phosphorylation compared to the parental peptide (*i.e.* **Nle**-
455 YPGKF-NH_2, AYPG**O**F-NH_2, AYPG-**(N_ε-Me-K)**-F-NH_2, AYPG-**Cit**-F-NH_2, AYPGK**Y**-
456 NH_2, AYPGK-**1Nal**-NH_2,) (Fig. 10, Table 1).
457
458 **PAR4-mediated MAPK signalling is $G\alpha_{q/11}$-dependent and β-arrestin independent.**
459 In order to further probe the contribution of different pathways downstream of PAR4 to p44/42
460 phosphorylation, we examined the effective of blocking $G\alpha_{q/11}$-signalling with the specific
461 antagonist YM254890 and examined the role of β-arrestins using a β-arrestin-1/-2 double
462 knockout HEK293 cell derived by CRISPR/Cas9 mediated targeting (Supp. Fig. 3). Pre-
463 treatment of PAR4-YFP HEK293 cells with 100 nM YM254890 for 20 minutes abolished
464 PAR4-AP (30 µM) stimulated activation of MAP kinase signalling and subsequent
465 phosphorylation of p-p44/42 at five minutes time (Fig. 11 A.). In contrast, there was no
466 significant difference in the phosphorylation of p44/42 MAPK between wild-type HEK293 and
467 β-arrestin-1/-2 knockout HEK293 cells stimulated with 30 µM PAR4-AP for 0-90 minutes
468 (Fig. 11 B.).
469
470 **Homology modelling of PAR4 and *in silico* docking of AYPGKF-NH_2.** In order to gain a
471 better understanding of the ligand-binding pocket in PAR4 we turned to homology modelling
472 and *in silico* docking experiments. A homology model of PAR4 was generated using known
473 coordinates of thermostabilized human PAR2 crystal structure in complex with AZ8838 (2.8Å
474 resolution, 5NDD.pdb, Cheng et al., 2017). Sequences of human PAR4 were aligned with the

475 structure-resolved residues of PAR2 using Clustal Omega (Madeira et al., 2019; Sievers et al.,
476 2011). We generated a homology model of wild-type PAR2 on the PAR2 structure, which
477 contained modifications necessary for crystallization. Twenty human PAR4 homology models,
478 using the wild-type human PAR2 model as a template, were generated in MODELLER (Webb
479 and Sali, 2014). The PAR4 model with the lowest discrete optimized protein energy (DOPE)
480 score was utilized for *in silico* analyses.
481
482 Docking AYPGKF-NH_2 to the PAR4 homology model (GalaxyPepDock; Lee et al., 2015)
483 revealed a number of highly predicted peptide-receptor interaction sites (Fig. 12 A.; Ser^{67},
484 Tyr^{157}, His^{229}, Asp^{230}, Leu^{232}, Leu^{234}, Asp^{235}, Ala^{238}, Gln^{242}, His^{306}, Tyr^{307}, Pro^{310}, Ser^{311}, Ala^{314},
485 Gly^{316}, Tyr^{319}, and Tyr^{322}). Of these, the most frequently predicted interactions were receptor
486 residues His^{229}, Asp^{230}, and Gln^{242}. In peptide-docked models, Gln^{242} made contact with
487 alanine, tyrosine, and lysine, with the most frequent prediction being with phenylalanine. His^{229}
488 was predicted to interact with lysine and phenylalanine. Asp^{230} was frequently predicted to
489 interact with lysine and phenylalanine and contacts with lysine appeared in 60% of predictions
490 (Fig. 12 B.). Interestingly, when visualizing receptor residues predicted to interact with the
491 peptide, we found that a large number of these residues were localized on extracellular loop 2
492 (ECL2) (Fig. 12 A. and B.).
493
494 **Calcium signalling and β-arrestin recruitment to predicted peptide binding-site mutant-**
495 **PAR4.** To experimentally examine *in silico* predictions, site-directed mutagenesis was
496 performed introducing alanine substitutions at the three most highly predicted interacting
497 residues, His^{229}, Asp^{230}, and Gln^{242}. Additionally, we generated a double mutation, $PAR4^{H229A,}$
498 ^{D230A}, to determine if combined loss of His^{229} and Asp^{230} would result in additive detriment to
499 receptor activation. We evaluated the functional consequences of these mutations by recording
500 calcium signalling in response to AYPGKF-NH_2 with all mutants. We observed no calcium
501 response in cells expressing $PAR4^{D230A}$-YFP or $PAR4^{H229A, D230A}$-YFP mutant receptors up to
502 300 μM AYPGKF-NH_2 (Fig. 13 A.). Similarly, peptide induced β-arrestin-1/-2 recruitment to
503 $PAR4^{D230A}$-YFP and $PAR4^{H229A, D230A}$-YFP was significantly reduced compared to the wild-
504 type PAR4. Both $PAR4^{H229A}$ and $PAR4^{Q242A}$ mutations were fully able to recruit β-arrestin-1/-
505 2 to the same levels observed with wild-type PAR4-YFP (Fig. 13 B. and C.).
506
507 To investigate whether these sites are important for tethered ligand activation of the receptor,
508 we stimulated cells expressing wildtype and mutant constructs with thrombin. Thrombin
509 cleavage of the receptor reveals the native tethered ligand, GYPGQV (Xu et al., 1998).
510 Comparable to activation with AYPGKF-NH_2, we observed significantly diminished calcium
511 signalling in HEK293 cells expressing $PAR4^{D230A}$-YFP and $PAR4^{H229A, D230A}$-YFP mutants,
512 even up to 10 units/mL thrombin (Fig. 13 D.). Additionally, β-arrestin-1/-2 recruitment was
513 also impaired to $PAR4^{D230A}$ and $PAR4^{H229A, D230A}$ mutants (Fig. 13 E and F). We observed no
514 appreciable difference in calcium signalling or β-arrestin recruitment when $PAR4^{H229A}$-YFP
515 and $PAR4^{Q242A}$-YFP mutants were stimulated with thrombin, with the exception of a modest
516 decrease in β-arrestin-1 recruitment to $PAR4^{Q242A}$-YFP mutant receptor.
517

518 **Platelet aggregation response to differential activation of PAR4 signalling.** To determine
519 the effects of targeted signalling observed with several peptides we investigated PAR4-
520 mediated platelet aggregation in response to the β-arrestin biased, calcium signalling-null
521 peptide, A**y**PGKF-NH_2, as well as a modestly more potent calcium agonist AYPG**R**F-NH_2
522 (compared to AYPGKF-NH_2). Thrombin (1 unit/mL) and 100 μM AYPGKF-NH_2 were used
523 as controls to ensure successfully washed platelet preparations. In response to thrombin
524 stimulation, we observed a characteristic aggregation trace resulting in 100% aggregation at 1
525 unit/mL. In agreement with previously published data, AYPGKF-NH_2 (100 μM) stimulation
526 resulted in approximately 50% platelet aggregation (Ramachandran et al., 2017). We observed
527 that platelet aggregation was not stimulated by 100 μM A**y**PGKF-NH_2. Interestingly, when
528 platelet preparations were stimulated with AYPG**R**F-NH_2, with which we observed a modest
529 increase in potency in calcium signalling assays, enhanced β-arrestin recruitment, and an
530 increased phosphorylation of p44/42, we observed platelet aggregation response comparable
531 to levels observed with thrombin (1 unit/mL) (Fig. 14).
532
533 **Discussion:**
534 PAR4 is emerging as a novel anti-platelet drug target. Here we examine structure activity
535 requirements for PAR4 activation of calcium signalling, β-arrestin recruitment and MAP
536 kinase activation. PAR cleavage by a number of different enzymes has been reported.
537 Canonically, thrombin has been described as a PAR1 and PAR4 activator while trypsin is
538 described as a PAR2 and PAR4 activator. While PAR3 can be cleaved by thrombin, its ability
539 to act as a signalling receptor remains ambiguous. In each case, cleavage by serine proteases
540 occurs at an arginine-serine site which reveals a unique tethered ligand specific to each PAR
541 (Hollenberg, 2003) - human PAR1- SFLLRNP… (Liu et al., 1991; Vu et al., 1991) , human
542 PAR2- SLIGKV… (Al-Ani et al., 2002; Nystedt et al., 1994) and human PAR4- GYPGQV…
543 (Kahn et al., 1998; Xu et al., 1998). While these tethered ligand sequences are diverse, they
544 retain some highly conserved properties including a highly conserved charged residue in
545 position five of the revealed tethered-ligand-mimicking peptide (arginine in PAR1; lysine in
546 PAR2). Additionally, PAR2 and PAR4 have a conserved glycine in position three and valine
547 in position six. The similarities of the proteolytically-revealed tethered ligands is observed in
548 the optimized tethered-ligand-mimicking synthetic agonist peptides. Hydrophobic residues
549 leucine, isoleucine, and proline are preferred in position three of PAR1, PAR2, and PAR4
550 agonist peptides, respectively. Additionally, there is a basic residue in position five of the
551 tethered ligand peptide in all three receptors (arginine in PAR1 and PAR2 and lysine in PAR4
552 activating peptides). These conserved residue properties highlight some of the key
553 requirements that a PAR4 agonist peptide must meet. Previous structure-activity work starting
554 with the proteolytically revealed sequences of human (GYPGQV) and murine (GYPGKF)
555 PAR4 identified the hexapeptide AYPGKF-NH_2 or SYPGKF-NH_2 to be potent and selective
556 agonists for PAR4 (Faruqi et al., 2000). In this study we started with the hexapeptide AYPGKF-
557 NH_2, as our parental peptide agonist, and incorporated various modifications at each of the six
558 positions in this peptide to investigate determinants of agonist-induced PAR4-coupling to
559 $G\alpha_{q/11}$, MAP kinase and β-arrestin-1/-2 recruitment to guide development of biased agonists
560 of PAR4.

561
562 Previously, it was demonstrated that substitution of alanine or serine in position one of the
563 GYPGKF-NH_2 activating peptide was sufficiently able to trigger tritiated inositol 1,4,5-
564 triphosphate release comparable to levels observed with thrombin activation and much higher
565 than release caused by the GYPGKF-NH_2 (Faruqi et al., 2000). Interestingly, substitution of
566 position 1 with threonine was reported to significantly reduce the potency of the activating
567 peptide (Faruqi et al., 2000). In keeping with results from previous studies, we find a
568 requirement for small aliphatic side chains in position 1 of PAR4 activating peptides, with
569 substitutions that increased bulk in this position consistently resulting in poor agonists for both
570 calcium signalling and β-arrestin recruitment (*N*-Me-A Fig. 3; *N*-Me-S, Aib, Inp, V, Nle – Fig
571 4; Table 1). Additionally, we observed that both stereochemical inversion of L-alanine to D-
572 alanine (D-alanine, Fig. 2) and backbone elongation (betaAla., Fig. 4) were detrimental to both
573 calcium signalling and β-arrestin recruitment. Additionally, we observed that capping of N-
574 terminal charge via acetylation significantly decreases agonist potency. Together these results
575 indicate that positive charge and the localization of that charge in addition to precise side-chain
576 positioning at position 1 are critical to effective PAR4-agonism.
577
578 The aromatic sidechain, and to a lesser extent the hydroxyl group, of the tyrosine[2] residue of
579 the parental peptide also proved to be important for peptide activity with alanine or D-isomer
580 substitutions resulting in decreased activity of all pathways investigated. These results are
581 consistent with previous findings that replacement of tyrosine with other aromatic residues,
582 such as phenylalanine, significantly reduced both specificity and potency of the activating
583 peptide (Faruqi et al., 2000). Interestingly, substituting L-tyrosine[2] for either D-tyrosine (Fig.
584 2 A., Fig. 10) or *N*-methyl-tyrosine (Fig. 3 A. & 10) resulted in loss of calcium and p44/42
585 signalling, but had more modest effects on β-arrestin recruitment (Fig, 2 B. & C., Fig. 3 B. &
586 C., respectively; Table 1). Also, substitution of tyrosine with either 4-fluoro-phenylalanine or
587 *O*-methyl-tyrosine did not significantly affect calcium, p44/42 phosphorylation or β-arrestin
588 recruitment in comparison to AYPGKF-NH_2 (Fig. 5 & 10; Table 1). Our findings, together
589 with previous reported data (Faruqi et al., 2000), suggest the necessity of an aromatic residue
590 in position 2 to maintain agonist potency. Further, our data reveal that backbone orientation in
591 position 2 is a key determinant of agonist potency. Future experiments fine-tuning the aromatic
592 substituents may be beneficial for peptide analogue development.
593
594 Our data reveal that alterations affecting proline conformation or glycine residue compactness
595 were not well-tolerated resulting in decreased calcium signalling, p44/42 MAP kinase
596 signalling, and β-arrestin recruitment to PAR4. Calcium signalling has previously been
597 reported to be negatively impacted by alterations to either of these two residues (Faruqi et al.,
598 2000). Both proline and glycine residues are frequently found in β-turns and these data support
599 the notion that the conformation (proline[3] and glycine[4]) and rigidity (proline[3]) of PAR4
600 agonists enabled by these residues is important for activity. To test this hypothesis further, we
601 made several substitutions in position 3 (proline) aimed at evaluating favoured backbone
602 conformations. We observed that a return to a predominantly trans-amide conformation by
603 substitution of proline with alanine (Fig. 1), results in decreased potency in all pathways

604 studied. Interestingly, this substitution did not abolish signalling but did significantly decrease
605 agonist potency, which suggests that the backbone conformation of proline may be necessary
606 for potency but not efficacy. Substitution of proline to pipecolic acid (Pip., Fig. 5), which has
607 a similar peptide backbone orientation to proline with a six-membered aromatic ring, decreased
608 β-arrestin recruitment with only a modest decrease in calcium signalling activation.
609 Interestingly, substitution of proline with nipecotic acid (Nip., Fig. 5) abolished calcium
610 signalling and p44/42 phosphorylation and also decreased β-arrestin recruitment. Nipecotic
611 acid is similar to pipecolic acid with the exception that nipecotic acid changes the direction of
612 the peptide backbone compared to that adopted by proline, while pipecolic acid favours a
613 similar backbone directionality and conformation similar to proline. Interestingly, we observed
614 a similar pharmacological profile observed with AY-**Nip**-GKF-NH_2 when we substitute D-
615 proline in position 3, which also changes the backbone orientation of the parental peptide.
616 These data demonstrate that the backbone conformation provided by proline in position 3 of
617 the parental peptide or by pipecolic acid substitution is necessary for agonism of PAR4
618 signalling pathways. Further, substitution of a proline[3] with alanine (AY**A**GKF-NH_2, Fig. 2)
619 significantly and detrimentally altered the pharmacological profile compared to the parental
620 peptide PAR4-AP, perhaps indicating that agonist competency contributed by position 3 is
621 largely conformational not chemical. Substitution of sarcosine or beta-alanine at position 4 also
622 negatively affected all signalling pathways, while substitution of glycine[4] with alanine resulted
623 in a rightward shift in potency with calcium signalling and a reduction of β-arrestin recruitment.
624 Together these substitutions reveal the necessity of a small flexible residue in position 4,
625 consistent with previous reports (Faruqi et al., 2000).
626
627 It has been previously demonstrated that substitution of position 5 glutamine in the native
628 tethered ligand (GYPGQV), with arginine or ornithine, resulted in decreased potency in the
629 PAR4 agonist peptide for calcium signalling pathways (Faruqi et al., 2000). However, there is
630 a basic residue found in position 5 of PAR1 (arginine, TFLL**R**), PAR2 (arginine, SLIG**R**L),
631 and PAR4 (lysine, AYPG**K**F) tethered-ligand mimicking peptides. Given the conservation of
632 charged residues in position 5 of PAR tethered-ligand mimicking peptides, we generated
633 PAR4-AP derivative peptides with lysine[5] substitutions that maintained or altered charge in
634 this position to determine if this is a requirement for activity at PAR4. Substitution of lysine[5]
635 with alanine had no appreciable effect on calcium or MAP kinase signalling, while resulting in
636 decreased β-arrestin recruitment (Fig. 1). Substitution of L-lysine[5] with D-lysine, however,
637 significantly reduced potency and efficacy in calcium signalling and β-arrestin recruitment and
638 did not stimulate MAP kinase signalling (Fig. 2). We continued our exploration of the position
639 with N_α-methyl-lysine substitution, which increases steric bulk through the addition of a methyl
640 group to the backbone, while also removing a hydrogen bond donor and increasing the amount
641 of peptide in the cis-transformation of the amide bond between position 4 and 5. We found this
642 substitution detrimental to calcium signalling but advantageous for β-arrestin recruitment,
643 resulting in saturated and comparable levels of recruitment than those observed with PAR4-AP
644 but at lower concentrations than PAR4-AP (Fig. 3). Thus, backbone conformation and bulk at
645 position 5 is important for agonism of calcium signalling and MAP kinase activation, while
646 perhaps being an important site for modification in the search for β-arrestin biased ligands.

647
648 We next turned our attention to analogues that resemble the side chain of lysine[5] with a specific
649 interest on structure-activity as well as ascertaining the importance of charge in this residue. In
650 contrast to what was observed with substitutions to the tethered-ligand that mimicked the native
651 tethered ligand, we find that both calcium signalling and β-arrestin recruitment were not
652 significantly impacted by substitution to ornithine, which decreases steric bulk and shortens
653 the distance between the backbone and the positively charged amine compared to lysine
654 (AYPG**O**F-NH_2; Fig. 6). Interestingly, however, we observed significantly increased p44/42
655 phosphorylation in response to AYPG**O**F-NH_2 stimulation (Fig. 10). This is somewhat
656 puzzling since we find p44/42 phosphorylation to be $G\alpha_{q/11}$-dependent (Fig. 11); however, it
657 is important to note that MAP kinase and other cellular signalling pathways downstream of
658 receptor activation are subject to amplification/deamplification processes within the cell
659 (Chidiac, 2016) and these observations may point to additional differences in signalling
660 stimulated by this peptide that needs to be examined. We further probed stericity in this position
661 through increasing bulk with substitution of lysine[5] with arginine (AYPG**R**F-NH_2).
662 Interestingly, this substitution also results in a delocalization of charge compared to the charge
663 on the lysine[5] side chain. This modification provided a similar calcium signalling profile
664 compared to that observed with ornithine substitution, however, resulted in a significant
665 increase of β-arrestin recruitment compared to the parental PAR4-AP. Interestingly, there was
666 no significant change in p44/42 phosphorylation like that observed with ornithine substitution.
667 Another peptide with increased steric bulk, N_ε-methyl-lysine substitution in position 5,
668 improved calcium signalling potency, modestly improved β-arrestin recruitment, and
669 significantly increased p44/42 phosphorylation [AYPG-**(N_ε-Me-K)**-F-NH_2, Fig. 6]. We further
670 investigated whether charge was a significant determinant of agonism by substituting lysine[5]
671 with citrulline (AYPG-**Cit**-F-NH_2), which lacks charge but retains a similar structure compared
672 to arginine and, to a lesser extent, lysine. We observed decreased calcium, equivalent β-arrestin
673 recruitment, and significantly increased p44/42 phosphorylation compared to the parental
674 peptide (Fig. 6 & 10). Together these data reveal that changes to side chain charge, bond
675 donors/acceptors, and steric bulk result in varied pharmacological responses that may be
676 exploited to bias signalling responses in favour of β-arrestin recruitment (AYPG**R**F-NH_2) or
677 p44/42 phosphorylation (AYPG**O**F-NH_2; AYPG-**(N_ε-Me-K)**-F-NH_2) with modest
678 improvements to potency in calcium signalling. Interestingly, we observed that charge is not
679 required for activation of some pathways as alanine and citrulline substitutions resulted in
680 agonism of PAR4.
681
682 Finally, our structure-activity investigation turned to position 6, phenylalanine, of the parental
683 peptide. Given the significant impact that alterations to position 2 (tyrosine) had on agonist
684 potency, we predicted that there may be a pi-pi (π-π) stacking interaction between tyrosine and
685 phenylalanine which is supported by the backbone kink provided by proline in position 3.
686 Substitution of position 6 with alanine or D-phenylalanine reduced calcium signalling potency
687 while reducing β-arrestin recruitment and p44/42 phosphorylation. These alterations suggest
688 that phenylalanine in position 6 is not essential for PAR4 activation by agonist peptide but is
689 important for agonist potency and full activation of all signalling pathways. Methylation of the

690 backbone nitrogen in phenylalanine (AYPGK-**(*N*-Me-F)**-NH_2) resulted in improved activation
691 of calcium signalling, β-arrestin recruitment, and p44/42 phosphorylation compared to
692 AYPGKF-NH_2 (Fig. 3). Addition of either methyl (AYPGK-**F(4-Me)**-NH_2; Fig. 7), fluorine
693 (AYPGK-**F(4-fluoro)**-NH_2; Fig. 7), or hydroxyl (AYPGK**Y**-NH_2; Fig. 7) off of the *para*-
694 position of the aromatic side chain of phenylalanine was deleterious to all signalling pathways
695 studied. Substitution of unnatural residues that increase the size of steric bulk and π-stacking
696 potential yielded mixed results based on the orientation of the naphthyl. Substitution of
697 phenylalanine with (1-naphthyl)-L-alanine (1Nal) increased p44/42 phosphorylation but
698 decreased both calcium signalling and β-arrestin recruitment (Fig. 7). Changing the alkyl chain
699 connection from position 1 to position 2 of the naphthyl (AYPGK-2Nal-NH_2; Fig 7) resulted
700 in activation similar to AYPGKF-NH_2. With (2-naphthyl)-L-alanine showing some flexibility
701 in the steric bulk of position 6, it would be interesting for future work to investigate increasing
702 the π-stacking potential at position 2 while simultaneously increasing the π-stacking potential
703 at position 6, since we hypothesize that these two residues' aromatic regions of the PAR4-AP
704 may interact.
705
706 To determine if any of the calcium signalling-null peptides were able to act as antagonists, cells
707 were pre-treated with calcium null peptides and subsequently stimulated with AYPGKF-NH_2
708 to see if the parental peptide was able to still elicit a signal. We observed that both AY-**Nip**-
709 GKF-NH_2 and AYP-**Sar**-KF-NH_2 were both able to significantly decrease the calcium signal
710 elicited by PAR4-AP (Fig. 8). Interestingly, both substitutions resulted in ablation of both
711 calcium and p44/42 signalling as well as significantly decreasing β-arrestin recruitment. These
712 results may indicate that targeting PAR4 with small molecules mimicking position 3 and 4
713 dipeptides may provide a starting place for the design of novel PAR4 antagonists. Additionally,
714 peptides that further explore modifications to position 3 and 4 could be investigated for potent
715 PAR4 antagonists.
716
717 In platelets, it has previously been demonstrated that PAR4-mediated calcium mobilization
718 induces activation and aggregation (Edelstein et al., 2014; Holinstat et al., 2006). Both
719 thrombin and AYPGKF-NH_2 initiated PAR4-dependent platelet aggregation to levels
720 comparable to those previously reported in the literature in the same rat platelet system
721 (Ramachandran et al., 2017). As was hypothesized, we observed that stimulation of washed
722 platelet samples with a calcium signalling null, β-arrestin biased peptide, A**y**PGKF-NH_2 (100
723 μM) did not stimulate platelet aggregation (Fig. 14). Further, stimulation of washed platelets
724 with the agonist peptide, AYPG**R**F-NH_2 (Fig. 6), enhanced platelet aggregation to levels
725 comparable to those observed with thrombin activation of PAR4 (Fig. 14). AYPG**R**F-NH_2
726 stimulates calcium signalling to levels comparable to that seen with AYPGKF-NH_2 but triggers
727 more β-arrestin-1 recruitment than the parental peptide. These data suggest that calcium
728 signalling is essential for triggering platelet activation, but arrestin recruitment may also play
729 a role.
730
731 Having ascertained some of the governing peptide residue characteristics enabling PAR4
732 activation and validated their signalling consequences in an *ex vivo* system, we turned our

733 attention to investigating the binding site of the receptor. The extracellular loops of many
734 GPCRs have been demonstrated to be important facilitators of ligand entry into the orthosteric
735 site, with ECL2 possessing the most diversity in sequence and structure (Venkatakrishnan et
736 al., 2014; Woolley and Conner, 2017). Analysis of common mechanisms of GPCR ligand
737 interaction derived from crystal structure and biochemical experiments reveal a possible role
738 of ECL2 secondary loop in binding and facilitating entry, while the diversity of residue
739 sequences across class A GPCRs is thought to confer their ligand specificity (Venkatakrishnan
740 et al., 2014; Woolley and Conner, 2017). In many class A GPCRs, a disulfide bond between
741 ECL2 and a transmembrane 3 cysteine ($Cys^{3.25}$, Ballesteros-Weinstein numbering) is thought
742 to stabilize the extracellular topology such that ligand recognition at ECL2 and subsequent
743 orthosteric binding can occur (Wheatley et al., 2012). All PAR receptors possess this canonical
744 TM3 $Cys^{3.25}$ (PAR1 $Cys175^{3.25}$, PAR2 $Cys148^{3.25}$, PAR3 $Cys166^{3.25}$, PAR4 $Cys149^{3.25}$) and
745 residues adjacent to this conserved cysteine are important for ligand binding and receptor
746 activation. Investigations into the role of PAR ECL2 domains have previously demonstrated
747 that all PAR receptors possess a homologous CHDxL motif (…CHDVL… - $PAR1^{C254\text{-}L258}$ and
748 $PAR2^{C226\text{-}L230}$; …CHDVH… $PAR3^{C245\text{-}L249}$ …CHDAL; … $PAR4^{C226\text{-}L230}$) in their ECL2 (Al-
749 Ani et al., 1999; Xu et al., 1998). Given that the activating peptides of PAR1 and PAR2 (Al-
750 Ani et al., 1999; Lerner et al., 1996) are similar (SFLLRN, PAR1; SLIGRL, PAR2),
751 additionally studies were conducted that revealed that ligand specificity is conferred by acidic
752 residues distal to the CHDxL motif (PAR1, $N^{259}ETL^{261}$; PAR2 $P^{231}EQL^{234}$; (Gerszten et al.,
753 1994; Lerner et al., 1996; Nanevicz et al., 1995). Interestingly, the equivalent human PAR4
754 ECL2 residues distal to the CHDAL domain, $P^{233}LDA^{236}$, share sequence homology with those
755 distal to the human PAR2 CHDVL domain ($P^{231}EQL^{234}$), both of which contain an acidic
756 residue. Al-Ani *et al.* (1999) demonstrated that glutamic acid residues in the rat PAR2 ECL2
757 (PEEVL) conferred specificity to PAR2 ligands. In previous studies, a series of aspartic acids
758 in the PAR4 extracellular loop 2 (ECL2) and amino terminal (N)-tail were proposed to be key
759 for thrombin binding to PAR4 (Nieman, 2008; Nieman and Schmaier, 2007; Sánchez Centellas
760 et al., 2017). Mutations of ECL2 aspartic acid residues $D^{224}A$, $D^{230/235}A$ (double mutation), and
761 $D^{224/230/235}A$ mutants were all sufficiently able to decrease thrombin cleavage of PAR4 and
762 activation in yeast models (Sánchez Centellas et al., 2017). Further, the activity of PAR4
763 agonist peptide AYPGKF-NH_2 was also abolished in PAR4 mutants lacking ECL2 single
764 mutant D224A, double mutant $D^{230/235}A$, or triple mutant $D^{224/230/235}A$ aspartic acid mutations
765 to alanine which the authors posit indicates that these aspartic acid residues may be important
766 for both agonist peptide and tethered ligand bindings and activation of PAR4. The $D^{230/235}A$
767 mutation to alanine removed two acidic residues in the highly conserved …$CHD^{230}AL$ domain
768 (PAR1 Asp^{256}; PAR2 Asp^{228}) as well as the homologous $PLD^{235}A$… specificity conferring
769 domain observed in PAR1 (Glu^{260}) and PAR2 (Glu^{232}) making it difficult to assess whether the
770 loss of cleavage and activation is due to the $CHD^{230}AL$ or $PLD^{235}A$ aspartic acid.
771
772 In the present study, *in silico* docking to a homology model of PAR4 revealed 17 predicted
773 sites of interaction with AYPGKF-NH_2 (Ser^{67}, Tyr^{157}, His^{229}, Asp^{230}, Leu^{232}, Leu^{234}, Asp^{235},
774 Ala^{238}, Gln^{242}, His^{306}, Tyr^{307}, Pro^{310}, Ser^{311}, Ala^{314}, Gly^{316}, Tyr^{319}, Tyr^{322}; Fig. 12 A.).
775 Interestingly, these predicted sites reveal residues that have been shown to or predicted to have
776 a role in PAR4 activation by thrombin or agonist peptide including aspartic acid residue Asp^{230}

found in the highly conserved CHDxL domain in PARs as well as Asp^{235} in the downstream region that is homologous to the specificity conferring motif found in PAR1 and PAR2 (Sánchez Centellas et al., 2017). Additionally, a previous *in silico* docking experiment revealed a role for aspartic acid and histidine in this motif in binding of AYPGKF-NH_2 to PAR4 (Moschonas et al., 2017). We generated mutations of the most frequently predicted interaction sites (His^{229}, Asp^{230}, Gln^{242}, His^{229}/Asp^{230}) to alanine which revealed that Asp^{230} is essential for interaction of the peptide with the receptor and activation as mutation to alanine abolished calcium signal potentiation as well as β-arrestin recruitment. Interestingly, these results were consistent with both peptide agonist AYPGKF-NH_2 as well as with thrombin stimulated activation of PAR4, which agrees with previous reports of the importance of these sites while also elucidating the importance of the conserved $CHD^{230}AL$ motif in PAR4 activation, consistent with the role of this domain in PAR1 and PAR2 (Al-Ani et al., 1999; Blackhart et al., 1996; Gerszten et al., 1994; Lerner et al., 1996; Nanevicz et al., 1995; Sánchez Centellas et al., 2017). Another highly predicted residue belonging to the CHDAL domain, His^{229}, when mutated to alanine did not alter the ability of either AYPGKF-NH_2 or the tethered ligand as revealed by thrombin to activate calcium signalling or β-arrestin recruitment pathways. Further, we observe that a double mutation of both of these sites to alanine (H229A, D230A) did not result in any additive detriment to PAR4 activation; therefore, we conclude that Asp^{230} interaction with PAR4 peptide and tethered ligand agonist performs an essential role in activation of PAR4.

Finally, in the context of platelet activation we find that our modified peptides that are able to cause a greater level of calcium signalling and β-arrestin recruitment than PAR4-AP also trigger more platelet aggregation. In our hands, PAR4-AP was never able to elicit greater than 50% of the aggregation seen with 1 unit/mL of thrombin, while the peptide AYPG**R**F-NH_2 was able to trigger aggregation comparable to that seen with thrombin. A role for PAR4 dependent calcium signalling is well established (Edelstein et al., 2014; French and Hamilton, 2016; Tourdot et al., 2018), and consistently our calcium signalling null peptide A**y**PGKF-NH_2 failed to activate platelets. A role for β-arrestin mediated PAR4 signalling in platelets has also been demonstrated (Khan et al., 2014; Ramachandran et al., 2017). Together these data suggest that calcium signalling is critical for initiating PAR4 mediated platelet aggregation, but the precise role hierarchy of the different PAR4 signalling pathways in platelet responses remains to be fully established.

In summary, these studies identify key mechanisms involved in PAR4 activation and signalling. We also present and characterize a novel toolkit of PAR4 agonist peptides that could be used to study biased signalling through PAR4 in platelets as well as other physiological systems. We further show that platelet activation by PAR4 critically depends on the $G\alpha_{q/11}$ pathway, and selective targeting of this pathway might yield a useful anti-platelet agent. Overall, our work advances our understanding of agonist binding to PAR4 and will support future efforts aimed at defining signalling contribution in homeostatic signalling and the discovery of novel therapeutics targeting PAR4.

819 **Materials and Methods:**
820 All chemicals were purchased from Millipore-Sigma (Burlington, Massachusetts, United
821 States), Thermo Fisher Scientific (Hampton, New Hampshire, United States), or BioShop
822 Canada Inc. (Burlington, Ontario, Canada) unless otherwise stated. AYPGKF-NH_2 was
823 purchased from and synthesized by Genscript (Piscataway, New Jersey, United States).
824 Thrombin from human plasma was obtained from Millipore-Sigma (Cat. # 605195, 5000 units;
825 Burlington, Massachusetts, United States).
826
827 ***Molecular Cloning and Constructs.*** The plasmid encoding PAR4-YFP was described
828 previously (Ramachandran et al., 2017). Plasmid DNA mutations in the predicted orthosteric
829 binding site of PAR4 were generated using the QuikChange XL Multi Site-Directed
830 Mutagenesis Kit (Agilent Technologies, Mississauga, ON, Canada) to generate all mutants
831 described in this study. All constructs were verified by sanger sequencing (Robarts DNA
832 sequencing facility, University of Western Ontario). β-arrestin-1/-2-rluc constructs were a kind
833 gift from Michel Bouvier (Université de Montréal). PX458 vector for CRISPR/Cas9 targeting
834 was a kind gift from Feng Zhang (Massachusetts Institute of Technology; Addgene # 48138)
835 *Site-directed mutagenesis of predicted PAR4 receptor-peptide interaction sites.* Site-directed
836 mutagenesis using Agilent QuikChange-XL was undertaken to generate mutations in highly
837 predicted receptor residues to validate GalaxyPepDock model and determine key binding site
838 residues for the native PAR4 tethered ligand and PAR4 agonist peptide AYPGKF-NH_2.
839 Residues were mutated by single-nucleotide substitutions replacing native residues with
840 alanine. Successful mutations were confirmed by DNA sequencing (London Regional
841 Genomics Centre, London, ON).
842
843 ***Cell Lines and Culture Conditions.*** All media and cell culture reagents were purchased from
844 Thermo Fisher Scientific (Hampton, New Hampshire, United States). HEK-293 cells (ATCC;
845 Manassas, Virginia, United States) and CRISPR/Cas9 HEK-293 β-arrestin double knockout
846 (β-arr knockout) cell lines were maintained in Dulbecco's modified Eagle's medium
847 supplemented with 10% fetal bovine serum, 1% sodium pyruvate, and 1% streptomycin
848 penicillin. Cells stably transfected with PAR4-YFP vector was routinely cultured in the above
849 media supplemented with 600 µg/mL G418 sulfate (Geneticin; ThermoFisher Scientific
850 Waltham, Massachusetts, United States). Since trypsin activates PAR4, cells were routinely
851 sub-cultured using enzyme-free isotonic phosphate-buffered saline (PBS), pH 7.4, containing
852 1 mM EDTA followed by centrifugation to remove PBS-EDTA and plated in appropriate
853 culture plates for further experimentation. Cells were transiently transfected with appropriate
854 vectors using a modified calcium phosphate transfection (Nuclease free water, 2.5M $CaCl_2$,
855 and 2x HEPES Buffered Saline). Transient transfections were rinsed with phosphate buffered
856 saline (PBS) 24 hours post-transfection and replaced with growth media. Transiently
857 transfected cells were assayed or imaged at 48 hours post-transfection. *Generation of β-*
858 *arrestin-1/-2 double knockout HEK-293 cells using CRISPR/Cas9*. A β-arrestin-1/-2 double
859 knockout HEK-293 cells cell line (β-arr. knockout) was generated using CRISPR/Cas9
860 mediated gene targeting. Guides sequences targeted to β-arrestin-1 or β-arrestin-2 were
861 designed using the design tool at http://crispr.mit.edu. Gene targeting guides (β-arrestin 1;

862 TGTGGACCACATCGACCTCG, β-arrestin 2; GCGGGACTTCGTAGATCACC, were
863 ligated into the PX458 vector (Kind gift from Dr. Feng Zhang, MIT, Addgene plasmid #48138),
864 verified by direct sequencing and transfected in HEK-293 cells via calcium phosphate
865 transfection (Ferguson and Caron, 2004; Graham and van der Eb, 1973). GFP expressing cells
866 were single-cell selected by flow cytometry (FACSAria III; London Regional Flow Cytometry
867 Facility) into wells of a 96-well plate. Clonal cell populations were expanded and screened by
868 western blot to identify successful knockout (anti-β-arrestin-1/-2 antibody, rabbit mAb D24H9;
869 Cell Signalling Technologies, Danvers, Massachusetts, United States; anti-β-actin antibody,
870 mouse mAb 8H10D10; Cell Signalling Technologies; Supplemental Figure 3).
871
872 ***General Methods for Peptide Synthesis***
873 All reagents were purchased from Sigma-Aldrich, ChemImpex, or Thermo Fisher Scientific
874 and used without further purification. Peptides were synthesized using standard Fmoc-solid
875 phase peptide synthesis (SPPS) on Rink amide MBHA resin (256 mg, 0.1 mmol, 0.39 mmol/g)
876 with a Biotage® Syrowave™ automated peptide synthesizer (0.4 mmol of HCTU, 0.4 mmol
877 of Fmoc-amino acids, 0.6 mmol of DIPEA, 1 h coupling). Some peptides also involved
878 additional manual synthesis (see procedures below). Following automated and manual
879 synthesis, peptides were cleaved off the resin by being shaken in a cleavage cocktail solution
880 of 95% TFA, 2.5% TIPS, and 2.5% H_2O (4 mL, 5 h), precipitated in ice cold *tert*-butyl methyl
881 ether, lyophilized, purified by preparative RP-HPLC, and further lyophilized to obtain a dry
882 powder. Purity was assessed by analytical RP-HPLC and characterized by mass spectrometry
883 (MS). The analytical RP-HPLC was performed on a system consisting of an analytical Agilent
884 Zorbax SB-C8 column (4.6 x 150 mm, 5 µm), Waters 600 controller, Waters in-line degasser,
885 and Waters Masslynx software (version 4.1). Two mobile phases were used; eluent A (0.1%
886 TFA in acetonitrile) and eluent B (0.1% TFA in MilliQ water). The flow rate was set at 1.5
887 $mLmin^{-1}$ over 10 minutes with an additional 5-minute wash (95% solvent A in solvent B). A
888 Waters 2998 Photodiode array detector (200-800 nm) and an ESI-MS (Waters Quattro Micro
889 API mass spectrometer) were used to monitor the column eluate. The preparative RP-HPLC
890 used the same system, eluents, and detection method as mentioned above for the analytical RP-
891 HPLC, except that a preparative Agilent Zorbax SB-C8 column (21.2 x 150 mm, 5 µm) at a
892 flow rate of 20 $mLmin^{-1}$ was used. The mass spectra for all peptides were determined in positive
893 mode using an ESI ion source on either a Bruker micrOToF II mass spectrometer or a Xevo
894 QToF mass spectrometer (Table S1). All peptides had purity >95% as determined by analytical
895 HPLC (see supplemental information, Figure S1).
896
897 ***Synthesis of Ac-AYPGKF-NH_2.*** The hexapeptide (AYPGKF) was synthesized using the
898 standard automated Fmoc-SPPS discussed in the general methods for peptide synthesis. While
899 still on resin, with all of the side chains protected, and with the N-terminal Fmoc-deprotection
900 completed, the N-terminus of this peptide was acetylated by being shaken in a solution of acetic
901 anhydride and DMF (v/v 1:4, 5 mL, 30 min). Following this, the peptide was cleaved, purified,
902 and analyzed as mentioned in the general methods for peptide synthesis.
903

904 ***Synthesis of Peptides Involving N-methylation of the Peptide Backbone*** Peptides [(*N*-Me-A)-
905 YPGKF-NH_2, (*N*-Me-S)-YPGKF-NH2, A-(*N*-Me-Y)-PGKF-NH2, AYPG-(N_α-Me-K)-F-
906 NH2, and AYPGK-(*N*-Me-F)-NH_2] were synthesized using abovementioned automated Fmoc-
907 SPPS up to the desired amino acid that was *N*-methylated (e.g. KF-resin for AYPG-(N_α-Me-
908 K)-F-NH_2). Following Fmoc-deprotection of the resin-bound N-terminal amino acid (e.g.
909 lysine for AYPG-(N_α-Me-K)-F-NH_2), site selective *N*-methylation of the N-terminal amino
910 acid was completed as follows: First, protection of the primary amine was completed to favour
911 monomethylation by adding 2-nitrobenzenesulfonyl chloride (110.8 mg, 0.5 mmol) and 2,4,6-
912 trimethylpyridine (132 µL, 1.0 mmol) in NMP (4 mL) to the on-resin peptide (0.1 mmol) and
913 shaken (15 min). Following completion of the protection reaction, the resin was washed thrice
914 with NMP (3X 5 mL) and dry THF (3X 5 mL). Second, *N*-methylation was completed through
915 Mitsunobu conditions by adding triphenylphosphine (131.2 mg, 0.5 mmol), diisopropyl
916 azodicarboxylate (98 µL, 0.5 mmol), and methanol (41 µL, 1.0 mmol) in dry THF (4 mL) to
917 the on-resin peptide and shaken under N_2 (10 min). Following completion of the *N*-methylation
918 reaction, the resin was washed thrice with dry THF (3X 5mL) and NMP (3X 5 mL). Third, the
919 methylated N-terminal amine was then deprotected by adding 2-mercaptoethanol (70 µL, 1.0
920 mmol) and 1,8-diazabicyclo(5.4.0)undec-7-ene (75 µL, 0.5 mmol) in NMP (4 mL) to the on-
921 resin peptide and shaken (5 min). The solution turned bright yellow as expected. The solution
922 was removed and then this third step was repeated, followed by being washed five times with
923 NMP (5X 5 mL) and thrice with DMF (3X 5 mL). Addition of the next sequential amino acid
924 (except for inapplicable peptides i.e. (*N*-Me-A)-YPGKF-NH_2 and (*N*-Me-S)-YPGKF-NH_2)
925 was added manually [0.3 mmol of HATU, 0.3 mmol of Fmoc-amino acid (e.g. Fmoc-Gly-OH
926 for AYPG-(N_α-Me-K)-F-NH_2), 0.6 mmol of DIPEA, 4 mL of DMF, 3 h coupling]. Following
927 completion of the sequential amino acid reaction, the resin was washed 5 times with DMF (5X
928 5mL) and then the next sequential amino acid was added (on applicable peptides i.e AYPG-
929 (N_α-Me-K)-F-NH_2 and AYPGK-(*N*-Me-F)-NH_2) using the automated procedure mentioned in
930 the general methods for peptide synthesis. Following completion of the synthesis, the peptide
931 was cleaved, purified, and analyzed as mentioned in the general methods for peptide synthesis.
932 The amino acid *N*-methylglycine, commonly known as sarcosine, was obtained from a
933 commercial source, and therefore, *N*-methylglycine containing peptides (i.e. Sar-YPGKF-NH_2
934 and AYP-Sar-KF-NH_2) were synthesized solely by the standard automated Fmoc-SPPS
935 discussed in the general methods for peptide synthesis.
936
937 ***Synthesis of AYPG-(N_ε-Me-K)-F-NH_2.*** The hexapeptide (AYPGKF) was synthesized using
938 the standard automated Fmoc-SPPS discussed in the general methods for peptide synthesis,
939 except that Fmoc-Lys(Alloc)-OH was used in place of standard Fmoc-Lys(Boc)-OH. While
940 still on resin, with all of the side chains protected, and with the N-terminal Fmoc-deprotection
941 completed, the N-terminus of this peptide was Boc protected by adding Boc-ON (98.5 mg, 0.4
942 mmol) and DIPEA (70 µL, 0.4 mmol) in DMF (4 mL) and shaken (4 hours). The solution was
943 removed and this Boc protection was repeated overnight (20 hours) to ensure reaction
944 completion. The resin was washed thrice with DMF (3X 5 mL) and dry DCM (3X 5 mL) and
945 was placed under N_2 for site selective Alloc deprotection of the on-resin lysine side chain.
946 Phenylsilane (296 µL, 2.4 mmol) in dry DCM (2 mL) was added to the resin.
947 Tetrakis(triphenylphosphine) palladium(0) (23.1 mg, 20 µmol) was dissolved in dry DCM (1

948 mL) and added to the resin. The peptide column was flushed with N_2 (2 min) followed by being
949 shaken (5 min). The resin was washed thrice with dry DCM (3X 5 mL). The procedure was
950 repeated and shaken again (30 min). The resin was washed four times with DCM (4X 5 mL)
951 and DMF (4X 5 mL). Following this N-terminal Boc protection and subsequent side chain
952 Alloc deprotection, *N*-methylation of the on-resin lysine side chain was completed through the
953 site selective *N*-methylation procedure mentioned above. Following completion of the
954 synthesis, the peptide was cleaved, purified, and analyzed as discussed in the general methods
955 for peptide synthesis.
956
957 ***SPPS Reaction Monitoring.*** Three methods were used to monitor SPPS reactions. Two
958 methods (the Kaiser Test and the small-scale resin cleavage) were used to monitor general
959 peptide synthesis. Three methods (the Kaiser Test, the small-scale resin cleavage, and the
960 Chloranil Test) were used to monitor synthesis of peptides involving *N*-methylation. For the
961 Kaiser Test, several resin beads were placed in a test tube followed by the addition of 42.5 mM
962 phenol in ethanol (50 µL), 20 µM potassium cyanide in pyridine (50 µL), and 280.7 mM
963 ninhydrin in ethanol (50 µL). The mixture was then heated (100 °C, 5 min); where a positive
964 test indicates the presence of a free primary amine. For the small-scale resin cleavage method,
965 several beads and cleavage cocktail (500 µL) are shaken, worked up as per the full cleavage of
966 the resin procedure described above, and the desired peptide was confirmed through HPLC-
967 MS. For the Chloranil Test, several resin beads were placed in a test tube followed by the
968 addition of 357.8 mM acetaldehyde in DMF (50 µL) and 81.3 mM *p*-chloranil in DMF (50 µL)
969 and allowed to stand at room temperature (5 min); where a positive test indicates the presence
970 of a free secondary amine.
971
972 ***Calcium Signalling Assay.*** HEK293 cells or HEK293 cells stably expressing PAR4-YFP were
973 loaded with calcium sensitive dye (Fluo-4 NW, F36206, Life Technologies, Thermo Fisher)
974 and aliquoted into cuvettes with Hanks buffered salt solution (HBSS containing Ca^{2+} and
975 Mg^{2+}). Samples were excited at 480nm and emission recorded at 530nm. Baseline fluorescence
976 from PAR4-YFP excitation remains constant throughout experiment. Following baseline
977 recording, agonist induced changes in fluorescence was recorded. Change in fluorescence from
978 baseline to maximum response at a given agonist concentration (delta) were expressed as a
979 percentage of maximum cellular response elicited by calcium ionophore (A23187, Sigma-
980 Aldrich). *Calcium Signalling Assay with PAR4 orthosteric site-directed mutants*. HEK293 cells
981 were transiently transfected with 2µg of wild-type YFP tagged PAR4 or PAR4 mutant
982 receptors (described above) using the calcium phosphate transfection protocol as described
983 above. Calcium signalling was investigated as described above for the wild type receptor.
984
985 ***β-arrestin Recruitment - Bioluminescence Resonance Energy Transfer (BRET).*** HEK293
986 cells were co-transfected with PAR4-YFP (2µg) or mutant PAR4-YFP and β-arrestin-1 or -2-
987 renilla luciferase (rluc, 0.2µg) using modified calcium phosphate transfection. Cells were re-
988 plated (24 hours post-transfection) into white 96-well plates (Corning). At 48-hours post-
989 transfection, agonist-stimulated β-arrestin recruitment to PAR4 was detected by measuring
990 BRET following 20 minutes of agonist stimulation. Coelenterazine (5µM; Nanolight

991 Technology, Pinetop, AZ) was added ten minutes prior to BRET collection using a Berthold
992 Mithras LB 940 plate reader.
993
994 ***Testing Peptide library specificity for PAR4*** Previous studies have pointed to the possibility
995 of PAR agonist peptides cross activating other members of this family. For example, the PAR1
996 tethered ligand peptide SFLLRN is able to activate PAR2 and substitution of a phenylalanine
997 residue in certain PAR4 agonist peptides confers PAR1 activity (Boitano et al., 2011; Faruqi
998 et al., 2000; Lerner et al., 1996). Activating peptides typically require an aromatic sidechain in
999 position 2 (F in PAR1) and we wondered if substitution of tyrosine for phenylalanine may
1000 decrease selectivity at PAR4 and increase crosstalk with PAR1. We examined whether
1001 substitutions made to AYPGKF-NH_2 affected their selectivity using a calcium signalling assay
1002 in HEK-293 cells that endogenously express PAR1 and PAR2. None of the peptides tested
1003 elicited a signalling greater than 5% of the calcium ionophore A23187 showing that they retain
1004 selectivity towards PAR4 (Supp. Fig. 4). Additionally, we investigated specificity using BRET
1005 for β-arrestin-2 recruitment to cells expressing PAR4-YFP or PAR2-YFP. None of the peptides
1006 were able to induce β-arrestin recruitment in PAR2-YFP expressing HEK-293 cells (NET
1007 BRET of 0.05 and over) with the exception of AYPGK-1Nal-NH_2 (Supp. Fig. 5).
1008
1009 ***PAR4-stimulated Mitogen-activated Protein Kinase (MAPK) signalling*** *HEK-293 and*
1010 *CRISPR/Cas9 β-arrestin-1/-2 double knockout HEK-293.* Agonist-stimulated mitogen-
1011 activated protein kinase (MAPK) signalling in CRISPR/Cas9 HEK-293 β-arrestin double
1012 knockout cells (β-arr. knockout) and wild-type HEK-293 cells transfected with PAR4-YFP
1013 were analysed by western blot. Cells were placed in serum free media (serum-free DMEM,
1014 Gibco) for 3 hours before beginning experiment. Cells were then stimulated with 30μM
1015 AYPGKF-NH_2 for varying time periods (0, 2, 5, 10, 20, 30, 60, 90 minutes) at 37 ˚C. Treated
1016 cells were placed on ice following stimulating period. Total protein was extracted adding kinase
1017 lysis buffer with phosphatase and protease inhibitors (20 mM Tris-HCl, pH 7.5, 100 mM NaCl,
1018 10 mM $MgCl_2$, 1 mM EDTA, 1 mM EGTA, 0.5% NP-40, 2.5 mM sodium pyrophosphate, 1
1019 mM b-glycerophosphate, 1 mM Na_3VO_4, 25 mM NaF, 1 mg/mL leupeptin, 1 mg/m aprotinin,
1020 1 mM phenylmethylsulfonyl fluoride, and 1mM dithiothreitol) for 20 minutes and cell
1021 membranes were cleared by centrifugation (13,300g for 3 minutes). Protein concentrations
1022 were measured using the Pierce BCA Protein Assay (Thermo Fisher Scientific). Protein
1023 samples were heat-denatured at 98°C for 8 minutes in denaturing Laemmli buffer (containing
1024 2-mercaptoethanol) and resolved on 4–12% gradient Invitrogen Bolt Bis-Tris Plus gels
1025 (Thermo Fisher Scientific). The resolved proteins were transferred via wet transfer in buffer
1026 (1X Tris-glycine, 20% methanol) to a polyvinylidene difluoride membrane and blocked in
1027 TBST buffer (TBS with 0.1% (v/v) Tween-20) supplemented with 1% ECL Advance Blocking
1028 Agent (GE Healthcare, Waukesha, WI) for 40 minutes at room temperature. p44/42
1029 (Thr202/Tyr204) phosphorylation was detected with specific antibodies (Cell Signalling
1030 Technology, Danvers, MA; diluted 1:1000 in TBST) overnight at 4°C. phospho-p44/42
1031 immunoreactivity was detected using the horseradish peroxidase-conjugated anti-rabbit
1032 secondary antibody (Cell Signalling Technology; 1:10,000 in TBST for 1 hour). After washing
1033 the membrane with TBST (3 x 10-minute washes), the peroxidase activity was detected with

1034 the chemiluminescence reagent ECL Advance (GE Healthcare) on iBright image Station
1035 (Invitrogen, Burlington, ON). Membranes were then stripped with blot stripping buffer
1036 (Thermo Fisher Scientific) at room temperature and blocked in TBST with 1% ECL Advance
1037 Blocking Agent before incubation with the p44/42 (1:1000 in TBST with 1% ECL Advance
1038 Blocking Agent) overnight at 4°C. Following incubation with primary antibody, blots were
1039 rinsed in TBST and incubated with appropriate horseradish peroxidase -conjugated anti-rabbit
1040 or anti-mouse secondary antibody (1:10,000 in TBST for 1 hour). Membranes were washed
1041 and imaged as previously described. Band intensities representing activated MAPK were
1042 quantified using FIJI (Schindelin et al., 2012). Phospho-kinase levels were normalized for
1043 differences in protein loading by expressing the data as a ratio of the corresponding total-p44/42
1044 signal. Data are expressed as a fold increase over unstimulated baseline control. *PAR4-*
1045 *stimulated MAPK signalling in HEK-293 +/- YM254890.* Agonist-stimulated MAPK signalling
1046 in wild-type HEK-293 cells transfected with PAR4-YFP were analysed by western blot. Cells
1047 were placed in serum free media (serum-free DMEM, Gibco) for 3 hours before beginning
1048 experiment. Prior to agonist stimulation cells were treated with either control (0.001% DMSO)
1049 or YM254890 (100nM) for 20 minutes. Cells were then stimulated with 30μM AYPGKF-NH_2
1050 for varying time periods (0, 2, 5, 10, 20, 30, 60, 90 minutes) at 37 degrees Celsius. Cells were
1051 lysed, protein quantified, and samples run and imaged as previously described. *MAPK*
1052 *signalling in PAR4-YFP stable cells with peptide library.* Agonist-stimulated mitogen-
1053 activated protein kinase (MAPK) signalling in HEK-293 cells stably expressing PAR4-YFP
1054 were analysed by western blot following stimulation with PAR4 peptide agonists. Cells were
1055 placed in serum free media (serum-free DMEM, Gibco) for 3 hours before beginning
1056 experiment. Cells were stimulated with either control (no agonist), AYPGKF-NH_2 or agonist
1057 peptides described at 100μM concentration. Cells were stimulated for 10 minutes with agonist
1058 and lysed, quantified, and blot as previously described.
1059
1060 ***Preparation of washed platelets and light-transmission aggregometry.*** Blood was drawn from
1061 the abdominal aorta or heart of Sprague-Dawley rats into trisodium citrate (3.4% w.v). The
1062 blood was centrifuged at 200g for 15 minutes at 22 degrees Celsius to isolate platelet-rich
1063 plasma (PRP). PRP was transferred to a 14 mL polypropylene round-bottom tube (Falcon) and
1064 centrifuged at 1800 rotations per minute (rpm.; 594g) for 10 minutes at 22˚C to pellet platelets
1065 and obtain platelet-poor plasma (PPP). PPP was decanted and used for 100% light transmission
1066 control. To obtain washed platelet sample, platelets were washed twice in Tyrode's buffer (12
1067 mM $NaHCO_3$, 127 mM NaCl, 5 mM KCl, 0.5 mM NaH_2PO_4, 1 mM $MgCl_2$, 5 mM glucose,
1068 and 10 mM HEPES; Ramachandran et al., 2017) and resuspended to a volume equivalent to
1069 that of the initial blood draw. Washed platelet sample was equilibrated for one hour at ambient
1070 temperature following the addition of 1M $CaCl_2$ (1 μl/mL). 400 μl of this washed platelet
1071 suspension was used for light transmission aggregometry on a platelet aggregometer (Model
1072 700; Chrono-Log Corp, Havertown, PA).
1073
1074 ***Structural homology modelling of PAR4.*** Residues resolved in the PAR2 crystal (5NDD.pdb)
1075 were used to generate a homology model of wild-type human PAR2. Homology model of wild-
1076 type human PAR2 was then aligned with the wild-type human PAR4 amino acid sequence
1077 [National Center for Biotechnology Information (NCBI) accession number NM_003950) using

Clustal Omega (Madeira et al., 2019; Sievers et al., 2011). Only residues resolved in the crystal structure of PAR2 were used as template coordinates for PAR4 homology modelling. Twenty human PAR4 homology models were generated using the human PAR2 crystal structure coordinates (5NDD.pdb; Cheng et al., 2017) as a template in MODELLER (version 9.16, Webb and Sali, 2017). The model with the lowest DOPE score was taken as the best structure and visualized using PyMOL (version 1.7.4, Schrödinger, LLC). Electrostatic surface potential was calculated after assignment of partial charges using PDB2PQR and using the Adaptive Poisson-Boltzmann Solver plugin in PyMOL (Dolinsky et al., 2004).

In silico docking of AYPGKF-NH_2 to the PAR4 homology model. *in silico* docking of PAR4 agonist peptide, AYPGKF-NH_2, to PAR4 homology model was undertaken using GalaxyPepDock (Lee et al., 2015). The lowest energy PAR4 homology model PDB file was loaded into GalaxyPepDock along with a text file of the PAR4 agonist peptide sequence which GalaxyPepDock uses to predict a peptide structure for docking analyses (Ala-Tyr-Pro-Gly-Lys-Phe; amidation is not included in the structure prediction). Ten models of PAR4-AP docking were generated. Frequency of receptor-peptide residue interactions, taken as atom-atom distances of less than 3 Angstroms, was quantified manually to determine highly recurrent interactions.

Data analysis and statistical tests. Data are shown as mean ± SEM. Calcium signalling and β-arrestin-1/-2 recruitment concentration effect curves were calculated using nonlinear regression curve fitting (three parameter; Prism7). EC_{50} values are reported (Table 1) where signal has saturated. Where signalling is not saturated EC_{50} is reported for calcium as not determined (*n.d.*). The F-statistic calculated to compare EC_{50} values was calculated using the extra sum-of-squares analysis (Kim et al., 2019). For table 1, values comparing percentage of signalling or recruitment at 100 μM to values obtained from the parental PAR4-AP, AYPGKF-NH_2, are shown. Significance was determined for comparisons with 100 μM AYPGKF-NH_2 and p44/42 phosphorylation by one-way analysis of variance (ANOVA). Western blot protein densitometry was quantified using FIJI. Transformation and analysis were conducted on raw data and significance is indicated by '*' ($p < 0.05$).

Acknowledgements and Funding. These studies were funded by a Canadian Institutes of Health Research (CIHR) grant (RR) and grants from the Natural Sciences and Engineering Research Council of Canada (LL and PS). PT is the recipient of a doctoral QEII Graduate Scholarships in Science and Technology. JCL is the recipient of a Canada Graduate Scholarship and an Ontario Graduate Scholarship.

Competing interests. The authors declare that no competing interests exist.

				% of AYPGKF-NH₂ Response (100μM)			
	Peptide (alterations shown in red)	**Ca^{2+} EC_{50} (μM)**	**Ca^{2+} Max. (% of A23187)**	**Ca^{2+} signaling**	**β-Arr-1 recruitment**	**β-Arr-2 recruitment**	**p-p44/42 (fold over baseline; 100 μM)**
PAR4-AP	**AYPGKF-NH_2**	12.1 ± 3.1	27.4 ± 1.7	100.0 ± 8.2	100.0 ± 3.9	100 ± 3.5	5.9 ± 1.5
Alanine	A**A**PGKF-NH_2	*n.d.*	51.8 ± 25.4	52.9 ± 12.4*	47.3 ± 3.6*	46.4 ± 3.2*	0.8 ± 0.1
	AY**A**GKF-NH_2	63.7 ± 20.8*	29.7 ± 3.4	75.4 ± 11.1	48.5 ± 7.9*	43.4 ± 7.1*	1.2 ± 0.3
	AYP**A**KF-NH_2	21.2 ± 6.6	22.4 ± 1.9	72.2 ± 6.3	56.4 ± 5.6*	54.6 ± 5.1*	1.0 ± 0.2
	AYPG**A**F-NH_2	9.8 ± 2.9	25.7 ± 1.8	96.7 ± 17.8	59.3 ± 7.2*	70.8 ± 6.5	6.5 ± 2.7
	AYPGK**A**-NH_2	17.3 ± 5.0	20.0 ± 1.5	69.4 ± 4.1	47.9 ± 3.8*	52.6 ± 3.5*	3.8 ± 2.2
D-isomer	**a**YPGKF-NH_2	*n.d.*	19.2 ± 4.8	24.0 ± 4.4*	48.7 ± 2.6*	47.5 ± 2.4*	0.8 ± 0.2
	A**y**PGKF-NH_2	*n.d.*	1.1 ± 0.5	3.9 ± 2.8*	50.7 ± 4.6*	46.4 ± 4.2*	0.6 ± 0.1
	AY**p**GKF-NH_2	*n.d.*	1.2 ± 0.4	6.1 ± 3.4*	45.2 ± 10.5*	38.1 ± 9.5*	0.7 ± 0.2
	AYPG**k**F-NH_2	*n.d.*	16.9 ± 5.3	25.2 ± 5.2*	47.4 ± 1.0*	36.5 ± 0.9*	1.0 ± 0.3
	AYPGK**f**-NH_2	22.2 ± 4.7	21.9 ± 1.2	76.7 ± 5.2	80.3 ± 6.6	74.1 ± 6.0	6.5 ± 2.9
***N*-methyl.**	**(*N*-Me-A)**-YPGKF-NH_2	*n.d.*	15.0 ± 7.5	13.3 ± 1.3*	119.2 ± 11.9	80.6 ± 10.8	1.3 ± 0.3
	A-**(*N*-Me-Y)**-PGKF-NH_2	*n.d.*	2.7 ± 0.2	9.8 ± 2.9*	71.4 ± 10.8	61.5 ± 9.8*	2.2 ± 0.2
	AYP-**Sar**-KF- NH_2	*n.d.*	2.4 ± 0.3	8.8 ± 1.5*	35.9 ± 4.3*	36.1 ± 3.9*	1.4 ± 0.2
	AYPG-**(N_α-Me-K)**-F-NH_2	*n.d.*	9.6 ± 1.9	18.3 ± 1.5*	126.7 ± 18.6	77.1 ± 16.9	1.8 ± 0.9
	AYPGK-**(*N*-Me-F)**-NH_2	7.6 ± 1.9	26.3 ± 1.4	99.4 ± 7.8	136.9 ± 18.0*	96.6 ± 16.9	15.7 ± 4.6
N-terminal	**Ac**-AYPGKF-NH_2	*n.d.*	11.0 ± 3.3	49.9 ± 16.5*	47.3 ± 3.1*	45.5 ± 2.8*	1.2 ± 0.4
Position 1	**V**YPGKF-NH_2	22.9 ± 8.3	16.8 ± 1.7	48.5 ± 4.6*	73.6 ± 13.0	55.2 ± 11.8*	2.3 ± 0.7
	Nle-YPGKF-NH_2	*n.d.*	1.1 ± 0.1	4.0 ± 1.1*	40.2 ± 9.7*	36.5 ± 8.8*	21.4 ± 7.0*
	Sar-YPGKF- NH_2	*n.d.*	1.6 ± 0.6	9.7 ± 8.5*	35.6 ± 2.0*	39.8 ± 1.8*	1.6 ± 1.1
	Aib-YPGKF-NH_2	50.2 ± 15.3*	25.1 ± 2.5	72.9 ± 12.0	38.6 ± 3.9*	37.3 ± 3.6*	7.8 ± 3.5
	(*N*-Me-S)-YPGKF-NH_2	*n.d.*	2.2 ± 0.5	8.8 ± 1.8*	78.1 ± 6.9	51.7 ± 6.3*	1.8 ± 0.4
	betaAla-YPGKF- NH_2	*n.d.*	1.9 ± 0.4	10.3 ± 3.9*	25.7 ± 4.8*	31.8 ± 4.4*	9.1 ± 3.4
	Inp-YPGKF-NH_2	*n.d.*	3.4 ± 0.8	18.9 ± 7.3*	32.0 ± 3.3*	26.9 ± 3.0*	1.3 ± 0.3
Position 2	A-**Tyr(Me)**-PGKF-NH_2	15.7 ± 4.0	25.7 ± 1.6	91.1 ± 10.1	77.9 ± 3.8	85.8 ± 3.4	12.7 ± 5.8
	A-**F-(4-fluoro)**-PGKF-NH_2	19.9 ± 5.4	35.1 ± 2.5	105.4 ± 9.0	72.1 ± 9.0	86.9 ± 8.1	10.1 ± 3.9
Position 3	AY-**Pip**-GKF- NH_2	30.7 ± 4.9	23.3 ± 1.1	74.2 ± 4.8	38.8 ± 3.0*	44.0 ± 2.7*	1.3 ± 0.3
	AY-**Nip**-GKF- NH_2	*n.d.*	2.5 ± 0.3	10.0 ± 1.8*	32.9 ± 4.9*	30.9 ± 4.5*	1.0 ± 0.3
Position 4	AYP-**betaAla**-KF- NH_2	*n.d.*	9.7 ± 2.4	19.8 ± 5.8*	42.5 ± 1.8*	24.9 ± 1.6*	1.8 ± 0.6
Position 5	AYPG**O**F- NH_2	4.2 ± 1.1	20.7 ± 1.1	77.3 ± 7.9	121.7 ± 8.5	112.1 ± 7.7	23.4 ± 7.2*
	AYPG**R**F-NH_2	4.0 ± 1.1	21.3 ± 1.2	82.0 ± 8.3	154.2 ± 10.3*	140.1 ± 9.4*	3.0 ± 0.3
	AYPG-**(N_ε-Me-K)**-F-NH_2	6.7 ± 1.9	23.8 ± 1.5	88.9 ± 9.3	122.5 ± 12.4	116.7 ± 11.2	20.5 ± 5.3*
	AYPG-**Cit**-F-NH_2	5.4 ± 0.8	18.2 ± 0.6	65.5 ± 1.3	94.1 ± 10.1	87.7 ± 9.2	25.1 ± 7.5*
Position 6	AYPGK**Y**-NH_2	5.2 ± 1.0	16.9 ± 0.7	61.2 ± 4.3*	120.5 ± 12.5	109.9 ± 11.4	20.2 ± 9.7*
	AYPGK-**F(4-Me)**-NH_2	9.4 ± 3.0	17.8 ± 1.3	62.0 ± 5.5*	56.4 ± 1.2*	63.2 ± 1.1*	0.9 ± 0.4
	AYPGK-**F(4-fluoro)**-NH_2	*n.d.*	*n.d.*	16.5 ± 10.2*	25.2 ± 6.5*	41.3 ± 5.9*	1.1 ± 0.5
	AYPGK-**1Nal**-NH_2	9.6 ± 1.9	18.7 ± 0.9	65.4 ± 7.4	77.5 ± 2.3	64.1 ± 2.0*	21.3 ± 10.8*
	AYPGK-**2Nal**-NH_2	11.1 ± 2.3	25.3 ± 1.3	93.9 ± 4.2	77.0 ± 7.0	91.6 ± 6.4	4.3 ± 1.7

Table 1. Summary table of all calcium, β-arrestin, and p44/42 data. Calcium data is displayed as EC_{50} or not determined (*n.d.*) if EC_{50} could not be calculated. Maximum calcium response achieved with each peptide is shown as a percentage of the maximum calcium response achievable in a given experiment revealed by calcium ionophore (% of A23187 calcium ionophore). Statistically significant shifts in EC_{50} compared to PAR4-AP, AYPGKF-NH_2, were found using the F-statistic (*$p < 0.05$). Given that saturation did not always occur, all peptides are compared to the parental PAR4-AP, AYPGKF-NH_2, and shown as a percent of

1124 the response obtained with PAR4-AP at a given concentration (100 μM). Finally, fold increase
1125 over unstimulated baseline is shown for phosphorylation of p44/42 MAP kinase activation.
1126 Statistical significance for comparisons at 100 μM and p44/42 phosphorylation are calculated
1127 using one-way ANOVA of response compared to PAR4-AP (*$p < 0.05$).

1128 **Figure 1. Alanine**
1129 **substitutions in positions 2-6**
1130 **significantly decreases β-**
1131 **arrestin recruitment and**
1132 **differentially affect calcium**
1133 **signalling compared to PAR4-**
1134 **AP. (A) Agonist-stimulated**
1135 **calcium signalling.** Calcium
1136 signalling is shown as a
1137 percentage of the maximum
1138 calcium signalling obtained by
1139 application of calcium
1140 ionophore (A23187, 3 µM). (*n*
1141 = *3-7*) **Agonist-stimulated**
1142 **recruitment of β-arrestin-1**
1143 **(B) and β-arrestin-2 (C) to**
1144 **PAR4.** Concentration effect
1145 curves of BRET values from
1146 cells treated increasing
1147 concentrations of peptide are
1148 presented as normalized net
1149 BRET ratio. (*n* = *3*).

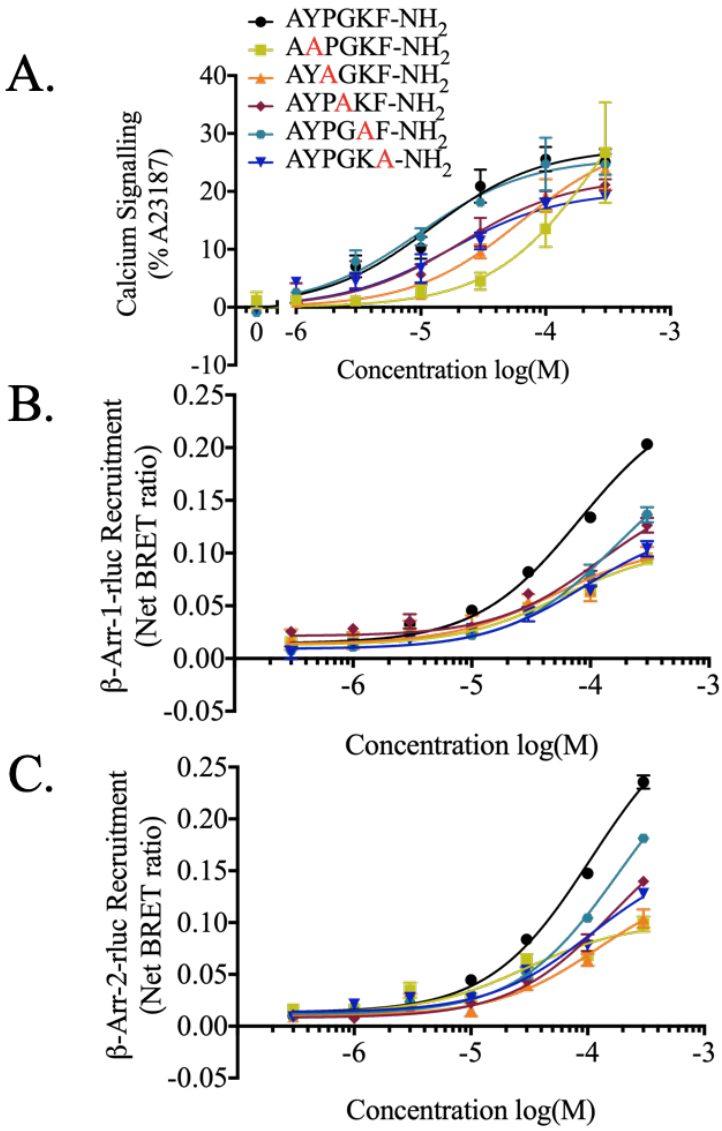

1150 **Figure 2. D-isomer amino acid**
1151 **substitutions in positions 1, 2,**
1152 **3, and 5 of the PAR4-AP,**
1153 **significantly reduces potency**
1154 **in calcium signalling and β-**
1155 **arrestin recruitment assays.**
1156 **(A) Agonist-stimulated**
1157 **calcium signalling.** Calcium
1158 signalling is shown as a
1159 percentage of the maximum
1160 calcium signalling obtained by
1161 application of calcium
1162 ionophore (A23187, 3 µM). (*n* =
1163 *3-4*) **Agonist-stimulated**
1164 **recruitment of β-arrestin-1 (B)**
1165 **and β-arrestin-2 (C) to PAR4.**
1166 Concentration effect curves of
1167 BRET values from cells treated
1168 increasing concentrations of
1169 peptide are presented as
1170 normalized net BRET ratio. (*n* =
1171 *3*).
1172

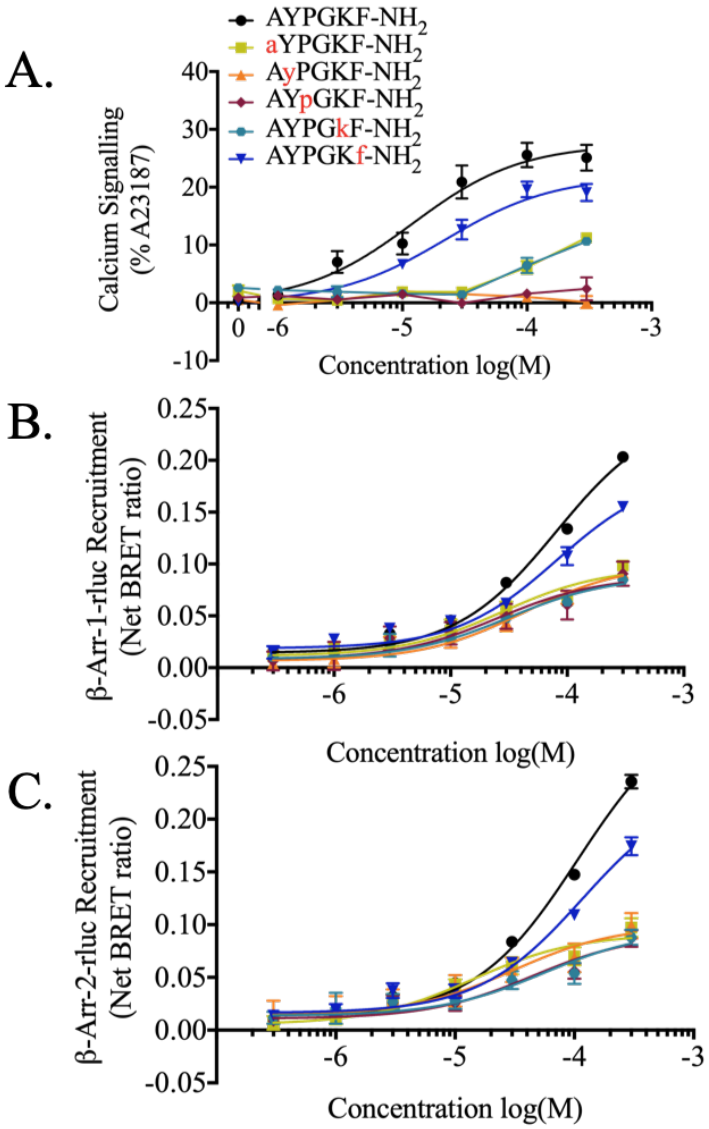

1173 **Figure 3. Peptides with *N*-**
1174 **methylation of either alanine[1] or**
1175 **lysine[5] do not initiate calcium**
1176 **signalling but enhance β-arrestin**
1177 **recruitment compared to PAR4-**
1178 **AP. *N*-methylation of**
1179 **phenylalanine[6] enhances β-**
1180 **arrestin recruitment while**
1181 **signalling calcium equipotently in**
1182 **comparison to PAR4-AP. (A)**
1183 **Agonist-stimulated calcium**
1184 **signalling.** Calcium signalling is
1185 shown as a percentage of the
1186 maximum calcium signalling
1187 obtained by application of calcium
1188 ionophore (A23187, 3 µM). (*n = 3-*
1189 *7)* **Agonist-stimulated recruitment**
1190 **of β-arrestin-1 (B) and β-arrestin-**
1191 **2 (C) to PAR4.** Concentration effect
1192 curves of BRET values from cells
1193 treated increasing concentrations of
1194 peptide are presented as normalized
1195 net BRET ratio. (*n = 3*).

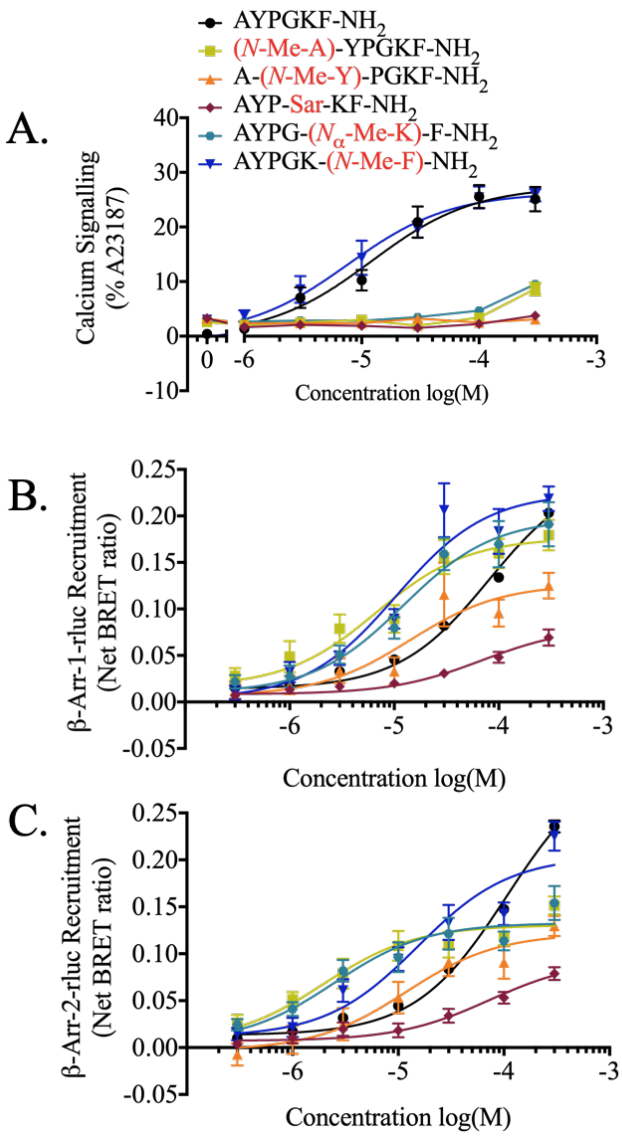

1196 **Figure 4. Calcium signalling and**
1197 **β-arrestin recruitment to PAR4 in**
1198 **response to AYPGKF-NH_2 or**
1199 **peptides with N-terminal**
1200 **acetylation or additional**
1201 **substitutions in position 1**
1202 **(alanine). (A) Agonist-stimulated**
1203 **calcium signalling.** Calcium
1204 signalling is shown as a percentage
1205 of the maximum calcium signalling
1206 obtained by application of calcium
1207 ionophore (A23187, 3 µM). (*n = 3-*
1208 *7)* **Agonist-stimulated recruitment**
1209 **of β-arrestin-1 (B) and β-arrestin-**
1210 **2 (C) to PAR4.** Concentration effect
1211 curves of BRET values from cells
1212 treated increasing concentrations of
1213 peptide are presented as normalized
1214 net BRET ratio. (*n = 3*).
1215

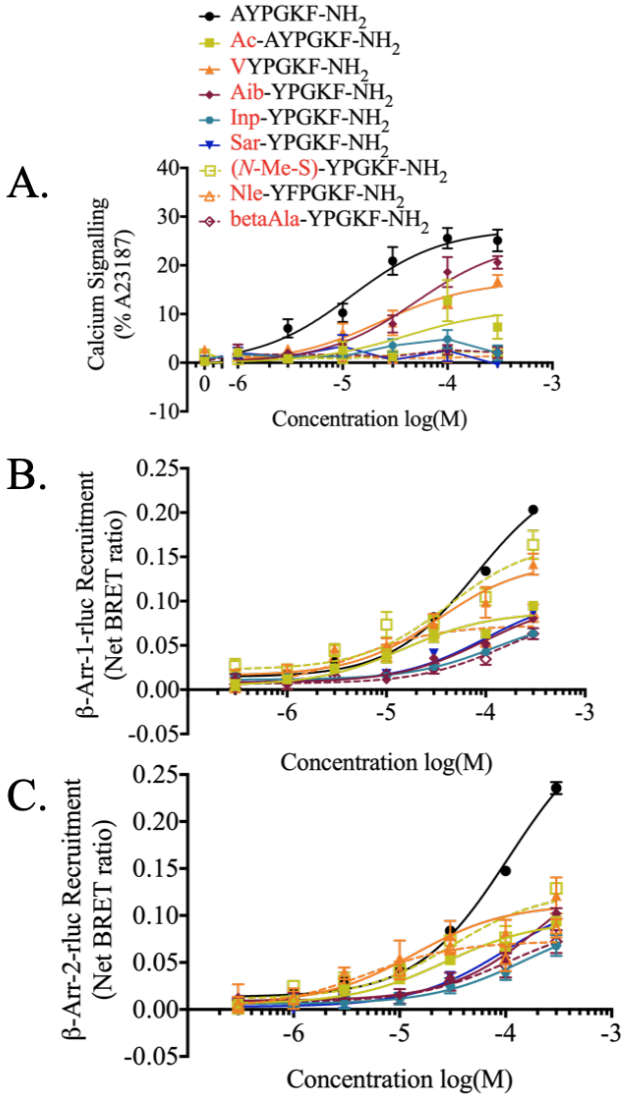

1216 **Figure 5. Calcium and β-arrestin**
1217 **recruitment to PAR4 in response**
1218 **to AYPGKF-NH_2 or peptides with**
1219 **additional substitutions in**
1220 **tyrosine[2], proline[3], or glycine[4]. (A)**
1221 **Agonist-stimulated calcium**
1222 **signalling.** Calcium signalling is
1223 shown as a percentage of the
1224 maximum calcium signalling
1225 obtained by application of calcium
1226 ionophore (A23187, 3 µM). (*n = 3-*
1227 *7)* **Agonist-stimulated recruitment**
1228 **of β-arrestin-1 (B) and β-arrestin-**
1229 **2 (C) to PAR4.** Concentration effect
1230 curves of BRET values from cells
1231 treated increasing concentrations of
1232 peptide are presented as normalized
1233 net BRET ratio. (*n = 3*).

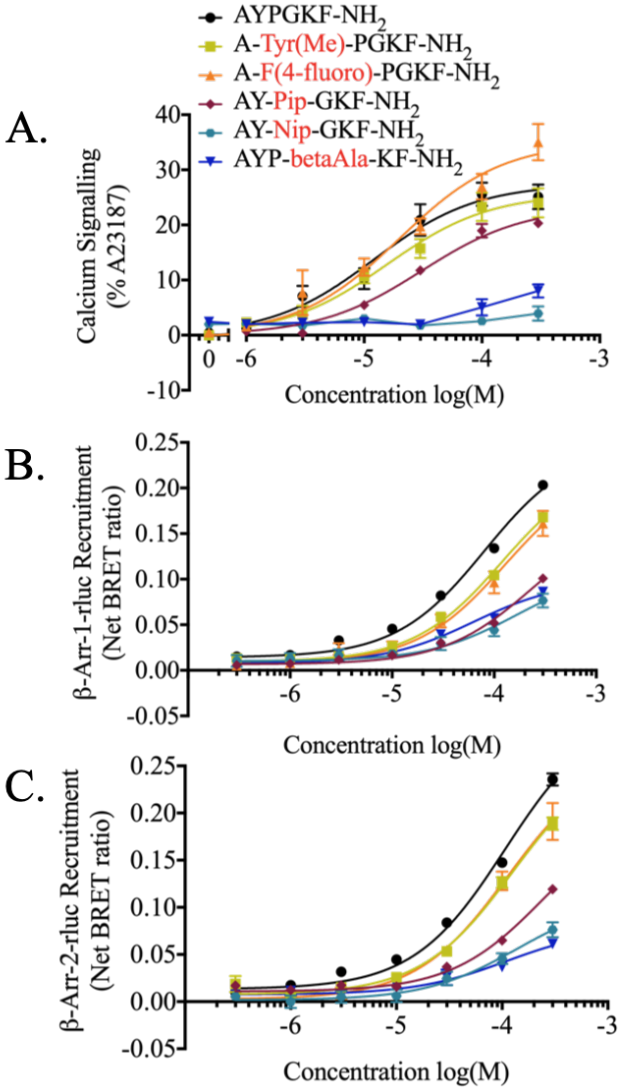

1234 **Figure 6. Calcium and β-arrestin**
1235 **recruitment to PAR4 in response**
1236 **to AYPGKF-NH_2 or peptides with**
1237 **additional substitutions in lysine[5].**
1238 **(A) Agonist-stimulated calcium**
1239 **signalling.** Calcium signalling is
1240 shown as a percentage of the
1241 maximum calcium signalling
1242 obtained by application of calcium
1243 ionophore (A23187, 3 µM). (*n = 3-*
1244 *7)* **Agonist-stimulated recruitment**
1245 **of β-arrestin-1 (B) and β-arrestin-**
1246 **2 (C) to PAR4.** Concentration effect
1247 curves of BRET values from cells
1248 treated increasing concentrations of
1249 peptide are presented as normalized
1250 net BRET ratio. (*n = 3*).
1251

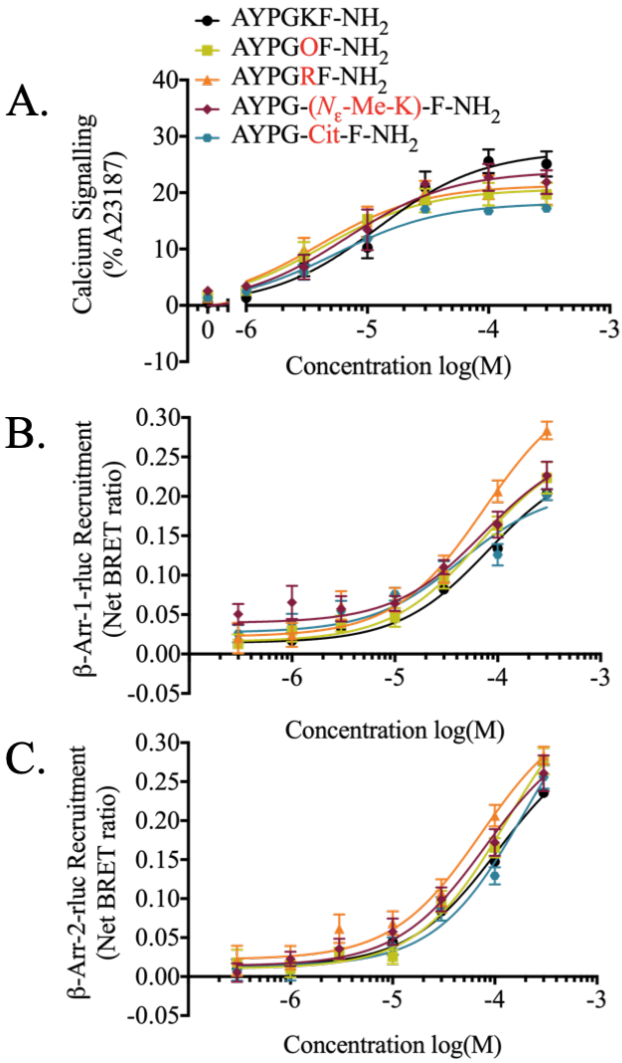

1252 **Figure 7. Calcium and β-arrestin**
1253 **recruitment to PAR4 in response**
1254 **to AYPGKF-NH_2 or peptides with**
1255 **additional substitutions in**
1256 **phenylalanine[6]. (A) Agonist-**
1257 **stimulated calcium signalling.**
1258 Calcium signalling is shown as a
1259 percentage of the maximum calcium
1260 signalling obtained by application of
1261 calcium ionophore (A23187, 3 µM).
1262 (*n = 3-7)* **Agonist-stimulated**
1263 **recruitment of β-arrestin-1 (B)**
1264 **and β-arrestin-2 (C) to PAR4.**
1265 Concentration effect curves of
1266 BRET values from cells treated
1267 increasing concentrations of peptide
1268 are presented as normalized net
1269 BRET ratio. (*n = 3*).

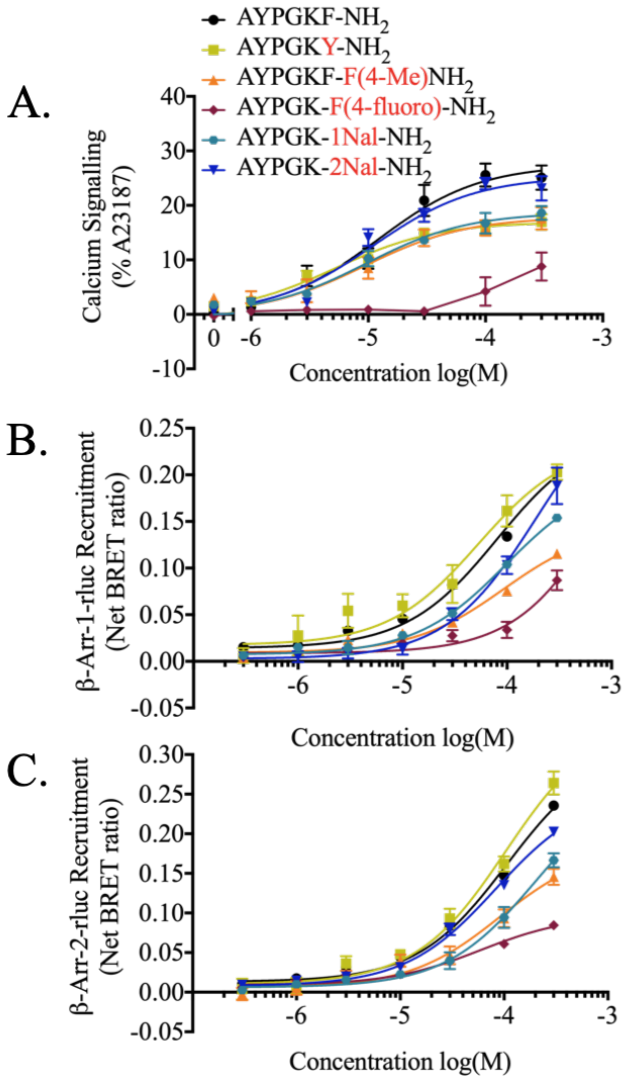

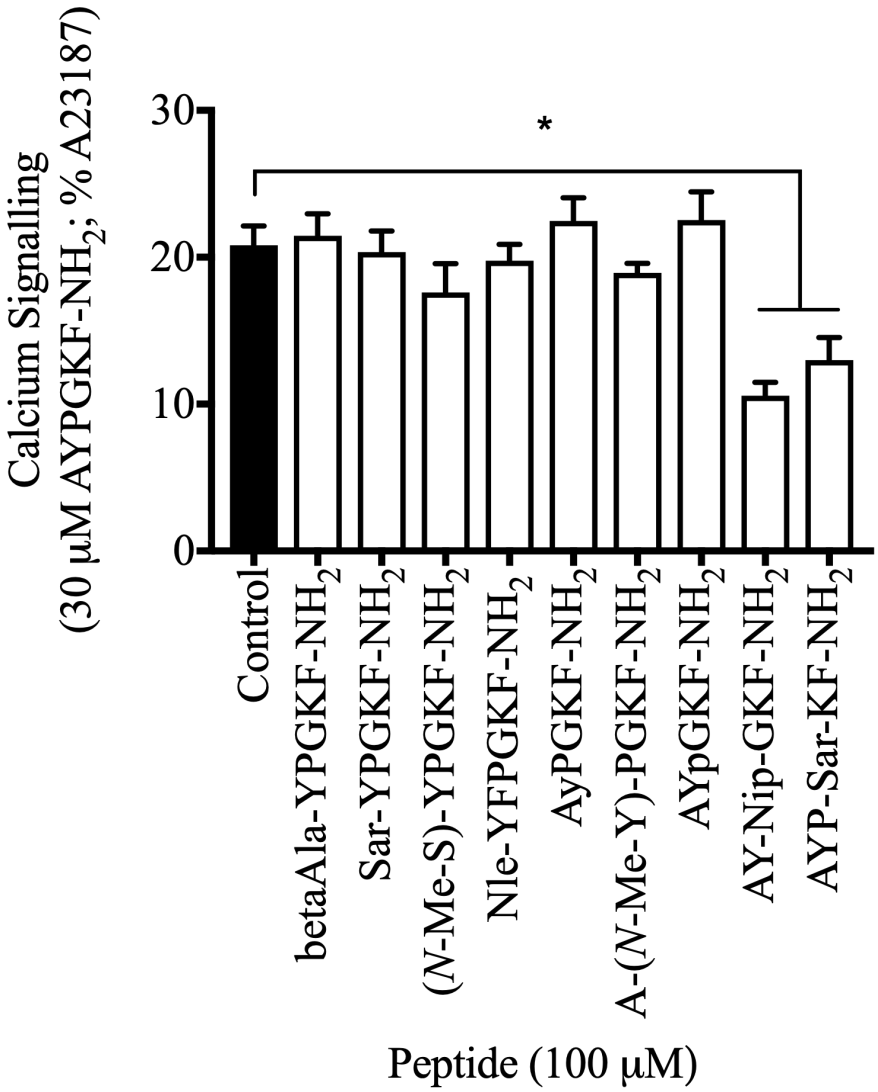

Figure 8. PAR4-AP (AYPGKF-NH_2) stimulated calcium signalling responses following pre-treatment with calcium signalling null peptides. Calcium signalling (Fluorescence Em: 530) in HEK293 cells stably expressing PAR4-YFP were recorded following 30 μM AYPGKF-NH_2 addition after 30-minute pre-treatment incubation with 100 μM of calcium signalling-null peptides. Data are shown as a percentage of maximum response obtained in cells treated with the calcium ionophore A23187 (3 μM). Agonist peptide concentrations are in M. Pre-treatment with calcium-null peptides did not affect AYPGKF-NH_2-stimulated calcium signalling in most cases with the exception of AY-Nip-GKF-NH_2 and AYP-Sar-KF-NH_2, which significantly decreased AYPGKF-NH_2 stimulated calcium signalling compared to vehicle treated control. (*$p > 0.05$; $n = 3$)

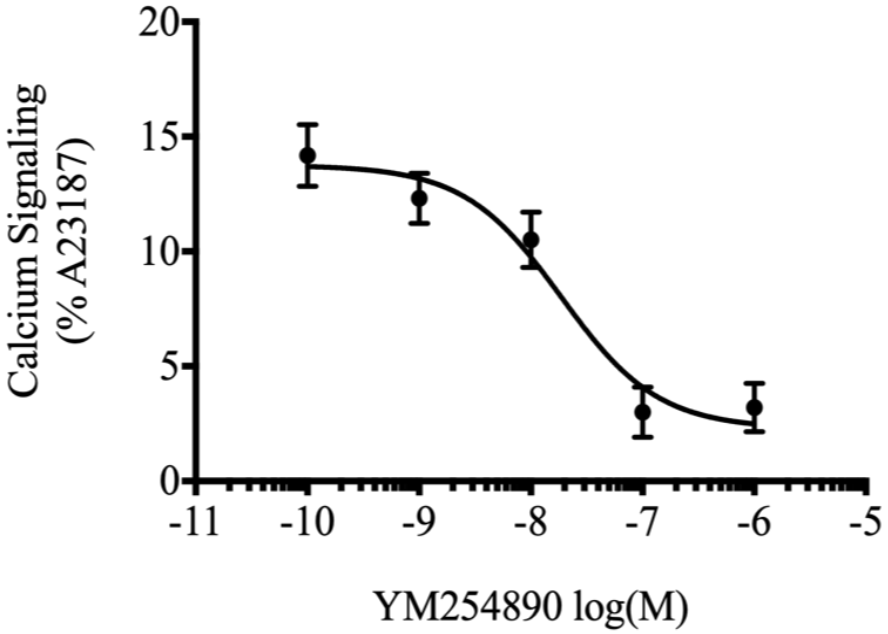

1280 **Figure 9. PAR4-mediated calcium signalling is $G\alpha_{q/11}$-dependent.** HEK293 cells stably
1281 expressing PAR4 were pre-treated with either DMSO vehicle control (0.001%) or increasing
1282 concentration of the selective $G\alpha_{q/11}$ inhibitor YM254890. Calcium signalling following
1283 stimulation with AYPGKF-NH_2 (100μM) was recorded. PAR4-mediated calcium signalling
1284 was blocked by YM254890 at concentrations greater than 100 nM. (*n = 4*)
1285

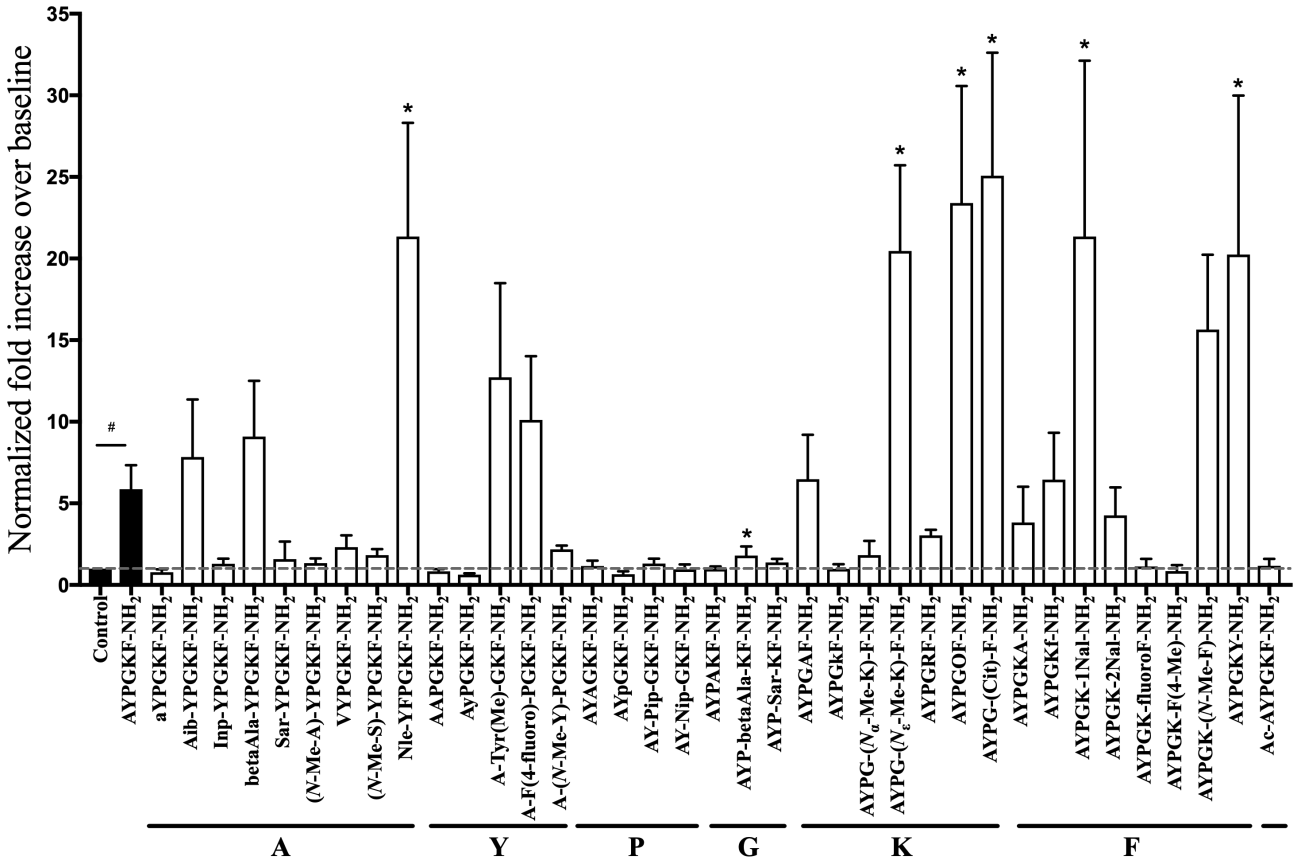

Figure 10. PAR4-mediated phosphorylation of p44/42(ERK) is attenuated upon stimulation of PAR4 with calcium-null peptide. HEK293 cells stably expressing PAR4-YFP were stimulated with AYPGKF-NH_2 (30 μM) or peptide (30 μM) from library of compounds and Western blot for p44/42 phosphorylation (p-p44/42). Data are shown as normalized fold increase over unstimulated control cells. Dashed baseline shows mean of unstimulated baseline for comparison. Dotted baseline shows mean response achieved following AYPGKF-NH_2 stimulation. (# $p > 0.05$ AYPGKF-NH_2 compared to untreated control; *$p > 0.05$ AYPGKF-NH_2 compared to other peptide agonists; one-way ANOVA). Peptides that were unable to stimulate calcium signalling were also generally unable to stimulate phosphorylation of p44/42. Interestingly, several peptides were able to significantly increase phosphorylation of p44/42 compared to AYPGKF-NH_2. (Representative blots shown in supplemental figure S2; *n = 4-5*)

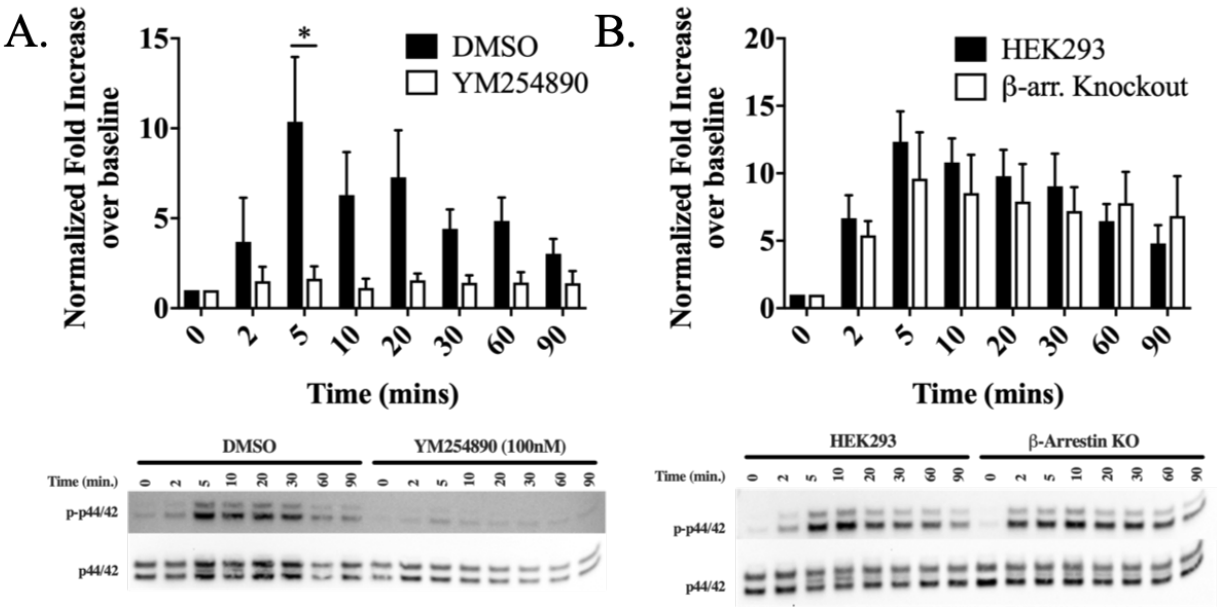

Figure 11. PAR4-mediated phosphorylation of p44/42 (ERK) is $G\alpha_{q/11}$-dependent and β-arrestin-independent. To evaluate contribution of $G\alpha_{q/11}$ and β-arrestin to p44/42 phosphorylation, p-p44/42 was monitored with western blot following stimulation with AYPGKF-NH_2 (30 μM) for various time points. To evaluate contribution of $G\alpha_{q/11}$-signalling cells were incubated with vehicle control (0.001% DMSO) or $G\alpha_{q/11}$-inhibitor, YM254890 (100 nM) prior to agonist stimulation (A). To determine contribution of β-arrestin-signalling to p44/42 phosphorylation, HEK293 and β-arrestin-1/2 CRISPR knockouts were assayed following agonist stimulation (B). Values are expressed as fold increase over unstimulated 0-minute time [(p-p44/22 / total p44/42) / (baseline p-p44/42 / total p44/42)]. Data are analysed with two-way ANOVA (*$p > 0.05$). We find that $G\alpha_{q/11}$ inhibition with YM254890 results in a significant reduction of p44/42 phosphorylation. We observe no statistical difference in ERK activation between HEK293 and β-arrestin-1/2 knockouts HEK293 cells. (Representative blots shown; *n = 4*)

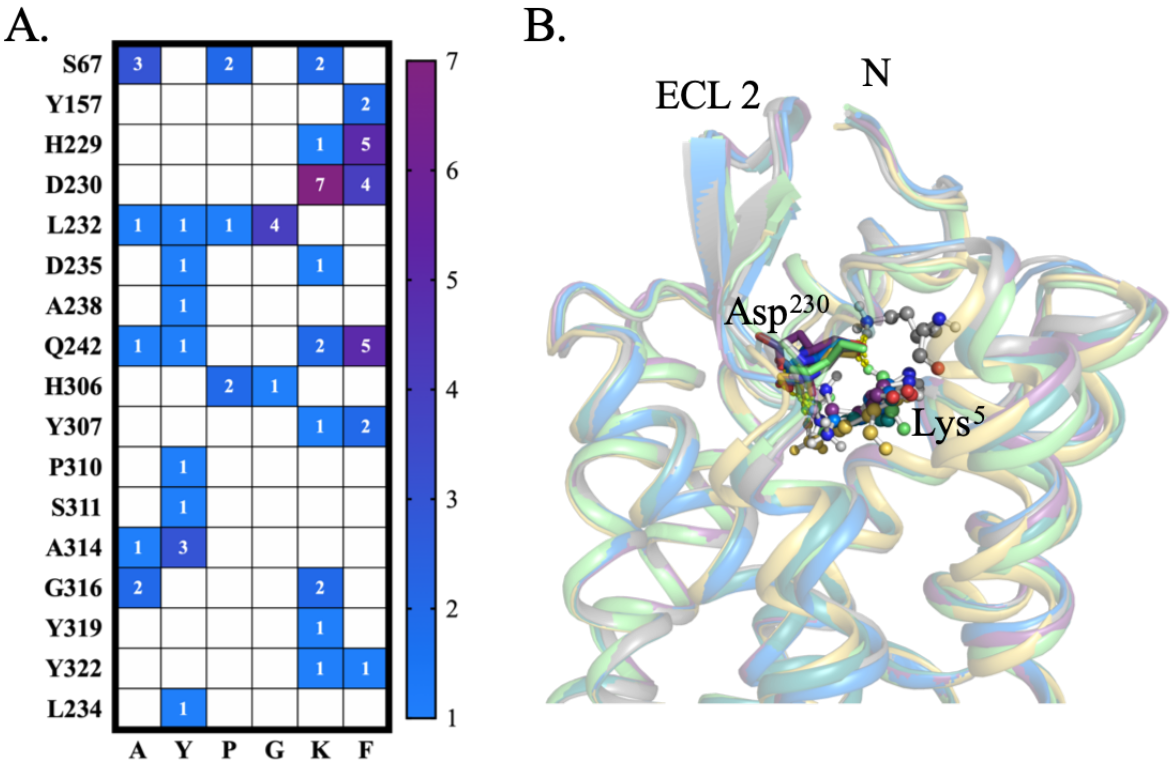

Figure 12. (A) Frequency table of PAR4/AYPGKF-NH_2 interactions as predicted by *in silico* peptide docking (GalaxyPepDock). Numbers represent the frequency with which an atom in a PAR4-AP residue was predicted to interact with an atom of a PAR4 residue. **(B) Representation of the most highly predicted AYPGKF-NH_2 binding site (Asp^{230}, shown as sticks) interacting (shown as yellow dashed lines) with position 5 (Lys^5; shown as ball and sticks) of AYPGKF-NH_2.** Interaction of Lys^5 and Asp^{230} was highly predicted in 7/10 models (B). Alignment of the receptor backbone (shown as transparent cartoon) reveals similar binding poses adopted by the side chain position of Asp^{230} and the position of Lys^5 of AYPGKF-NH_2.

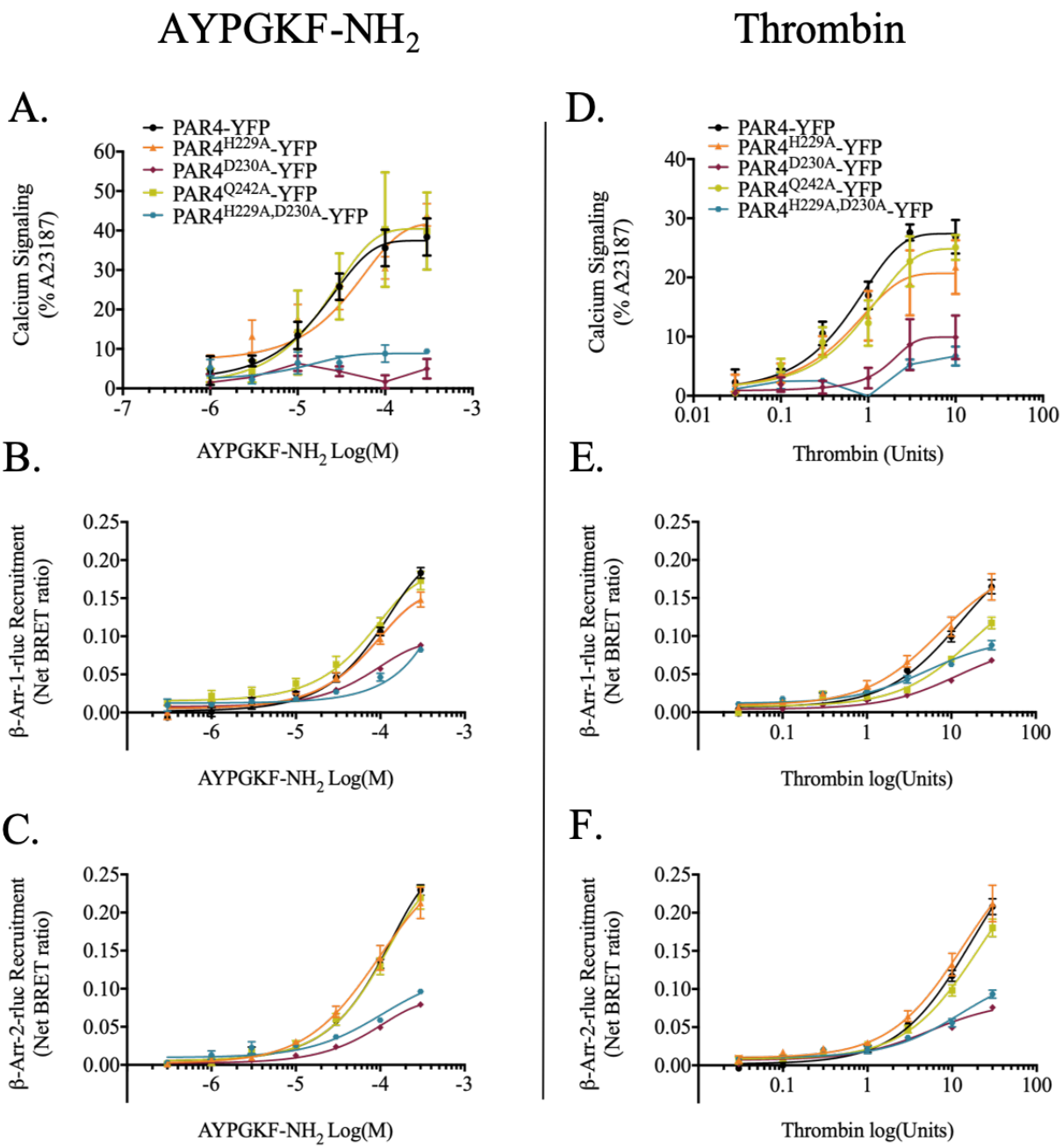

Figure 13. AYPGKF-NH$_2$-stimulated calcium signalling and β-arrestin-1/-2 recruitment in PAR4 extracellular loop 2 mutants. Agonist-stimulated Calcium signalling Calcium signalling in response to AYPGKF-NH$_2$ (A) or thrombin (D) was recorded in HEK293 cells transiently expressing PAR4-YFP, single site-directed mutant PAR4-YFP (PAR4^{H229A}-YFP, PAR4^{D230A}-YFP, PAR4^{Q242A}-YFP), or double site-directed mutant PAR4-YFP (PAR4$^{H229A, D230A}$-YFP, PAR4$^{H229D, A231D}$-YFP). Data are shown as a percentage of maximum response obtained in cells treated with the calcium ionophore A23187 (3 μM) for each transient cell line, per experimental day. AYPGKF-NH$_2$ concentration is in M and thrombin concentration is shown as units. (N=3-5) **Agonist-stimulated β-arrestin-1/-2 recruitment** HEK293 cells were transiently transfected with BRET pair of either β-arrestin-1-rluc or -2-rluc and PAR4-YFP or site-directed mutant PAR4-YFP (described above) and agonist-stimulated arrestin recruitment to PAR4 was monitored. Cells were incubated with increasing concentration of either

1331 AYPGKF-NH_2 (B, C) or thrombin (E, F) for 20 minutes and BRET values were recorded.
1332 BRET values from cells treated with HBSS were also collected to normalize the data. Renilla-
1333 luciferase substrate coelenterazine-h (5 μM) was added 10 minutes prior to data collection.
1334 Data are presented as the normalized net BRET ratio [eYFP/rluc - baseline (HBSS control)].
1335 AYPGKF-NH_2 concentration is in M and thrombin concentration is shown as units. ($n = 4$).

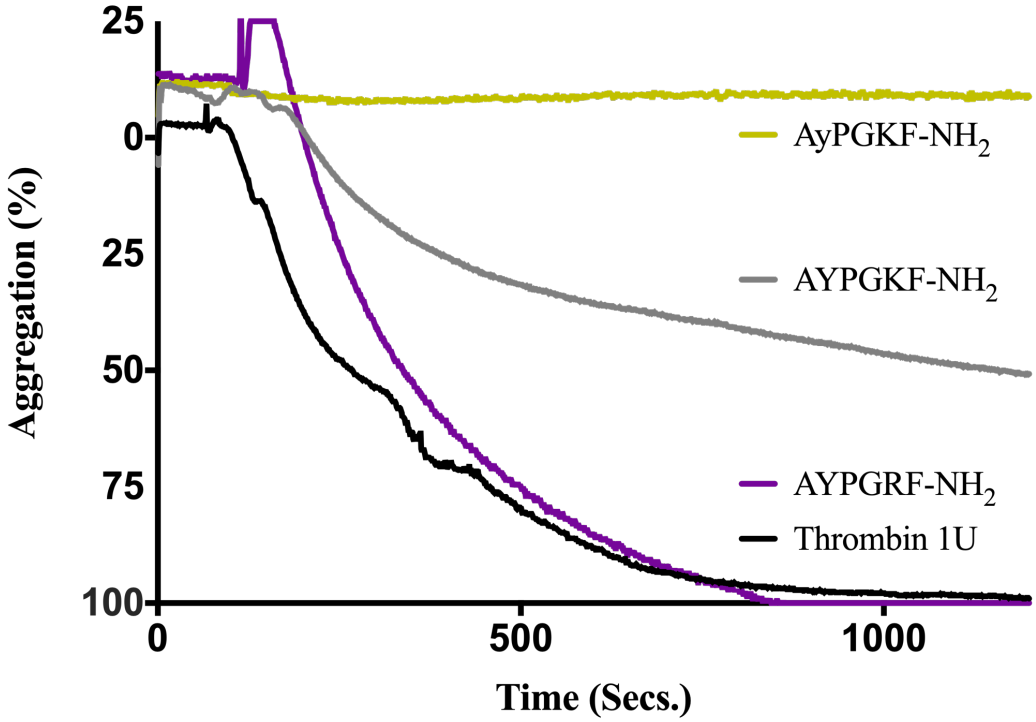

1336 **Figure 14. PAR4 agonist-mediated platelet aggregation.** Both thrombin (1 unit/mL; shown
1337 in black) and AYPGKF-NH_2 (100 µM; shown in grey) initiated PAR4-dependent rat platelet
1338 aggregation. We observed that stimulation of washed platelet samples with a calcium signalling
1339 null, β-arrestin biased peptide, AyPGKF-NH_2 (100 µM; shown in yellow) did not stimulate
1340 platelet aggregation. Further, stimulation of washed platelets with the peptide agonist
1341 AYPGRF-NH_2 (100 µM; shown in purple), caused a robust platelet aggregation comparable to
1342 the response with 1unit/mL thrombin response (*n = 2-4*).

References.

Adams MN, Ramachandran R, Yau M-K, Suen JY, Fairlie DP, Hollenberg MD, Hooper JD. 2011. Structure, function and pathophysiology of protease activated receptors. *Pharmacology & therapeutics* **130**:248–282.

Al-Ani B, Saifeddine M, Kawabata A, Hollenberg MD. 1999. Proteinase activated receptor 2: Role of extracellular loop 2 for ligand-mediated activation. *Br J Pharmacol* **128**:1105–1113.

Al-Ani B, Wijesuriya SJ, Hollenberg MD. 2002. Proteinase-activated receptor 2: differential activation of the receptor by tethered ligand and soluble peptide analogs. *The Journal of pharmacology and experimental therapeutics* **302**:1046–1054.

Bar-Shavit R, Maoz M, Kancharla A, Jaber M, Agranovich D, Grisaru-Granovsky S, Uziely B. 2016. Protease-activated receptors (PARs) in cancer: Novel biased signaling and targets for therapy. *Methods in cell biology* **132**:341–358. doi:10.1016/bs.mcb.2015.11.006

Blackhart BD, Emilsson K, Nguyen D, Teng W, Martelli AJ, Nystedt S, Sundelin J, Scarborough RM. 1996. Ligand cross-reactivity within the protease-activated receptor family. *The Journal of biological chemistry* **271**:16466–16471.

Boitano S, Flynn AN, Schulz SM, Hoffman J, Price TJ, Vagner J. 2011. Potent Agonists of the Protease Activated Receptor 2 (PAR2). *J Med Chem* **54**:1308–1313. doi:10.1021/jm1013049

Cheng RKY, Fiez-Vandal C, Schlenker O, Edman K, Aggeler B, Brown DG, Brown GA, Cooke RM, Dumelin CE, Doré AS, Geschwindner S, Grebner C, Hermansson N-O, Jazayeri A, Johansson P, Leong L, Prihandoko R, Rappas M, Soutter H, Snijder A, Sundström L, Tehan B, Thornton P, Troast D, Wiggin G, Zhukov A, Marshall FH, Dekker N. 2017. Structural insight into allosteric modulation of protease-activated receptor 2. *Nature* **545**:112–115. doi:10.1038/nature22309

Chidiac P. 2016. RGS proteins destroy spare receptors: Effects of GPCR-interacting proteins and signal deamplification on measurements of GPCR agonist potency. *Methods* **92**:87–93. doi:10.1016/j.ymeth.2015.08.011

Coughlin SR. 2005. Protease-activated receptors in hemostasis, thrombosis and vascular biology. *J Thromb Haemost* **3**:1800–1814.

Coughlin SR. 1999. How the protease thrombin talks to cells. *Proceedings of the National Academy of Sciences of the United States of America* **96**:11023–11027.

Covic L, Misra M, Badar J, Singh C, Kuliopulos A. 2002. Pepducin-based intervention of thrombin-receptor signaling and systemic platelet activation. *Nature Medicine* **8**:1161–1165.

Dolinsky TJ, Nielsen JE, McCammon JA, Baker NA. 2004. PDB2PQR: an automated pipeline for the setup of Poisson-Boltzmann electrostatics calculations. *Nucleic Acids Res* **32**:W665-667. doi:10.1093/nar/gkh381

Edelstein LC, Simon LM, Lindsay CR, Kong X, Teruel-Montoya R, Tourdot BE, Chen ES, Ma L, Coughlin S, Nieman M, Holinstat M, Shaw CA, Bray PF. 2014. Common variants in the human platelet PAR4 thrombin receptor alter platelet function and differ by race. *Blood* **124**:3450–3458. doi:10.1182/blood-2014-04-572479

Erlandson SC, McMahon C, Kruse AC. 2018. Structural Basis for G Protein–Coupled Receptor Signaling. *doi.org* **47**:annurev–biophys–070317–032931.

Faruqi TR, Weiss EJ, Shapiro MJ, Huang W, Coughlin SR. 2000. Structure-function analysis of protease-activated receptor 4 tethered ligand peptides. Determinants of specificity and utility in assays of receptor function. *The Journal of biological chemistry* **275**:19728–19734.

Ferguson SSG, Caron MG. 2004. Green Fluorescent Protein-Tagged β-Arrestin Translocation as a Measure of G Protein-Coupled Receptor Activation In: Smrcka AV, editor. G Protein Signaling: Methods and Protocols, Methods in Molecular Biology™. Totowa, NJ: Humana Press. pp. 121–126. doi:10.1385/1-59259-430-1:121

1396 Fredriksson R, Schioth HB. 2005. The repertoire of G-protein-coupled receptors in fully
1397 sequenced genomes. *Molecular pharmacology* **67**:1414–1425.
1398 doi:10.1124/mol.104.009001
1399 French SL, Hamilton JR. 2016. Protease-activated receptor 4: from structure to function and
1400 back again. *Br J Pharmacol* **173**:2952–2965. doi:10.1111/bph.13455
1401 Gerszten RE, Chen J, Ishii M, Ishii K, Wang L, Nanevicz T, Turck CW, Vu TK, Coughlin SR.
1402 1994. Specificity of the thrombin receptor for agonist peptide is defined by its
1403 extracellular surface. *Nature* **368**:648–651.
1404 Graham FL, van der Eb AJ. 1973. A new technique for the assay of infectivity of human
1405 adenovirus 5 DNA. *Virology* **52**:456–467.
1406 Hilger D, Masureel M, Kobilka BK. 2018. Structure and dynamics of GPCR signaling
1407 complexes. *Nature structural & molecular biology* **25**:4–12. doi:10.1038/s41594-017-
1408 0011-7
1409 Hoffmann W, Langenhan J, Huhmann S, Moschner J, Chang R, Accorsi M, Seo J,
1410 Rademann J, Meijer G, Koksch B, Bowers MT, von Helden G, Pagel K. 2019. An
1411 Intrinsic Hydrophobicity Scale for Amino Acids and Its Application to Fluorinated
1412 Compounds. *Angewandte Chemie International Edition* **58**:8216–8220.
1413 doi:10.1002/anie.201813954
1414 Holinstat M, Voss B, Bilodeau ML, McLaughlin JN, Cleator J, Hamm HE. 2006. PAR4, but
1415 not PAR1, signals human platelet aggregation via Ca2+ mobilization and synergistic
1416 P2Y12 receptor activation. *The Journal of biological chemistry* **281**:26665–26674.
1417 Hollenberg MD. 2003. Proteinase-activated receptors: Tethered ligands and receptor-
1418 activating peptides. *Drug Dev Res* **59**:336–343. doi:10.1002/ddr.10301
1419 Hollenberg MD, Mihara K, Polley D, Suen JY, Han A, Fairlie DP, Ramachandran R. 2014.
1420 Biased signalling and proteinase-activated receptors (PARs): targeting inflammatory
1421 disease. *British journal of pharmacology* **171**:1180–1194.
1422 Ishihara H, Connolly AJ, Zeng D, Kahn ML, Zheng YW, Timmons C, Tram T, Coughlin SR.
1423 1997. Protease-activated receptor 3 is a second thrombin receptor in humans.
1424 *Nature* **386**:502–506.
1425 Jacques SL, Kuliopulos A. 2003. Protease-activated receptor-4 uses dual prolines and an
1426 anionic retention motif for thrombin recognition and cleavage. *The Biochemical*
1427 *journal* **376**:733–740.
1428 Jacques SL, LeMasurier M, Sheridan PJ, Seeley SK, Kuliopulos A. 2000. Substrate-assisted
1429 catalysis of the PAR1 thrombin receptor. Enhancement of macromolecular
1430 association and cleavage. *The Journal of biological chemistry* **275**:40671–40678.
1431 Jean-Charles P-Y, Kaur S, Shenoy SK. 2017. GPCR signaling via β-arrestin-dependent
1432 mechanisms. *J Cardiovasc Pharmacol* **70**:142–158.
1433 doi:10.1097/FJC.0000000000000482
1434 Kahn ML, Zheng YW, Huang W, Bigornia V, Zeng D, Moff S, Farese RVJ, Tam C, Coughlin
1435 SR. 1998. A dual thrombin receptor system for platelet activation. *Nature* **394**:690–
1436 694.
1437 Khan A, Li D, Ibrahim S, Smyth E, Woulfe DS. 2014. The Physical Association of the P2Y12
1438 Receptor with PAR4 Regulates Arrestin-Mediated Akt Activation. *Molecular*
1439 *pharmacology* **86**:1–11.
1440 Kim BH, Wang FI, Pereverzev A, Chidiac P, Dixon SJ. 2019. Toward Defining the
1441 Pharmacophore for Positive Allosteric Modulation of PTH1 Receptor Signaling by
1442 Extracellular Nucleotides. *ACS Pharmacol Transl Sci* **2**:155–167.
1443 doi:10.1021/acsptsci.8b00053
1444 Lee H, Heo L, Lee MS, Seok C. 2015. GalaxyPepDock: a protein–peptide docking tool
1445 based on interaction similarity and energy optimization. *Nucleic Acids Res* **43**:W431–
1446 W435. doi:10.1093/nar/gkv495
1447 Lerner DJ, Chen M, Tram T, Coughlin SR. 1996. Agonist recognition by proteinase-activated
1448 receptor 2 and thrombin receptor. Importance of extracellular loop interactions for
1449 receptor function. *The Journal of biological chemistry* **271**:13943–13947.

1450 Li D, D'Angelo L, Chavez M, Woulfe DS. 2011. Arrestin-2 differentially regulates PAR4 and
1451 ADP receptor signaling in platelets. *The Journal of biological chemistry* **286**:3805–
1452 3814.
1453 Liu LW, Vu TK, Esmon CT, Coughlin SR. 1991. The region of the thrombin receptor
1454 resembling hirudin binds to thrombin and alters enzyme specificity. *The Journal of*
1455 *biological chemistry* **266**:16977–16980.
1456 Madeira F, Park YM, Lee J, Buso N, Gur T, Madhusoodanan N, Basutkar P, Tivey ARN,
1457 Potter SC, Finn RD, Lopez R. 2019. The EMBL-EBI search and sequence analysis
1458 tools APIs in 2019. *Nucleic Acids Res* **47**:W636–W641. doi:10.1093/nar/gkz268
1459 Miller MM, Banville J, Friends T, Gagnon M, Hangeland JJ, Lavalee J-F, Martel A, O'Grady
1460 H, Remillard R, Ruediger EH, Tremblay F, Posy S, Allegretto N, Guarino VR, Harden
1461 D, Harper TW, Hartl K, Josephs J, Malmstrom S, Watson CA, Yang Y, Zhang G,
1462 Wong PC, Yang J, Bouvier M, Seiffert DA, Wexler RR, Lawrence RM, Priestley ES,
1463 Marinier A. 2019. Discovery of Potent Protease-Activated Receptor 4 Antagonists
1464 with in vivo Antithrombotic Efficacy. *J Med Chem*.
1465 doi:10.1021/acs.jmedchem.9b00186
1466 Morrow DA, Braunwald E, Bonaca MP, Ameriso SF, Dalby AJ, Fish MP, Fox KA, Lipka LJ,
1467 Liu X, Nicolau JC, Ophuis AJ, Paolasso E, Scirica BM, Spinar J, Theroux P, Wiviott
1468 SD, Strony J, Murphy SA. 2012. Vorapaxar in the secondary prevention of
1469 atherothrombotic events. *The New England journal of medicine* **366**:1404–1413.
1470 Morrow DA, Scirica BM, Fox KA, Berman G, Strony J, Veltri E, Bonaca MP, Fish P, McCabe
1471 CH, Braunwald E. 2009. Evaluation of a novel antiplatelet agent for secondary
1472 prevention in patients with a history of atherosclerotic disease: design and rationale
1473 for the Thrombin-Receptor Antagonist in Secondary Prevention of Atherothrombotic
1474 Ischemic Events (TRA 2 degrees P)-TIMI 50 trial. *Am Heart J* **158**:335–341 e3.
1475 Moschonas IC, Kellici TF, Mavromoustakos T, Stathopoulos P, Tsikaris V, Magafa V, Tzakos
1476 AG, Tselepis AD. 2017. Molecular requirements involving the human platelet
1477 protease-activated receptor-4 mechanism of activation by peptide analogues of its
1478 tethered-ligand. *Platelets* **28**:812–821. doi:10.1080/09537104.2017.1282607
1479 Nanevicz T, Ishii M, Wang L, Chen M, Chen J, Turck CW, Cohen FE, Coughlin SR. 1995.
1480 Mechanisms of thrombin receptor agonist specificity. Chimeric receptors and
1481 complementary mutations identify an agonist recognition site. *The Journal of*
1482 *biological chemistry* **270**:21619–21625.
1483 Nieman MT. 2008. Protease-Activated Receptor 4 Uses Anionic Residues To Interact with α-
1484 Thrombin in the Absence or Presence of Protease-Activated Receptor 1.
1485 *Biochemistry* **47**:13279–13286. doi:10.1021/bi801334s
1486 Nieman MT, Schmaier AH. 2007. Interaction of Thrombin with PAR1 and PAR4 at the
1487 Thrombin Cleavage Site. *Biochemistry* **46**:8603–8610. doi:10.1021/bi700597p
1488 Nystedt S, Emilsson K, Wahlestedt C, Sundelin J. 1994. Molecular cloning of a potential
1489 proteinase activated receptor. *Proceedings of the National Academy of Sciences of*
1490 *the United States of America* **91**:9208–9212.
1491 Pierce KL, Premont RT, Lefkowitz RJ. 2002. Seven-transmembrane receptors. *Nature*
1492 *Reviews Molecular Cell Biology* **3**:639–650.
1493 Ramachandran R, Mihara K, Thibeault P, Vanderboor CM, Petri B, Saifeddine M, Bouvier M,
1494 Hollenberg MD. 2017. Targeting a Proteinase-Activated Receptor 4 (PAR4) Carboxyl
1495 Terminal Motif to Regulate Platelet Function. *Molecular pharmacology* **91**:287–295.
1496 Rwibasira Rudinga G, Khan GJ, Kong Y. 2018. Protease-Activated Receptor 4 (PAR4): A
1497 Promising Target for Antiplatelet Therapy. *Int J Mol Sci* **19**.
1498 doi:10.3390/ijms19020573
1499 Sánchez Centellas D, Gudlur S, Vicente-Carrillo A, Ramström S, Lindahl TL. 2017. A cluster
1500 of aspartic residues in the extracellular loop II of PAR 4 is important for thrombin
1501 interaction and activation of platelets. *Thrombosis Research* **154**:84–92.
1502 doi:10.1016/j.thromres.2017.04.006
1503 Scarborough RM, Naughton MA, Teng W, Hung DT, Rose J, Vu TK, Wheaton VI, Turck CW,
1504 Coughlin SR. 1992. Tethered ligand agonist peptides. Structural requirements for

1505 thrombin receptor activation reveal mechanism of proteolytic unmasking of agonist
1506 function. *The Journal of biological chemistry* **267**:13146–13149.
1507 Schindelin J, Arganda-Carreras I, Frise E, Kaynig V, Longair M, Pietzsch T, Preibisch S,
1508 Rueden C, Saalfeld S, Schmid B, Tinevez J-Y, White DJ, Hartenstein V, Eliceiri K,
1509 Tomancak P, Cardona A. 2012. Fiji: an open-source platform for biological-image
1510 analysis. *Nature Methods* **9**:676–682. doi:10.1038/nmeth.2019
1511 Scirica BM, Bonaca MP, Braunwald E, De Ferrari GM, Isaza D, Lewis BS, Mehrhof F, Merlini
1512 PA, Murphy SA, Sabatine MS, Tendera M, Van de Werf F, Wilcox R, Morrow DA.
1513 2012. Vorapaxar for secondary prevention of thrombotic events for patients with
1514 previous myocardial infarction: a prespecified subgroup analysis of the TRA 2°P-TIMI
1515 50 trial. *The Lancet* **380**:1317–1324. doi:10.1016/S0140-6736(12)61269-0
1516 Seyedabadi M, Ghahremani MH, Albert PR. 2019. Biased signaling of G protein coupled
1517 receptors (GPCRs): Molecular determinants of GPCR/transducer selectivity and
1518 therapeutic potential. *Pharmacol Ther* **200**:148–178.
1519 doi:10.1016/j.pharmthera.2019.05.006
1520 Shapiro MJ, Weiss EJ, Faruqi TR, Coughlin SR. 2000. Protease-activated receptors 1 and 4
1521 are shut off with distinct kinetics after activation by thrombin. *The Journal of biological*
1522 *chemistry* **275**:25216–25221.
1523 Sievers F, Wilm A, Dineen D, Gibson TJ, Karplus K, Li W, Lopez R, McWilliam H, Remmert
1524 M, Söding J, Thompson JD, Higgins DG. 2011. Fast, scalable generation of high-
1525 quality protein multiple sequence alignments using Clustal Omega. *Molecular*
1526 *Systems Biology* **7**:539. doi:10.1038/msb.2011.75
1527 Sriram K, Insel PA. 2018. G Protein-Coupled Receptors as Targets for Approved Drugs:
1528 How Many Targets and How Many Drugs? *Molecular pharmacology* **93**:251–258.
1529 Tourdot BE, Stoveken H, Trumbo D, Yeung J, Kanthi Y, Edelstein LC, Bray PF, Tall GG,
1530 Holinstat M. 2018. Genetic Variant in Human PAR (Protease-Activated Receptor) 4
1531 Enhances Thrombus Formation Resulting in Resistance to Antiplatelet Therapeutics.
1532 *Arterioscler Thromb Vasc Biol* **38**:1632–1643. doi:10.1161/ATVBAHA.118.311112
1533 Venkatakrishnan AJ, Deupi X, Lebon G, Tate CG, Schertler GF, Babu MM. 2014. Molecular
1534 signatures of G-protein-coupled receptors. *Nature* **494**:185–194.
1535 doi:10.1038/nature11896
1536 Vu TK, Hung DT, Wheaton VI, Coughlin SR. 1991. Molecular cloning of a functional
1537 thrombin receptor reveals a novel proteolytic mechanism of receptor activation. *Cell*
1538 **64**:1057–1068.
1539 Webb B, Sali A. 2017. Protein Structure Modeling with MODELLERFunctional Genomics.
1540 New York, NY: Humana Press, New York, NY. pp. 39–54. doi:10.1007/978-1-4939-
1541 7231-9_4
1542 Wheatley M, Wootten D, Conner MT, Simms J, Kendrick R, Logan RT, Poyner DR, Barwell
1543 J. 2012. Lifting the lid on GPCRs: the role of extracellular loops. *Br J Pharmacol*
1544 **165**:1688–1703. doi:10.1111/j.1476-5381.2011.01629.x
1545 Wilson SJ, Ismat FA, Wang Z, Cerra M, Narayan H, Raftis J, Gray TJ, Connell S, Garonzik
1546 S, Ma X, Yang J, Newby DE. 2017. PAR4 (Protease-Activated Receptor 4)
1547 Antagonism With BMS-986120 Inhibits Human Ex Vivo Thrombus Formation.
1548 *Arteriosclerosis, Thrombosis, and Vascular Biology* ATVBAHA.117.310104.
1549 doi:10.1161/ATVBAHA.117.310104
1550 Wong PC, Seiffert D, Bird JE, Watson CA, Bostwick JS, Giancarli M, Allegretto N, Hua J,
1551 Harden D, Guay J, Callejo M, Miller MM, Lawrence RM, Banville J, Guy J, Maxwell
1552 BD, Priestley ES, Marinier A, Wexler RR, Bouvier M, Gordon DA, Schumacher WA,
1553 Yang J. 2017. Blockade of protease-activated receptor-4 (PAR4) provides robust
1554 antithrombotic activity with low bleeding. *Science translational medicine* **9**:eaaf5294.
1555 doi:10.1126/scitranslmed.aaf5294
1556 Woolley MJ, Conner AC. 2017. Understanding the common themes and diverse roles of the
1557 second extracellular loop (ECL2) of the GPCR super-family. *Molecular and Cellular*
1558 *Endocrinology*, Pleiotropic GPCR signaling in health and disease **449**:3–11.
1559 doi:10.1016/j.mce.2016.11.023

1560 Wu CC, Huang SW, Hwang TL, Kuo SC, Lee FY, Teng CM. 2000. YD-3, a novel inhibitor of
1561 protease-induced platelet activation. *Br J Pharmacol* **130**:1289–1296.
1562 Xu WF, Andersen H, Whitmore TE, Presnell SR, Yee DP, Ching A, Gilbert T, Davie EW,
1563 Foster DC. 1998. Cloning and characterization of human protease-activated receptor
1564 4. *Proceedings of the National Academy of Sciences of the United States of America*
1565 **95**:6642–6646.
1566 Young SE, Duvernay MT, Schulte ML, Nance KD, Melancon BJ, Engers J, Wood MR,
1567 Hamm HE, Lindsley CW. 2010. A Novel and Selective PAR4 Antagonist:
1568 ML354Probe Reports from the NIH Molecular Libraries Program. Bethesda (MD):
1569 National Center for Biotechnology Information (US).
1570

1571 # Supplemental tables and figures:

1572

1573 **Table S1: MS data of synthesized peptides.**

1574

Compound	Molecular Formula (M)	Calc. $[M+H]^+$ (*m/z*)	Found $[M+H]^+$ (*m/z*)
Ac-AYPGKF-NH$_2$	$C_{36}H_{50}N_8O_8$	723.38	723.43
AAPGKF-NH$_2$	$C_{28}H_{44}N_8O_6$	589.35	589.30
AYAGKF-NH$_2$	$C_{32}H_{46}N_8O_7$	655.36	655.43
AYPAKF-NH$_2$	$C_{35}H_{50}N_8O_7$	695.39	695.46
AYPGAF-NH$_2$	$C_{31}H_{41}N_7O_7$	624.31	625.36
AYPGKA-NH$_2$	$C_{28}H_{44}N_8O_7$	605.34	606.42
aYPGKF-NH$_2$	$C_{34}H_{48}N_8O_7$	681.37	681.44
AyPGKF-NH$_2$	$C_{34}H_{48}N_8O_7$	681.37	681.44
AYPGkF-NH$_2$	$C_{34}H_{48}N_8O_7$	681.37	681.46
AYPGKf-NH$_2$	$C_{34}H_{48}N_8O_7$	681.37	681.48
Aib-YPGKF-NH$_2$	$C_{35}H_{50}N_8O_7$	695.39	695.49
Sar-YPGKF-NH$_2$	$C_{34}H_{48}N_8O_7$	681.37	681.38
Inp-YPGKF-NH$_2$	$C_{37}H_{52}N_8O_7$	721.40	721.50
betaAla-YPGKF-NH$_2$	$C_{34}H_{48}N_8O_7$	681.37	681.46
A-Tyr(Me)-PGKF-NH$_2$	$C_{35}H_{50}N_8O_7$	695.39	695.48
A-F(4-fluoro)-PGKF-NH$_2$	$C_{34}H_{47}N_8O_6F$	683.37	683.36
AY-Pip-GKF-NH$_2$	$C_{35}H_{50}N_8O_7$	695.39	695.39
AY-Nip-GKF-NH$_2$	$C_{35}H_{50}N_8O_7$	695.39	695.39
AYP-Sar-KF-NH$_2$	$C_{35}H_{50}N_8O_7$	695.39	695.39
AYP-betaAla-KF-NH$_2$	$C_{35}H_{50}N_8O_7$	695.39	695.48
AYPGK-1Nal-NH$_2$	$C_{38}H_{50}N_8O_7$	731.38	731.48
AYPGK-2Nal-NH$_2$	$C_{38}H_{50}N_8O_7$	731.38	731.50
AYPGK-F(4-fluoro)-NH$_2$	$C_{34}H_{47}N_8O_7F$	699.36	699.38
AYPGK-F(4-Me)-NH$_2$	$C_{35}H_{50}N_8O_7$	695.39	695.39
AYpGKF-NH$_2$	$C_{34}H_{48}N_8O_7$	681.37	681.37
AYPGK-(*N*-Me-F)-NH$_2$	$C_{35}H_{50}N_8O_7$	695.39	695.39
AYPG-(N_α-Me-K)-F-NH$_2$	$C_{35}H_{50}N_8O_7$	695.39	695.39
A-(*N*-Me-Y)-PGKF-NH$_2$	$C_{35}H_{50}N_8O_7$	695.39	695.39
(*N*-Me-A)-YPGKF-NH$_2$	$C_{35}H_{50}N_8O_7$	695.39	695.39
VYPGKF-NH$_2$	$C_{36}H_{52}N_8O_7$	709.40	709.40
(*N*-Me-S)-YPGKF-NH$_2$	$C_{35}H_{50}N_8O_8$	711.38	711.38
Nle-YPGKF-NH$_2$	$C_{37}H_{54}N_8O_7$	723.42	723.42
AYPGRF-NH$_2$	$C_{34}H_{48}N_{10}O_7$	709.38	709.38
AYPGOF-NH$_2$	$C_{33}H_{46}N_8O_7$	667.36	667.36
AYPG-Cit-F-NH$_2$	$C_{34}H_{47}N_9O_8$	710.36	710.36
AYPG-(N_ε-Me-K)-F-NH$_2$	$C_{35}H_{50}N_8O_7$	695.39	695.39
AYPGKY-NH$_2$	$C_{34}H_{48}N_8O_8$	697.37	697.37

1575

Figure S1: Analytical RP-HPLC UV detection chromatograms of synthesized peptides. Purity of all peptides are > 95% as determined by analytical RP-HPLC UV detection (see traces below).

Ac-AYPGKF-NH_2:

t_R = 10.50 min; gradient = 10% to 50% (solvent A in solvent B, 0 to 10 min)

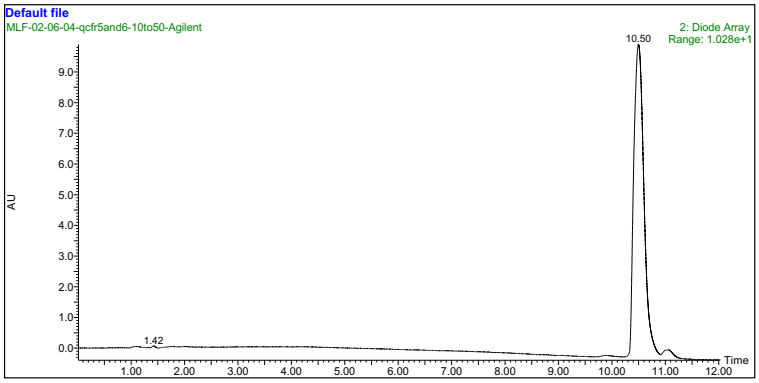

AAPGKF-NH_2:

t_R = 8.08 min; gradient = 10% to 70% (solvent A in solvent B, 0 to 10 min)

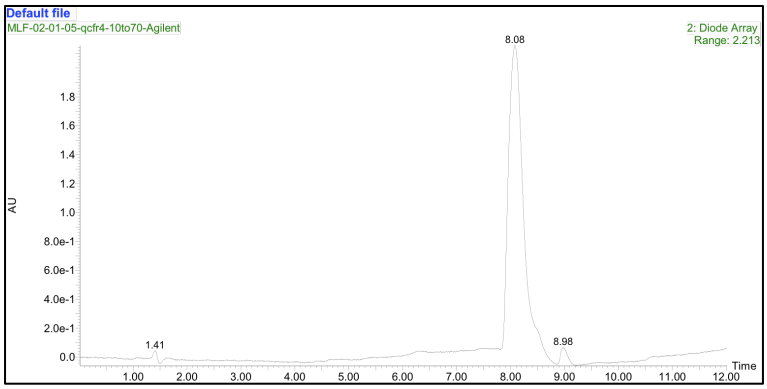

AYAGKF-NH_2:

t_R = 9.14 min; gradient = 10% to 60% (solvent A in solvent B, 0 to 10 min)

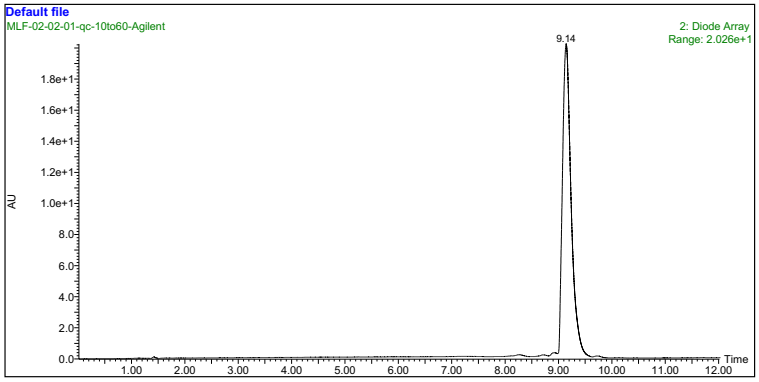

AYPAKF-NH_2:

t_R = 10.53 min; gradient = 10% to 50% (solvent A in solvent B, 0 to 10 min)

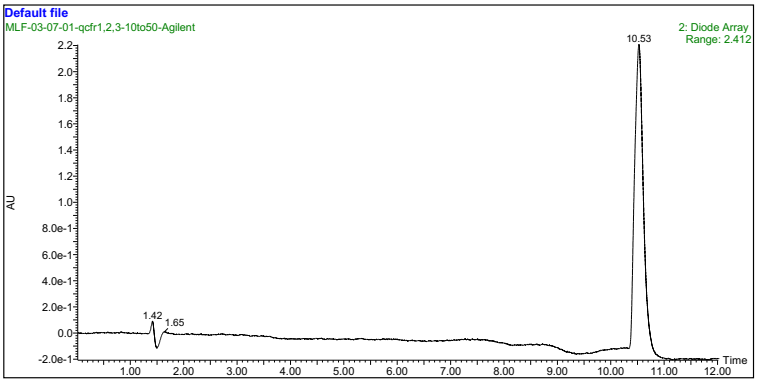

AYPGAF-NH_2:

t_R = 10.83 min; gradient = 10% to 50% (solvent A in solvent B, 0 to 10 min)

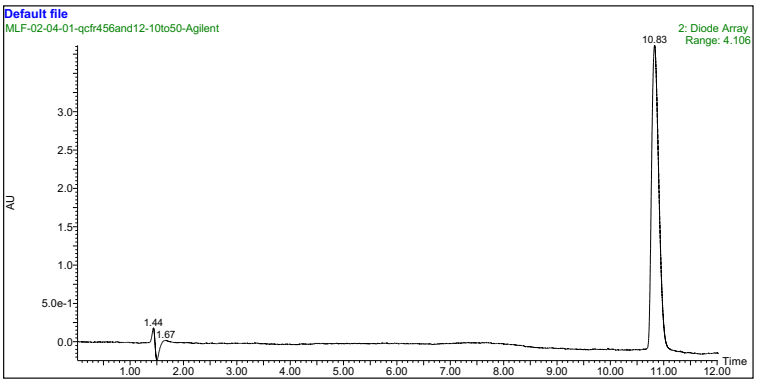

AYPGKA-NH_2:

t_R = 9.71 min; gradient = 5% to 30% (solvent A in solvent B, 0 to 10 min)

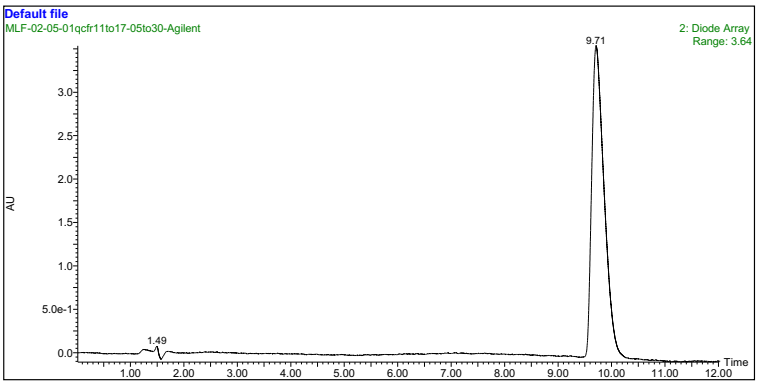

aYPGKF-NH_2:

t_R = 10.06 min; gradient = 10% to 50% (solvent A in solvent B, 0 to 10 min)

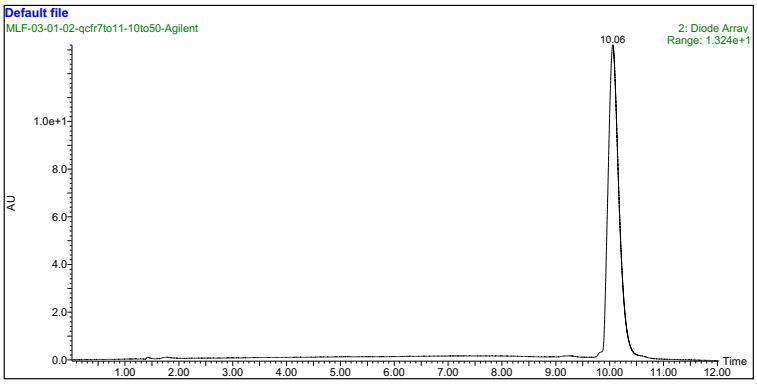

AyPGKF-NH_2:

t_R = 9.49 min; gradient = 15% to 50% (solvent A in solvent B, 0 to 10 min)

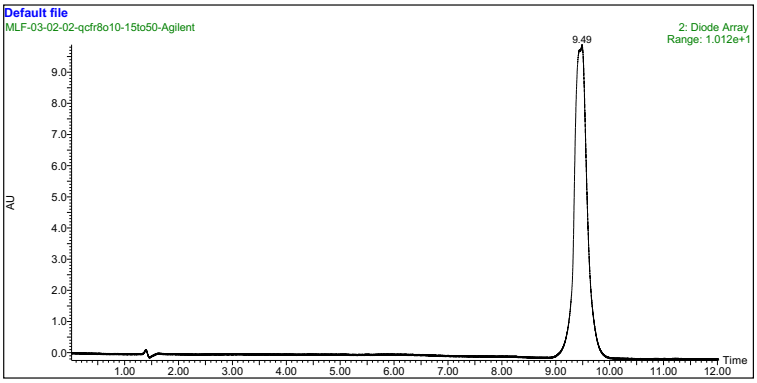

AYPGkF-NH_2:

t_R = 9.17 min; gradient = 10% to 70% (solvent A in solvent B, 0 to 10 min)

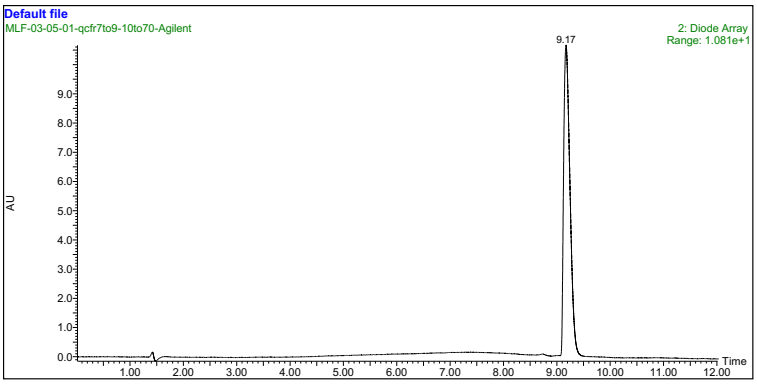

AYPGKf-NH_2:

t_R = 9.04 min; gradient = 10% to 70% (solvent A in solvent B, 0 to 10 min)

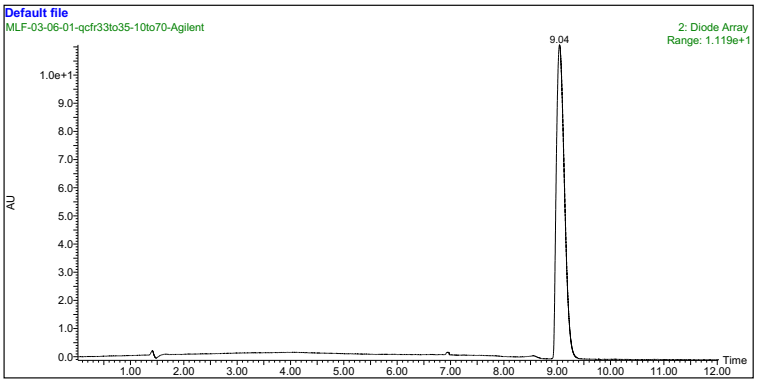

Aib-YPGKF-NH_2:

t_R = 9.35 min; gradient = 10% to 70% (solvent A in solvent B, 0 to 10 min)

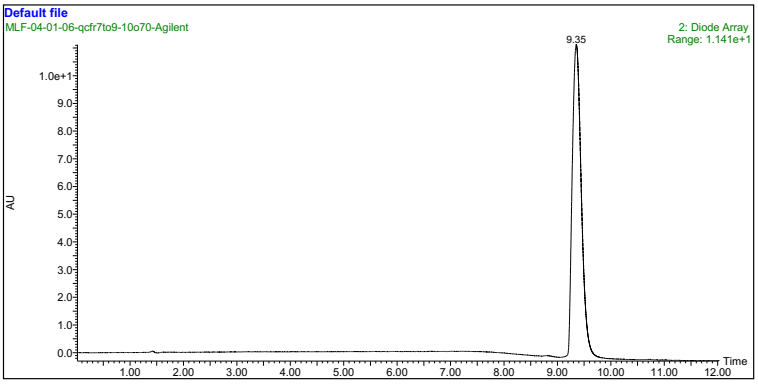

Sar-YPGKF-NH_2:

t_R = 9.23 min; gradient = 10% to 70% (solvent A in solvent B, 0 to 10 min)

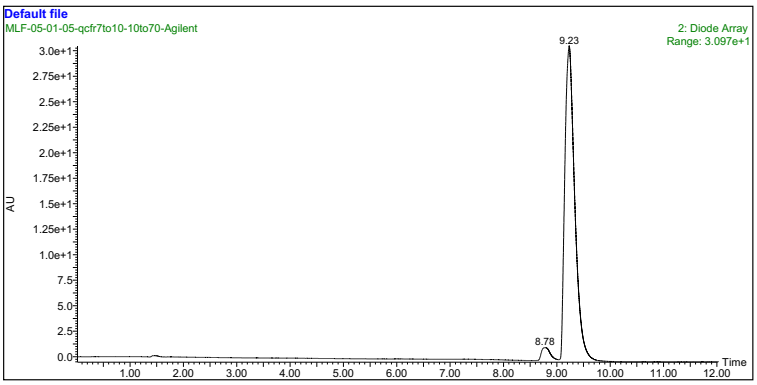

Inp-YPGKF-NH_2:

t_R = 9.26 min; gradient = 10% to 70% (solvent A in solvent B, 0 to 10 min)

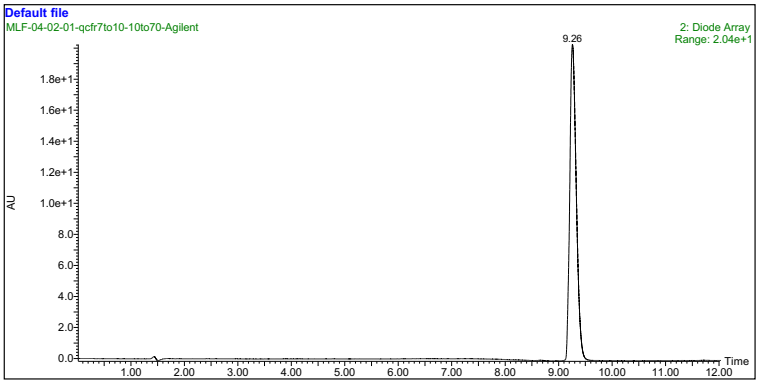

betaAla-YPGKF-NH_2:

t_R = 9.34 min; gradient = 10% to 70% (solvent A in solvent B, 0 to 10 min)

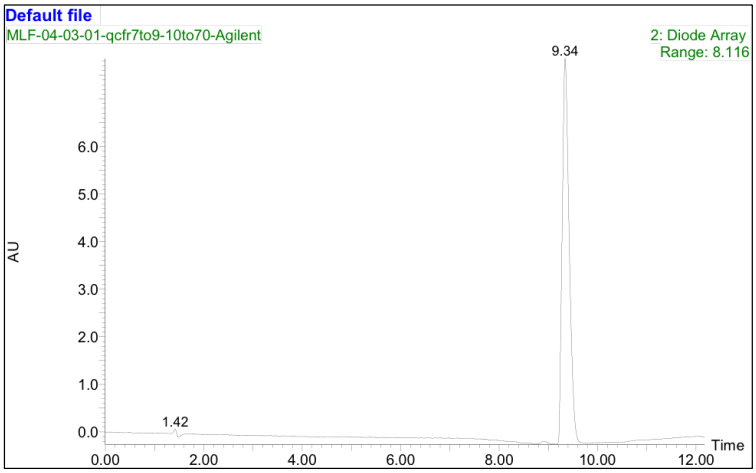

A-Tyr(Me)-PGKF-NH_2:

t_R = 9.57 min; gradient = 13% to 70% (solvent A in solvent B, 0 to 10 min)

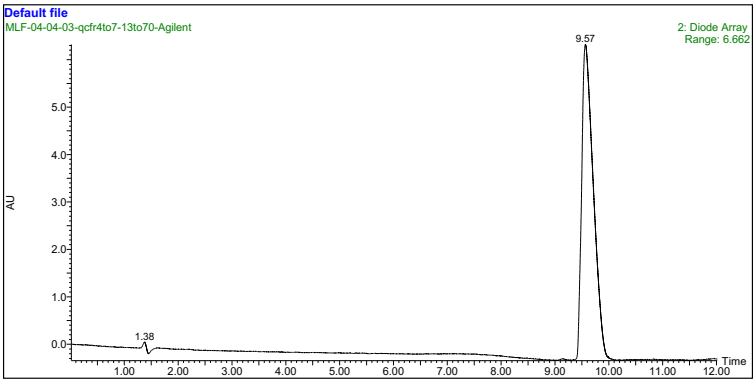

A-F(4-fluoro)-PGKF-NH_2:

t_R = 9.63 min; gradient = 13% to 70% (solvent A in solvent B, 0 to 10 min)

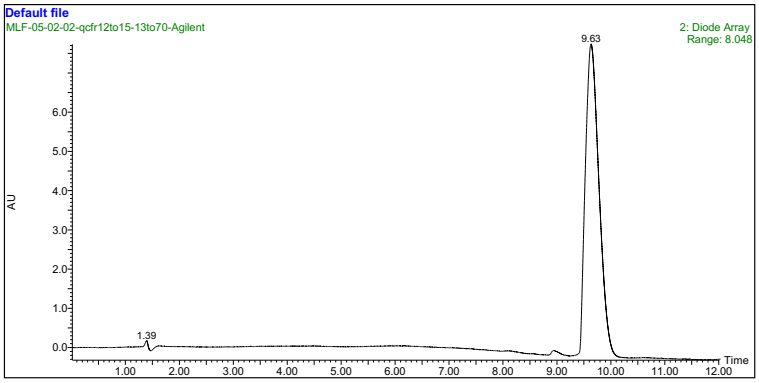

AY-Pip-GKF-NH_2:

t_R = 9.25 min; gradient = 13% to 70% (solvent A in solvent B, 0 to 10 min)

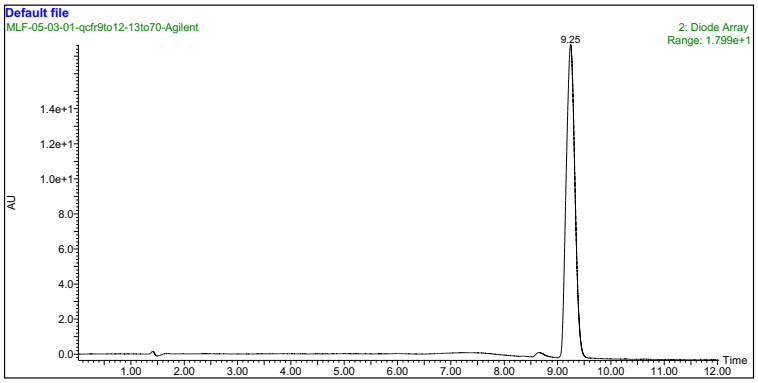

AY-Nip-GKF-NH_2:

t_R = 8.77 min; gradient = 13% to 70% (solvent A in solvent B, 0 to 10 min)

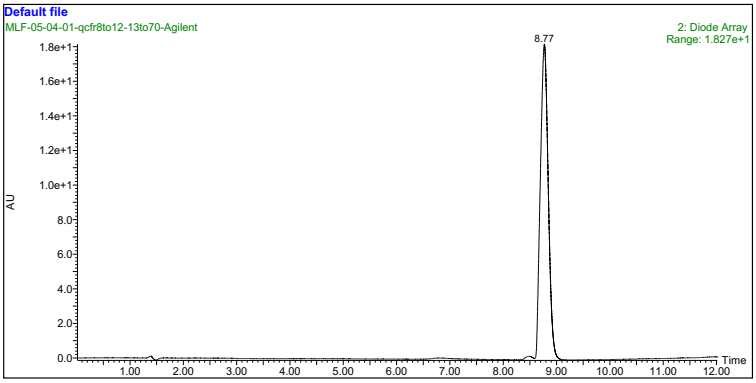

AYP-Sar-KF-NH_2:

t_R = 9.56 min; gradient = 10% to 60% (solvent A in solvent B, 0 to 10 min)

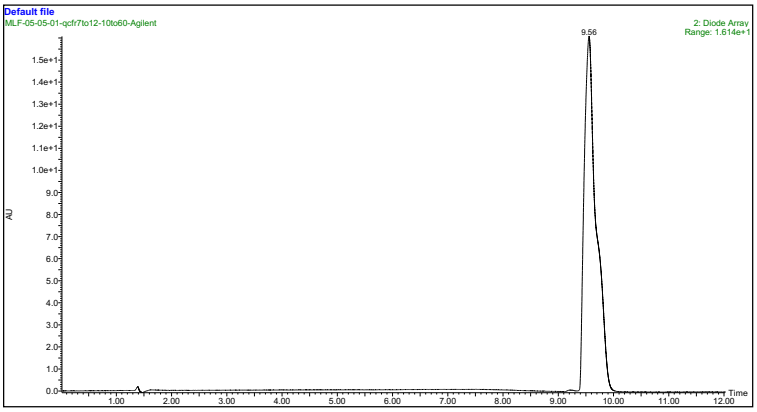

AYP-betaAla-KF-NH_2:

t_R = 9.38 min; gradient = 10% to 70% (solvent A in solvent B, 0 to 10 min)

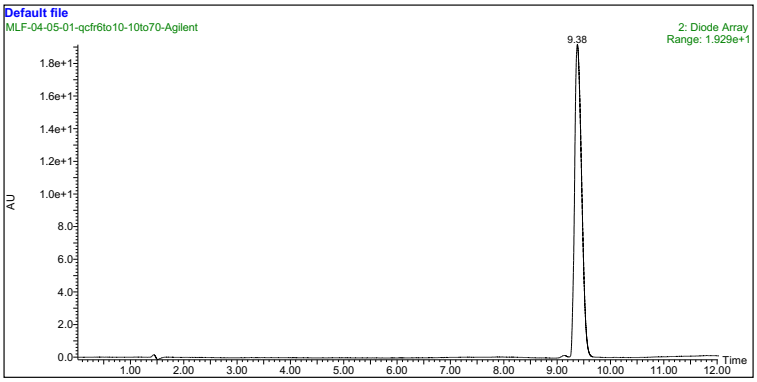

AYPGK-1Nal-NH_2:

t_R = 9.71 min; gradient = 13% to 70% (solvent A in solvent B, 0 to 10 min)

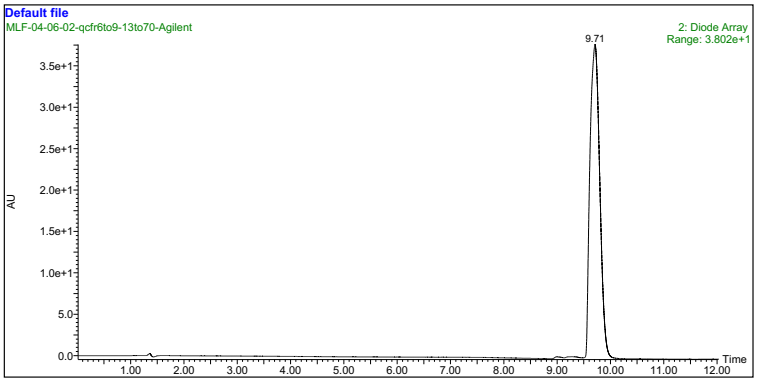

AYPGK-2Nal-NH_2:

t_R = 9.72 min; gradient = 13% to 70% (solvent A in solvent B, 0 to 10 min)

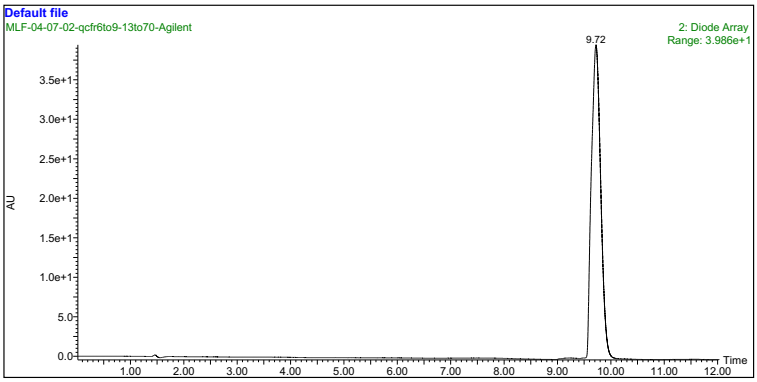

AYPGK-F(4-fluoro)-NH_2:

t_R = 8.91 min; gradient = 13% to 70% (solvent A in solvent B, 0 to 10 min)

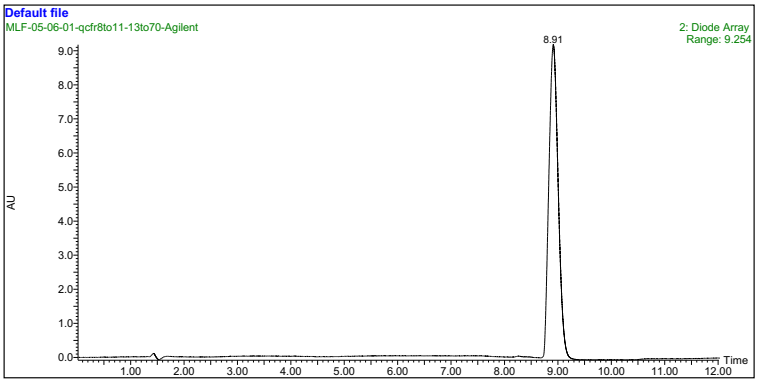

AYPGK-F(4-Me)-NH_2:

t_R = 9.32 min; gradient = 13% to 70% (solvent A in solvent B, 0 to 10 min)

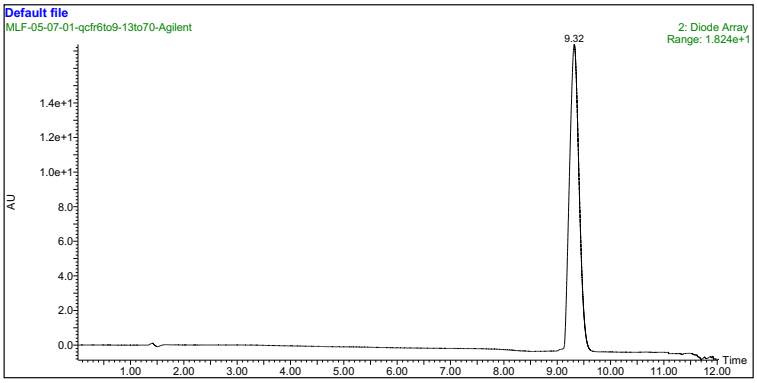

AYpGKF-NH_2:

t_R = 9.02 min; gradient = 12% to 75% (solvent A in solvent B, 0 to 10 min)

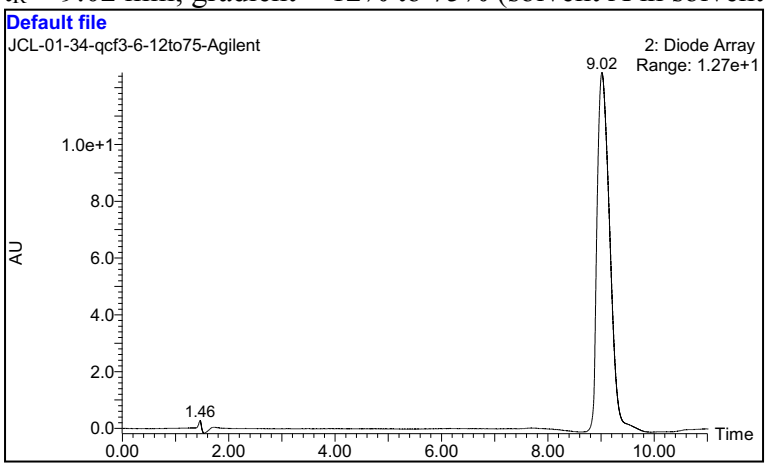

AYPGK-(*N*-Me-F)-NH_2:

t_R = 8.73 min; gradient = 12% to 80% (solvent A in solvent B, 0 to 10 min)

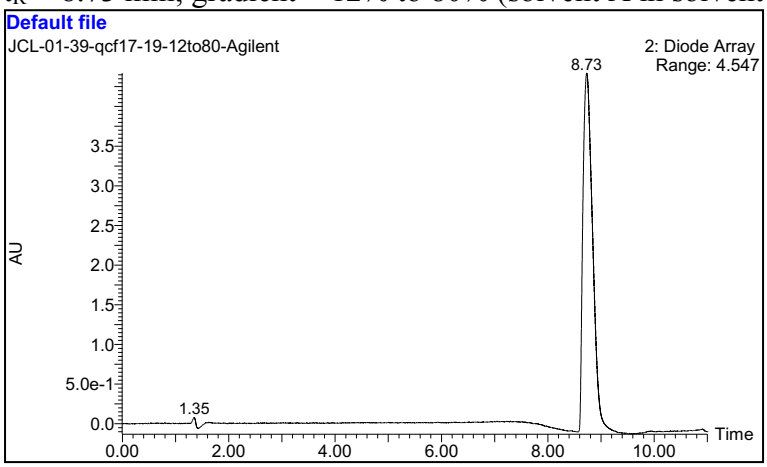

AYPG-(N_α-Me-K)-F-NH_2:

t_R = 8.33 min; gradient = 15% to 70% (solvent A in solvent B, 0 to 10 min)

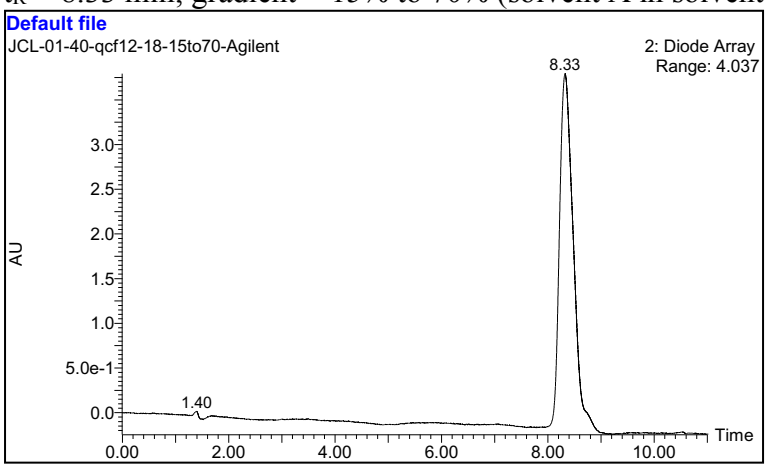

A-(*N*-Me-Y)-PGKF-NH_2:

t_R = 8.74 min; gradient = 12% to 70% (solvent A in solvent B, 0 to 10 min)

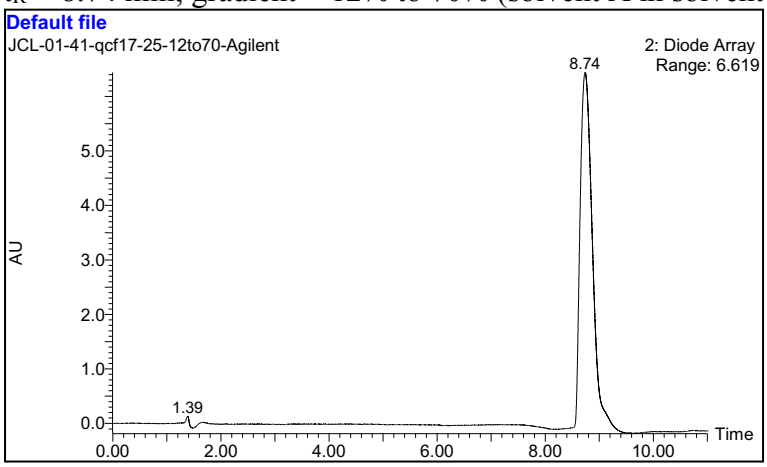

(*N*-Me-A)-YPGKF-NH_2:

t_R = 8.88 min; gradient = 12% to 70% (solvent A in solvent B, 0 to 10 min)

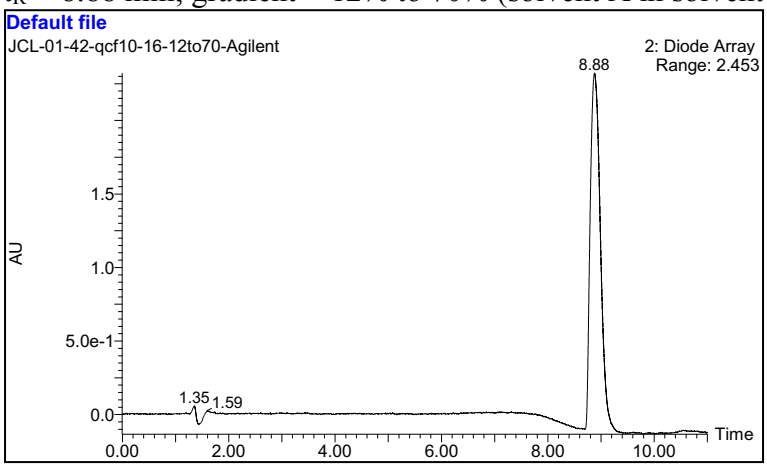

VYPGKF-NH_2:

t_R = 8.90 min; gradient = 12% to 70% (solvent A in solvent B, 0 to 10 min)

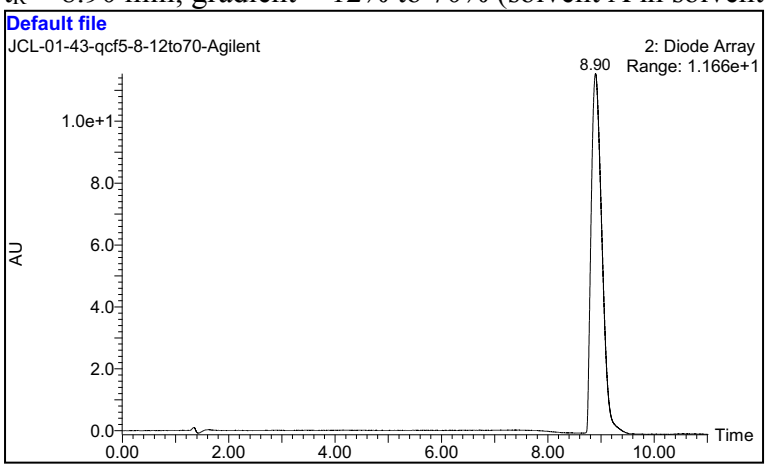

(*N*-Me-S)-YPGKF-NH_2:

t_R = 9.00 min; gradient = 13% to 70% (solvent A in solvent B, 0 to 10 min)

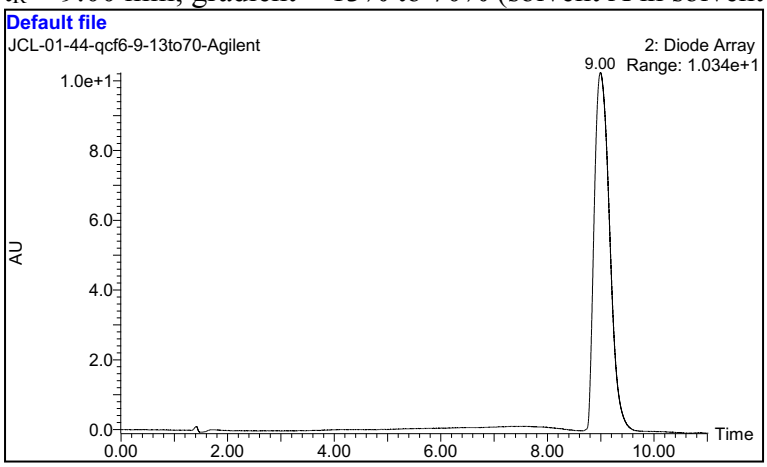

Nle-YPGKF-NH_2:

t_R = 8.88 min; gradient = 15% to 70% (solvent A in solvent B, 0 to 10 min)

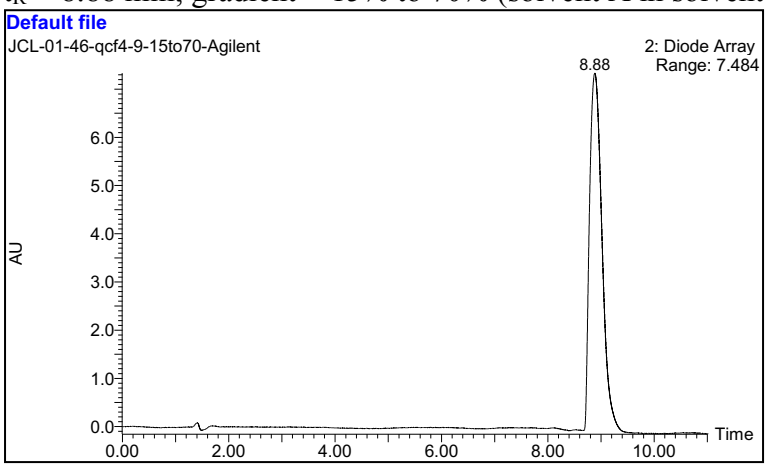

AYPGRF-NH_2:

t_R = 8.73 min; gradient = 13% to 70% (solvent A in solvent B, 0 to 10 min)

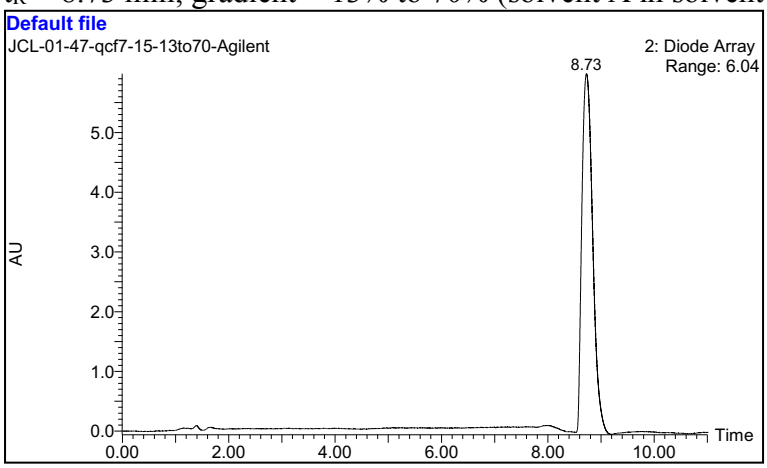

AYPGOF-NH_2:

t_R = 9.16 min; gradient = 12% to 80% (solvent A in solvent B, 0 to 10 min)

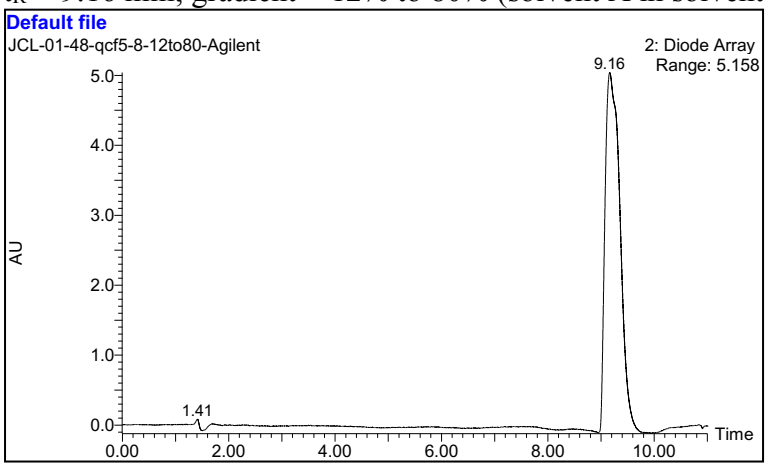

AYPG-Cit-F-NH_2:

t_R = 8.82 min; gradient = 13% to 80% (solvent A in solvent B, 0 to 10 min)

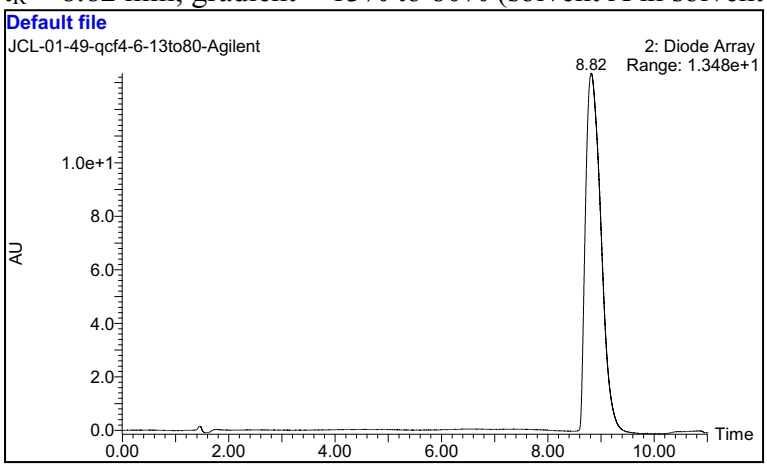

AYPG-(N_ε-Me-K)-F-NH_2:

t_R = 8.74 min; gradient = 12% to 70% (solvent A in solvent B, 0 to 10 min)

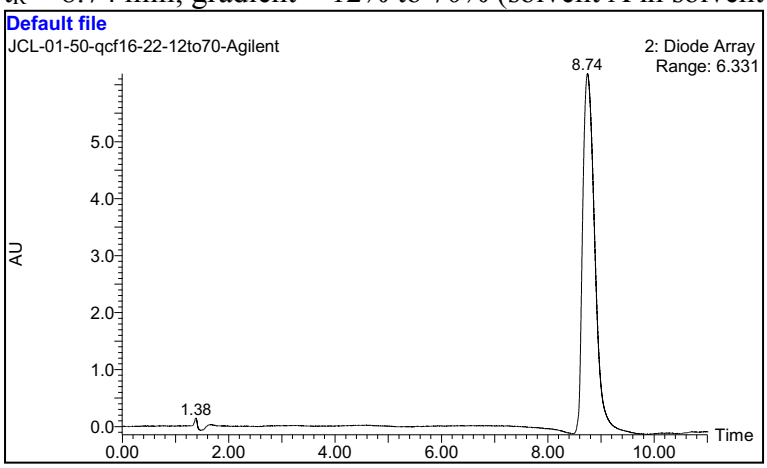

AYPGKY-NH_2:

t_R = 8.88 min; gradient = 8% to 80% (solvent A in solvent B, 0 to 10 min)

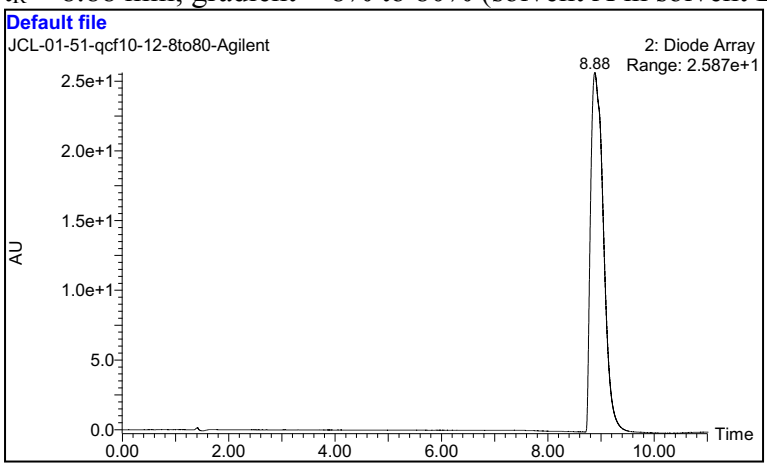

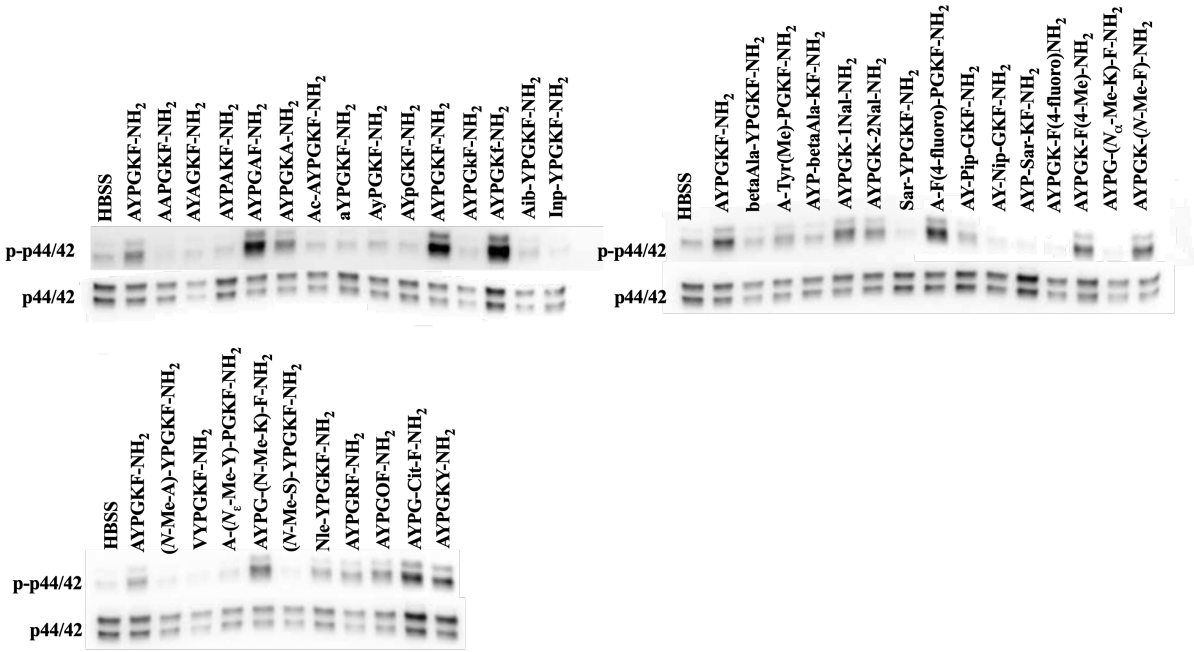

1807 **Figure S2. Representative blots of ERK phosphorylation in response to 100 µM of**
1808 **AYPGKF-NH$_2$ and derivative peptides. Data are summarized in figure 10.**

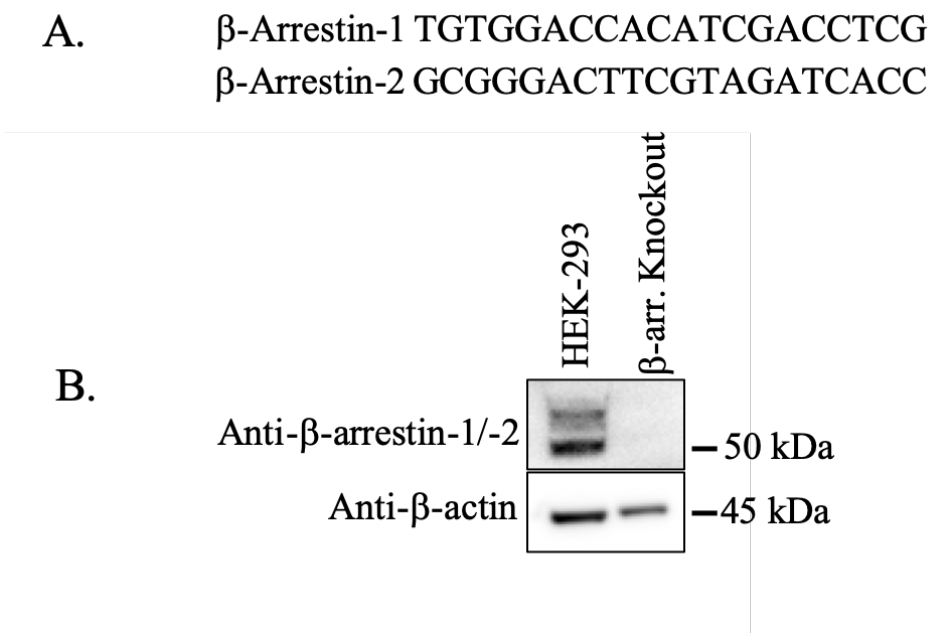

1809 **Figure S3. (A) Guide RNA sequences designed to target either β-arrestin-1 or -2. (B)**
1810 **Representative blots of β-arrestin-1/-2 protein from HEK-293 and β-arrestin-1/-2 double**
1811 **knockout HEK-293 (β-arr. Knockout) cells.** We observe no β-arrestin-1/-2 protein in the β-
1812 arr. knockout HEK-293 cell line.

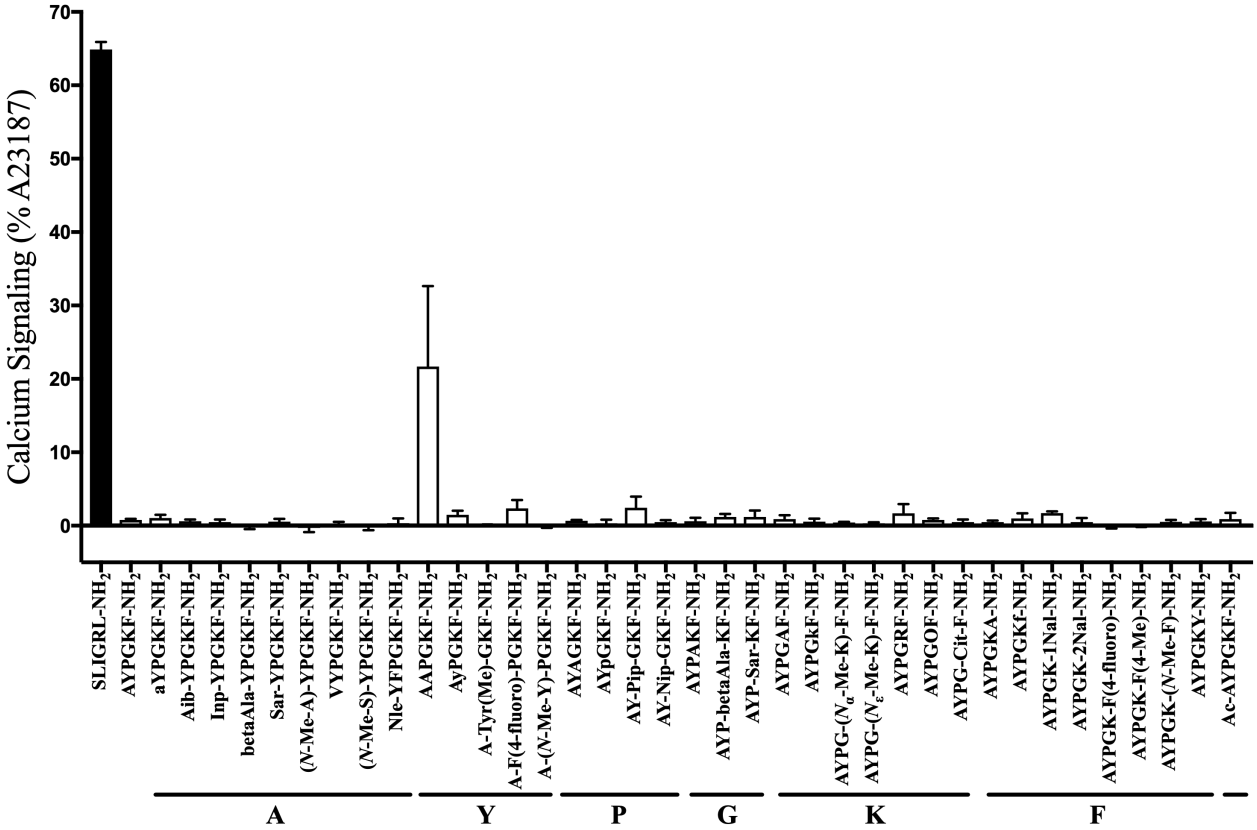

1813 **Figure S4. PAR4 peptide library is specific for PAR4 as shown by lack of calcium**
1814 **signalling in HEK293 cells which do not endogenously express PAR4. Peptide AAPGKF-**
1815 **NH_2 was found to have basal fluorescence even in the absence of cells. (*n* = *3*)**

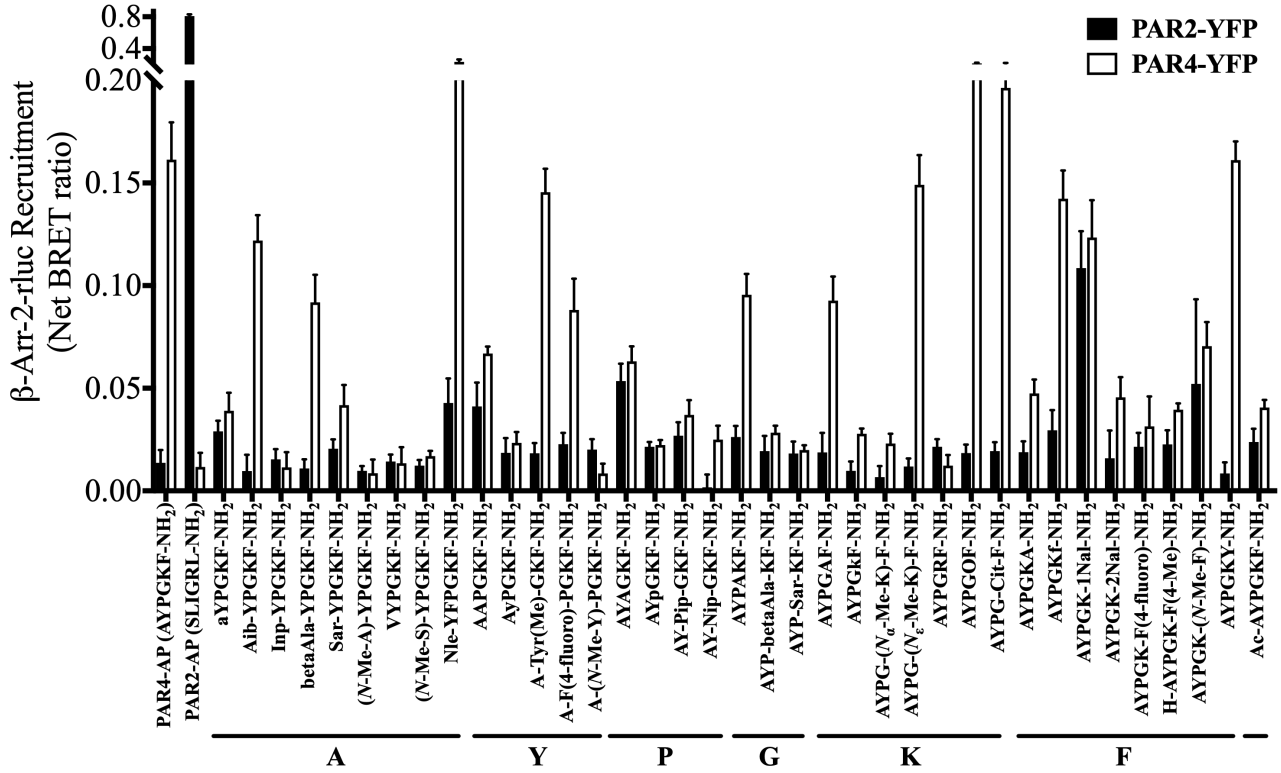

Figure S5. PAR4 peptide library is specific for PAR4 and does not cause recruitment of β-arrestin-2 to PAR2 (shown as black bars) at 100 µM, with the exception of AYPGK-1Nal-NH_2 which shows some β-arrestin recruitment to PAR2. BRET ratios obtained with the parental peptides for both PAR4 (AYPGKF-NH_2) and PAR2 (SLIGRL-NH_2) are shown. (*n* = *3*)